Living on the edge: Analysis of *Zostera marina* and the potential for restoration in Peconic Bay (Long Island, NY)

A Thesis Presented

by

Kaitlyn O'Toole

to

The Graduate School

in Partial Fulfillment of the

Requirements

for the Degree of

Master of Science

in

School of Marine and Atmospheric Sciences

Marine Sciences

Stony Brook University

May 2020

Stony Brook University

The Graduate School

Kaitlyn O'Toole

We, the thesis committee for the above candidate for the

Master of Science degree, hereby recommend

acceptance of this thesis.

Bradley J. Peterson
Associate Professor
School of Marine and Atmospheric Sciences
Stony Brook University

Donna Selch
Visiting Assistant Professor
School of Marine and Atmospheric Sciences
Stony Brook University

Bradley Furman
OPS Research Scientist
Florida Fish and Wildlife Research Institute

This thesis is accepted by the Graduate School

Eric Wertheimer
Dean of the Graduate School

Abstract of the Thesis

Living on the edge: Analysis of *Zostera marina* and the potential for restoration in Peconic Bay (Long Island, NY)

by

Kaitlyn O'Toole

Master of Science

in

School of Marine and Atmospheric Sciences

Marine Sciences

Stony Brook University

2020

As global ocean temperatures continue to rise, concern has arisen over the economic and environmental ramifications. As an integral part of coastal ecosystems, seagrasses provide nurseries for shellfish and juvenile fish, reduce currents, and improve water quality. Since the 1930's, *Zostera marina* (a northern seagrass species) has declined in Peconic Bay, Long Island (NY, USA). Sensitive to both light and temperature, light attenuation below photosynthetic demands and/or elevated temperatures over 25°C causes a metabolic imbalance in *Z. marina*. Severe or extended imbalances exhaust carbon reserves, inducing mortality. Temperature and sediment characteristics typically influence minimum light requirements (between 10 and 30% of surface light attenuation) of *Z. marina*. To determine minimum light requirements for Peconic Bay *Z. marina* populations, the light attenuation coefficient (K_d) was modeled using multiple linear regression. Collected concentrations of total suspended solids (TSS), chlorophyll-a, and colored dissolved organic matter (CDOM) were used with collected K_d. The light model explained only 25% of the K_d variance and further analysis suggested influence of other factors. A habitat suitability model developed from light, depth, temperature, hardened shorelines, and wave exposure, effectively modeled *Z. marina* presence in Peconic Bay–with 99.4% accuracy. This random forest model ranked variable importance as follows: wave exposure (highest), hardened shorelines, temperature, depth, and light (lowest). Model accuracy increased with removal of the light variable. Additionally, this model calculated survival thresholds, areas of high restoration probability, and predicted impacts of climate change—specifically temperature increases and sea level rise—in Peconic Bay.

Table of Contents

List of Figures

Chapter 1

Chapter 2

List of Tables

Chapter 1

Chapter 2

Acknowledgments

I would first like to thank my advisor, Bradley Peterson, for all his advice, encouragement, and constant support throughout this process. From boat donuts to boat tacos, you have contributed tremendously to my love for science and field work. I found a second family in the lab through your promotion of an environment of encouragement, free-thinking, support, and understanding.

Thank you to my readers, Dr. Bradley Furman and Dr. Donna Selch, for assisting and supporting me in the creation of this thesis with countless edits and advice. Your advice and encouragement brought my work to a place I may not have been able to reach on my own.

Thank you to the Peterson Lab, past and present, for teaching me how to think critically and efficiently, especially in the field. You all have always been willing to lend a helping hand, no matter the task. Thank you to Dr. Rebecca Kulp, Dr. Diana Chin, Stephen Heck, Amanda Tinoco, Leah Reidenbach, Dylan Cottrell, Alyson Lowell, and Brittney Scannell for making field days and hours in the office that much more enjoyable. I can't wait to see where you all go in the future!

I'd also like to thank many of the people who have been involved in this process, by way of friendship, advice, and willingness to answer any question I may have. Thank you to Scott "Indy" Hughes, Dr. Stephen Tettelbach, Jordan Raphael, Stephen Schott, and Maria Brown. Thank you to the boat captains Brian Gagliardi and Andy Brosnan for not pitching me overboard, and Chris Paparo for pointing out all the things I'm not noticing. Thank you to Courtney Ferland and Ginny Clancy for quickly and efficiently answering questions and processing paperwork, you saved me quite a bit of stress.

Thank you to the Peconic Estuary Program for providing the funding for my project, specifically to Sarah Schaefer, Elizabeth Hornstein, and Joyce Novak for supporting and promoting my work.

And finally, thank you to my friends and family. Without you, none of this would be possible. I have always had a love of the ocean and nature and decided early on that marine science was my passion. Their love and support have been unwavering, and I couldn't have done it without you.

Chapter 1

INTRODUCTION

Seagrasses are an integral part of coastal estuarine systems that provide a multitude of ecosystem services including nurseries for shellfish and finfish, sediment stability, current/wave reduction, and increased water quality (Dennison et al. 1993, Hughes et al. 2013). Seagrasses integrate carbon from the water column into tissues during photosynthesis. Anaerobic sediments cover the resulting detritus and create a sink of carbon, known as "blue carbon" (Fourqurean et al. 2012, Greiner et al. 2013, Lavery et al. 2013). Globally, seagrass coverage has declined dramatically due to wasting disease, light limitation, human activity, and temperature stress (Orth et al. 2006, Hughes et al. 2013). Without sufficient light, seagrass respiration rates outpace photosynthesis, resulting in net negative production (Dennison & Alberte 1985). Higher water temperatures require higher light levels to compensate for higher metabolic demand. Although higher temperatures and lower light levels are detrimental to the survival and productivity of seagrasses, improvements in either environmental variable helps to alleviate the stress associated with the other (Zimmerman et al. 2015).

Zostera marina, or eelgrass, is the dominant seagrass found in the eastern bays of Long Island, NY, USA (NYS Seagrass Taskforce 2009). New York has experienced a 90% decrease in *Z. marina* cover (as of 2009). During the 1930s, seagrass losses were driven by a wasting disease caused by the protist, *Labyrinthula macrocystis* (Short et al. 1987). More recent declines have been caused by light limitation and, to a lesser degree, fishing/shellfishing practices. Excess nitrogen causes algal blooms and excess epiphytic growth, which block light from seagrass in high densities (NYS Seagrass Taskforce 2009). *Zostera marina* requires a minimum of ~10–30% surface light attenuating to depth; this range is dependent on environmental conditions such as temperature and percent organic matter (Dennison et al. 1993, Dixon & Leverone 1995, Batiuk et al. 2000, Kemp et al. 2004, Kenworthy et al. 2014). Increasing water temperature raises the metabolic rates of *Z. marina*, exacerbating physiological stress on the plant. The optimal temperature range for *Z. marina* is between 10–25°C, and signs of stress are observed above 25°C (Zimmerman et al. 1989). Prolonged exposure (30+ days) over 25°C is lethal as well as short exposure from 27–35°C (Zimmerman et al. 1989). *Zostera marina* typically grows in sediment with less than 5–13% organic matter (Kenworthy et al. 2014). High organic matter sediments are generally associated with anoxia and high levels of hydrogen sulfide, a lethal by-product of anaerobic microbial respiration. Elevated hydrogen sulfide levels (>4μM) increases the need for

radial oxygen loss from roots and rhizomes, which can increase the photosynthetic demand. If not met, hydrogen sulfide penetration into the roots at high concentrations kills the plant (Krause-Jensen et al. 2011, Kenworthy et al. 2014). These factors act individually and synergistically to control *Z. marina* light requirements and survival.

Peconic Bay, an estuary comprised of several small bays, lies between the North and South "Forks" of eastern Long Island, NY (Figure 1). Plagued by wasting disease in the 1930s and brown tide (*Aureococcus anophagefferens*) beginning in 1985, there was a significant die-off of *Z. marina* in Peconic Bay. Populations of the bay scallop (*Argopecten irradians*), an economically important fishery to New York State, were also decimated by the brown tide events (Dennison et al. 1989, Tettelbach et al. 2015) . Brown tide, in high densities, will block light from reaching submerged aquatic vegetation, especially at the deep edges of *Z. marina* beds (Dennison et al. 1989). Shallower populations might meet photosynthetic needs, but these areas often fall outside optimal ranges of other key environmental conditions, such as temperature and wave energy. Brown tide is estimated to have reduced *Z. marina* coverage by 40% in Great South Bay and the Peconic Estuary during the 1980s (Dennison et al. 1989, Gobler & Sunda 2012). The continued loss of this important juvenile bay scallop habitat may prevent scallop recovery to pre-bloom densities; however, Carroll et. al (2010) found the invasive seaweed *Codium fragile* to provide a potentially suitable habitat. A brown tide event in Peconic Bay has not occurred since 1995, yet *Z. marina* coverage has declined by approximately 50% from 2000 to 2014 (Tettelbach et al. 2015, Pickerell & Schott 2017).

Water quality declines from east (Gardiner's Bay) to west (Flanders Bay), as the estuary gets shallower, more stratified, and less hydrologically connected. The Peconic River, the main tributary to the estuary, drains into Flanders Bay but is not the main source of freshwater. The majority of freshwater input in Peconic Bay is through submarine groundwater discharge (Hardy 1976). Residential, commercial, and agricultural land surrounds the embayment which contributes substantially to nutrient loading in the area (Pickerell & Schott 2017). The historical influence of nitrogen and phosphorus discharge due to sewage treatment plants in Riverhead has since lessened over time, but the impact of leaky septic systems and cesspools has increased. These leaks contribute a majority (50%) of total nitrogen loading to the Peconic Bay Estuary (Hardy 1976, Lloyd 2014). Fertilizers and agriculture, particularly on the North Fork, contribute an additional 26% of total nitrogen loading in the estuary. Nutrients may run off directly into the estuary or

leach into the groundwater where they remain for 100s of years. Atmospheric deposition contributes the remaining 24% of total nitrogen (Lloyd 2014). Nitrogen typically acts as the limiting nutrient for phytoplankton growth (Thayer 1974, Boynton et al. 1982). Nitrogen levels in Peconic Bay from 1998–2014 were below Peconic Estuary Program established criteria (0.45mg/L TN) for a majority of the year (Schaefer 2017).

Despite low nitrogen levels, *Z. marina* beds have continued to decline in Peconic Bay. Extended temperatures (~30 days) above 25°C and lower light availability west of Shelter Island resulted in unsuccessful *Z. marina* restoration attempts by CCE (Cornell Cooperative Extension; Pickerell & Schott 2017). Meadows west of Shelter Island (Bullhead Bay) are only found in areas of significant submarine groundwater discharge. Pickerell and Schott (2017) hypothesized that groundwater keeps the roots and rhizomes cooler than the surrounding water, which results in reduced respiration demands and thus lower light requirements. Determining the spatial resolution of groundwater discharge in Peconic Bay has been identified as a research priority for this estuary. This study excluded areas knowingly influenced by groundwater.

Studying the effects of light and temperature limitations on *Z. marina* in Peconic Bay is essential. Understanding how eutrophication, disease, and climate change affect seagrass locally improves the efficacy of restoration work. Water quality improvements in bays along the Atlantic coast of the United States have led to successful restoration of seagrass in many urbanized estuaries (Greening et al. 2014, Reynolds et al. 2016). The NYS Seagrass Taskforce, established in 2009 to study the mechanisms behind the *Z. marina* decline in Long Island waters, recommended the creation of a bio-optical model for Peconic Bay. Creating a bio-optical model to determine light-limiting factors in Peconic Bay is necessary to understand the continued declines in *Z. marina* and how improvements in water quality will aid restoration.

A bio-optical model allows for the addition of multiple light absorption, scattering, and refraction parameters to model light attenuation with depth. Bio-optical models determine water column irradiance by representing the effect of biological material on optical properties (Baker & Smith 1981). These models typically compute euphotic zone depths in the open ocean and similarly determine light limiting depths for seagrass restoration in coastal areas (Gallegos & Kenworthy 1996, Gallegos 2001, Koch 2001, Biber et al. 2008, Zimmerman et al. 2015). Bio-optical modeling conducted in the Chesapeake Bay focused primarily on *Z. marina* light requirements. Extensive water quality monitoring to determine light requirements of resident *Z.*

marina populations resulted in increased management towards protecting and restoring this seagrass in the bay (Batiuk et al. 2000, Lefcheck et al. 2018). The availability of previous bio-optical models for *Z. marina* introduces the parameters and methods for future models and systems. These models are variations on one another, but rely on the same underlying elements: chlorophyll-a (chl-a), total suspended solids (TSS), colored dissolved organic matter (CDOM), and the light attenuation coefficient (K_d) (Dennison et al. 1993, Stevenson et al. 1993, Kemp et al. 2004, Biber et al. 2008, Zimmerman et al. 2015). A bio-optical model, combined with temperature, sediment characteristics (porewater sulfide concentrations, organic content, and grain size), water column properties (salinity and dissolved oxygen), depth and tidal stage, wind speed, and wave exposure, can be used to produce a habitat suitability model. The habitat suitability model uses spatially explicit information on key biotic and abiotic parameters to predict species occurrence in the landscape. This knowledge will focus restoration efforts on high probability locations.

Water quality sampling for chlorophyll, TSS, CDOM, and K_d took place over two summers at 15 locations throughout Peconic Bay. Multiple linear regression was used to model K_d from collected chlorophyll, TSS, and CDOM. Percent light to bottom for each day sampled determined the days of minimum percent light needed for *Z. marina* survival in Peconic Bay. Sampling of CDOM had not been conducted in Peconic Bay prior to this study and a spectrophotometric and fluorometric relationship was determined. This study hopes to demonstrate the importance of light to *Z. marina* populations and to encourage further water quality improvements in the estuary. By determining light requirements, the combined effects of increased water quality and climate change (temperature and sea level rise) can be evaluated.

METHODS

Study Area

Located between the North and South Forks of Long Island, New York (Figure 1), the Peconic Bay estuary, comprised of five smaller bays, totals 218km^2. The only tributary to the bay, the Peconic River, discharges into westernmost Flanders Bay. Most of the freshwater input discharges as groundwater through porous sediments. Peconic Bay gradually deepens west to east from Flanders Bay (avg. depth: 1.6m) to Shelter Island Sound (avg. depth: 4.6m; Hardy 1976). Characterized by warmer temperatures and higher nutrients, western bays historically contained *Z. marina*, however, complete loss occurred prior to 1988 (Dennison et al. 1989). Eastern Shelter Island Sound and Gardiner's Bay contain the last two areas in Peconic Bay with *Z. marina* present. High-resolution orthoimagery, when available, was used to delineate *Z. marina* beds (Figure 2). Heavily tidally influenced, these areas receive cooler and clearer waters. The average flushing time increases from 22 days in Shelter Island Sound to 55 days in Flanders Bay (Hardy 1976).

Water Quality Monitoring

This study focuses on water quality sampling from Flanders Bay to western Gardiner's Bay (Figure 3). Fifteen sites were chosen throughout Peconic Bay at depths less than 5m (MLW). Sites were classified into two categories: "historic", or areas with historic but no present *Z. marina*; and "current", or sites with *Z. marina* as of 2017. No "current" sites lost notable *Z. marina* coverage during the sampling period. Of these 15 sites, four sites within western Peconic Bay (Flanders, Great Peconic, and Little Peconic Bay) were selected to incorporate historic *Z. marina* coverage and subsequent losses prior to the 1980s. The remaining 11 sites were distributed throughout eastern Peconic Bay (Shelter Island Sound and western Gardiner's Bay) — composed of six historic sites and five current sites. Sites were labeled as: WQ 1–10 (without *Z. marina*) and SG 1–5, with *Z. marina* (Figure 3).

The deep edge, considered to be the area of highest environmental stress for *Z. marina*, integrates the plant's response to stresses from both light and sediment (Kenworthy et al. 2014, Zimmerman et al. 2015). However, while increased depths result in greater light stress, the deep edge experiences lower temperature stress in warmer months. To monitor light requirements at

this “light stressed” area, sampling occurred at the deep edge of *Z. marina* beds where present (SG1-5). Light requirements from the deep edge demonstrate the minimum light requirements of that *Z. marina* bed. The constituents of the water column that were included in the bio-optical model were: chlorophyll-a (an indicator of shading by phytoplankton present in the water column), CDOM (colored dissolved organic matter), and TSS (total suspended solids). Water quality parameters were recorded using YSI 6600 (2017) or EXO 1 sonde (2018) from a boat monthly in May, June and October, and bi-weekly from July through September. At each station, water depth, dissolved oxygen (DO), water temperature, salinity, and turbidity (NTU’s), were measured <1m from the bottom. The YSI instruments were calibrated monthly.

Measurements of the irradiation values and percent light from surface were measured from at least three depths using a Li-Cor LI-1400 datalogger equipped with an underwater quantum sensor (LI-192SA) and deck sensor (LI-190SA). In-situ light attenuation values, K_d (m^{-1}), were determined by the Beer-Lambert exponential decay function (Carruthers et al. 2001). Whole water grab samples were taken in duplicate below the water surface (~10 cm) using 1L amber polyethylene bottles at each station for TSS and chlorophyll-a. Chlorophyll-a was extracted using the USEPA fluorometric method 445.0 (Arar & Collins 1997), and concentration determined with a Turner Trilogy Laboratory Fluorometer. Chlorophyll-a filtration was performed within eight hours of collection and frozen at -20°C, extracted within three weeks, and analyzed within 48 hours of acetone addition. Total suspended solids concentration was determined using USEPA method 160.2 (USEPA 1999) and filtered within one week of collection.

CDOM samples were taken monthly to minimize cost and processing time. Samples were taken in duplicate at each station and filtered on site through a 0.7-µm pore size GF/F filter into amber borosilicate 20mL vials and frozen at -20°C until analysis. CDOM absorption measurements were run on a Perkin Elmer dual beam UV-vis spectrophotometer using 10-cm quartz cuvettes from 350–700 nm and a slit length of 2 nm. CDOM absorption coefficients were determined at 440 and 350 nm after correcting raw values for scattering and normalizing to a standard path length (Branco & Kremer 2005). CDOM fluorometric measurements (ppb) were run on a Turner Trilogy Laboratory Fluorometer using the UV module (excitation = 350 nm and emission wavelength= 410–450 nm) and calibrated using quinine sulfate at known concentrations (Rochelle-Newall et al. 2014). Both fluorometric and spectrophotometer measurements were made for CDOM to determine a correlation between the two methods: this was performed for 3 sampling

dates at all sites (n=45). While absorption measurements are standard practice due to the heterogeneity of sample particle size, fluorometric measurements are much easier and less expensive to run. Determining a method for converting between fluorometric and spectrophotometric measurements has been successful for smaller water bodies and is useful when including CDOM measurements in routine water quality sampling (Branco 2007). Bio-optical modeling typically uses CDOM absorption measurements at 440 nm. However, when comparing absorption and fluorometric measurements, it is important to use the same excitation wavelength, in this case, 350 nm (Hoge et al. 1993, Rochelle-Newall et al. 2014). Relationships between a_{350}, a_{440}, and concentration (ppb) were evaluated using linear regression.

Creation of bio-optical model

To model the light attenuation coefficient (K_d) from collected chlorophyll-a (µg/L), TSS (mg/L), and CDOM samples (a_{350}), a multiple linear regression (MLR) technique was used based on the assumption that each constituent contributed individually to light attenuation (Batiuk et al. 2000):

$$K_d = K_{water} + k_c[Chl] + k_s[TSS] + k_g[CDOM] \quad (1)$$

where K_{water} represents the partial coefficient of light attenuation through pure seawater (intercept), and k_c, k_s, k_g represents the specific light attenuation coefficient of chlorophyll, TSS, and CDOM respectively (Batiuk et al. 2000, Gallegos 2001). MLR was performed with and without CDOM measurements for Peconic Bay, at each site sampled, and grouped by spatial designation, "regions" (A–E, Figure 4). Sites were grouped into "regions", A–E based on proximity to one another. Grouping spatially allows for a lower chance of error by increasing data points. Outliers were removed from data using the Bonferroni test ($p < 0.05$) and Cook's Distance.

Percent light to bottom

Percent light reaching the bottom, PLW (percent light through water), was calculated by using Gallegos (2001):

$$PLW = exp^{K_d * Z} * 100 \quad (2)$$

where K_d is the observed light attenuation coefficient and Z is the depth (m) at mean low water (MLW). Bathymetry was obtained from the NCEI NOAA LIDAR data taken in 2014 as part of the Hurricane Sandy DEM imagery. Bathymetry taken from the 2014 imagery provided the highest horizontal and vertical resolution at 10cm each. The vertical datum was transformed into MLW from NAVD88 by the NOAA vertical datum converter (VDatum 4.0.1). Observed K_d values were interpolated over the bay from sampling sites using inverse distance weighting (IDW). These values, along with bathymetry (Z) were then used in Equation 2 to determine PLW throughout the bay for the 18 sampling days. A binary classification scheme was used to determine the percent light threshold needed for *Z. marina* to survive in this system. Seven threshold values were tested based on the literature value range of 10–30% required surface light: 10, 15, 18.5, 20, 22.5, 25, and 30% light to bottom (Dennison et al. 1993, Dixon & Leverone 1995, Kemp et al. 2004, Kenworthy et al. 2014). For every day of sampling each cell was classified by 0, below the threshold, or 1, above or equal to the threshold using the 'reclassify' function in R (Hijmans 2019). Seven layers were created for each threshold with a maximum value of 18 for each cell. Interquartile values, 25th, 50th, and 75th, of PLW values (0–100) for all days of sampling were also calculated. A 50,000 random point file was constructed within a 0–5-m depth region (MLW), corresponding to the minimum and maximum depth where *Z. marina* was present in 2017 imagery delineations. For the entire point file, 2.5% of points were within *Z. marina* beds due to the low coverage in Peconic Bay. A stratified random design was used to avoid leading to a high Type-2 error rate; 5,000 random points were taken within *Z. marina* sites and combined with a 45,000 random point file outside of *Z. marina* sites. Cell values from each threshold (PLW 10–30, interquartile values) were extracted to these points using the 'extract' function in R. These points were then used in model evaluations for determining the importance and value of each threshold in predicting *Z. marina* presence or absence.

Statistical analysis and model assessment

Differences between years, sites, and groupings were assessed through ANOVA and subsequent Tukey HSD tests. Significant results in all tests were evaluated using a p-value of less than or equal to 0.05. Outliers for all regressions were evaluated using the Bonferroni test and Cook's Distance.

Linear regression was performed to determine possible correlation between K_d and each parameter: chlorophyll, TSS, and CDOM. These parameters were also evaluated against one another to ensure independence. When parameters were correlated, the variance inflation factor (VIF) was computed to determine collinearity using the 'car' R package (Fox et al. 2020). Scores higher than 5 (conservative)–10 are considered to have a problematic amount of collinearity and should be removed (James et al. 2013). MLR was used to model K_d with the possible additive effects of chlorophyll, TSS, and CDOM. This was also performed without CDOM as many water quality management agencies do not sample for this parameter. MLR was used with individual sites, regions, and the entire bay to determine the relationship between K_d and multiple parameters.

Evaluating light thresholds for Peconic Bay *Z. marina* was performed using the evaluate function in R package 'dismo' (Hijmans et al. 2017). Light levels at each threshold (PLW 10–30) and 25th, 50th, and 75th interquartile values were extracted to 50,000 points and each point was determined to be present or absent for *Z. marina*. Boxplots of days at each threshold were created to display median and range of values (0–18) at points where *Z. marina* is present. The evaluate function then calculated the value at which the true positive and negative rate were concurrently at their maximum (Hijmans et al. 2017). Each cell was classified as present or absent based on the value computed by the function. The best light value for prediction of *Z. marina* presence or absence was determined by comparing overall accuracy, correlation, true positive/negative rates, and false positives/negative rates.

RESULTS

Site characteristics

Significant differences between individual sites and regions were evaluated through ANOVA and Tukey HSD tests. Data for 2017 and 2018 were pooled for all linear regressions. Chlorophyll values were between 1.19 and 39.74 (µg/L), had a median of 6.12 (µg/L), and differed only slightly among sites (Table 1). One of the two most western sites, WQ2, had significantly higher chlorophyll values than several of the eastern sites (Figure 5). Values for TSS ranged from 3.7 to 50.6 (mg/L), had a median value of 12.4 (mg/L), and had no significant differences between individual sites (Figure 6). CDOM values ranged between 0.27 and 2.86 (m^{-1}), had a median value of 1.31 (m^{-1}), and had no significant differences between sites (Figure 7). K_d was also variable, ranging from 0.25 to 1.69 (m^{-1}), had a median of 0.68 (m^{-1}), and had significant differences for two sites (Figure 8). The proximity of one site to the mouth of Hashomomuck Pond, WQ4, and the other to a Shelter Island town wastewater outfall, SG1, likely accounts for differences in K_d. These two sites were not significantly different from each other.

There were few statistical differences between sites within regions. Minimum, maximum, and median values for chlorophyll, TSS, CDOM, and K_d were also computed for the regions (Table 2). Significant differences between regions were found for chlorophyll (Figure 9) and K_d (Figure 12). Region A, the most western region, had statistically higher chlorophyll values when compared to regions C, D, and E, the more eastern regions. Region B, located in Shelter Island Sound to eastern Little Peconic Bay, had significantly higher K_d values when compared with all other regions. No significant differences were found for TSS (Figure 10) and CDOM (Figure 11).

Linear Regression Modeling

Linear regression was performed with chlorophyll-a (µg/L) and TSS (mg/L) concentrations, and CDOM absorption (a_{350}) to determine correlation with K_d. Individual sites, regions, and the bay were separately analyzed to determine if any parameter was a sufficient predictor of K_d. Individual parameters against K_d yielded largely insignificant results. Chlorophyll-a was the best predictor for K_d at two out of fifteen sites (Table 3), TSS at one site (Table 4), and CDOM at three sites (Table 5). However, the slope of the line at one of the two chlorophyll and

all CDOM significant sites was negative, rendering these results of little value to the model. Grouping spatially uses more data points and although the coefficient of determination was reduced, the significance of the models was increased and the chance of Type II error decreased. Among these models, one of the five chlorophyll-a models (Table 6), two TSS models (Table 7), and one CDOM model (Table 8) were significant. When correlation was modeled for the entire bay between the light attenuation coefficient and each parameter, TSS was significant, but chlorophyll and CDOM were not (Table 9). The best predictor of the light attenuation coefficient was total suspended solids: however, the coefficient of determination (R^2= 0.06) was not high enough to be appropriate for modeling, simply indicating a weak relationship between the parameters.

Multiple linear regression was used to model the contributions of chlorophyll, TSS, and CDOM to the light attenuation coefficient. MLR was performed similarly to the previous linear modeling (i.e. individual sites, spatial groups, and the entire bay). Five of the fifteen sites had significant correlation: however, four of the five significant regressions also included negative coefficients for at least one parameter (Table 10). All spatially grouped models were significantly correlated with relatively high coefficients of determination (R^2=0.3–0.7). Chlorophyll and/or CDOM were negative in three of the five models, suggesting that one, or both, of the variables were not important to the light attenuation coefficient in that area (Table 11). The model for the entire bay was significant: all parameter coefficients were positive in the model, but chlorophyll and CDOM coefficients were not statistically significant., indicating they were not as important as TSS to light attenuation in this estuary (Table 11). Multicollinearity was found between all parameters; however, the variables were not found to inflate the variance of the regression coefficient due to low VIF scores (< 1.25).

The CDOM parameter was removed from the modeling, as many agencies do not test for this constituent, and re-run with the same methods. Five of the fifteen sites were significantly correlated between K_d and chlorophyll/TSS. All models included negative parameter coefficients, but four of the five were positive for TSS parameter coefficients (Table 12). When spatially grouped, three of the five models showed significant correlation and two of those included negative parameter coefficients for chlorophyll (Table 13). The full bay model was highly significant, and all values were positive, though the chlorophyll coefficient was not significant (Table 13).

Threshold analysis of light levels in Peconic Bay

Interpolated percent light through water (PLW) was determined throughout Peconic Bay for each day sampled using Equation 2. Days over threshold values of PLW were calculated at 10% (Figure 13, 14), 15% (Figure 15, 16), 18.5% (Figure 17, 18), 20% (Figure 19, 20), 22.5% (Figure 21, 22), 25% (Figure 23, 24), and 30% (Figure 25, 26) of incident light. *Zostera marina* appeared to require a percent light of over 10% for all days sampled but varied between a minimum 18 and 6 days at 30%, excluding outliers (Figure 27). All PLW thresholds had a median value of 18 days, excluding the PLW of 30%, which had a median value of 17 days. The inter-quartile ranges for PLW thresholds increased as percent light increased, suggesting that populations had varying light requirements. Points with present *Z. marina* also received higher PLW than those without (Figure 28). Correlation of *Z. marina* presence to light threshold values remained low (0.26–0.35) but was highest at the PLW of 22.5% (Table 16). *Z. marina* presence or absence based on the threshold PLW of 22.5% of 11 days yielded a high false positive rate, 0.38 (38%). Out of 50,000 points, about 20,000 points were misclassified as having *Z. marina* where none was present. In addition, 25, 50, and 75th interquartile values of percent light through water (0–100 %) from all days sampled (18 days) were used as a different metric to determine typical light levels needed for *Z. marina* to survive (Figure 20). These light levels were also run through the evaluate function and performed similarly to the days over PLW thresholds (correlation 0.29–0.31). The cut-off threshold was between 21.61 and 26.30% (25–75th IQR), which encompasses the days over PLW of 22.5% (Table 16). The high false positive rate suggests that there were other parameters outside of light affecting *Z. marina* distribution in Peconic Bay.

CDOM

In Peconic Bay there was a significant positive relationship (R^2=0.37) between CDOM absorption (a_{440}) and concentration (ppb; Figure 29). There was also a significant relationship between a_{440} and a_{350} (R^2=0.72; Figure 30). The relationship between a_{350} and concentration measurements (ppb) was much stronger than using a_{440} (Figure 23). Equation 3 relating concentration (ppb) to a_{350} was as follows:

$$a_{350} = 1.03803 * \left[CDOM_{ppb}\right] + 0.97509 \quad (3)$$

This equation can be used to estimate CDOM in Peconic Bay (R^2=0.69, Figure 23). The relationship between fluorescence and absorbance is important because CDOM had not been systematically monitored in Peconic Bay prior to this study.

DISCUSSION

Declines in *Z. marina* may be caused by the plant's inability to compensate for metabolic demands due to insufficient light. Determining a model for light attenuation is imperative for the management of *Z. marina* to predict effects of proposed changes to water quality management. When depth is known, percent light to bottom can be calculated with K_d from collected water quality samples; when percent light to bottom is known, *Z. marina* populations can be monitored for insufficient light. The model also has the capability to predict percent light to bottom from modified water constituent concentrations, e.g. via nitrogen management or lack thereof (Gallegos & Kenworthy 1996, Gallegos 2001, Kemp et al. 2004, Biber et al. 2008). The predictions of the bio-optical model will be useful with future climate change scenarios of increasing water temperatures and sea level rise. Higher water temperatures and the corresponding increase in seagrass respiration will increase the photosynthetic requirement, especially when light is limiting (Biber et al. 2005, Kenworthy et al. 2014, Abdelrhman 2016, 2017). Conversely, higher water clarity may protect *Z. marina* in surviving in future warmer temperatures (Zimmerman et al. 2015).

Zostera marina has been continuously losing area from western to eastern Peconic Bay, even as water quality thresholds have been met (Pickerell & Schott 2017, Schaefer 2017). Unexpectedly, differences in CDOM or TSS were not detected between sites and regions, especially on a west to east gradient. Limited differences between sites and regions were present in chlorophyll concentrations and the light attenuation coefficient. The site differences that were present for chlorophyll existed between western sites (WQ 1 and 2) and eastern sites due to longer residence times (Hardy 1976). The light attenuation coefficient and TSS concentrations were not significantly different between these areas. Concentrations of model constituents were within

bounds of several other water quality sampling programs focused on *Z. marina* light requirements (Kemp et al. 2004, Biber et al. 2008, Kenworthy et al. 2014, Zimmerman et al. 2015, Abdelrhman 2017). However, sampling typically took place on days where the sea-state was calm (wind speed < 17 knots) from May-October, which may affect the light attenuation value and concentrations of the constituents. Total suspended solids would likely be higher with wind events, and CDOM and chlorophyll would likely increase following heavy rain. Both events could increase light attenuation (Ward et al. 1984, Jordan et al. 1991, Stevenson et al. 1993, Koch 1999, Dixon et al. 2014).

Linear regression between the light attenuation coefficient and individual parameters yielded low correlation on site, region, and bay levels. The best predictor in the system was TSS, explaining only 6% of the variance in light attenuation. The low correlation values suggested that no one parameter accurately explains light attenuation. Modeling regions with all parameters for light attenuation and only considering the coefficient of determination yielded the best results. However, this method generated negative coefficients for chlorophyll and TSS, undermining the assumption that all constituents were additive. Similar coefficients between clustered sites were expected but not produced (Batiuk et al. 2000). In modeling the entire bay, the coefficient of determination doubled when CDOM was included in the model (R^2=0.25) versus not (R^2=0.12). These models did not produce a high enough coefficient of determination to effectively predict the light attenuation coefficient despite being statistically significant. To create an accurate model, a follow up study that uses an in-situ spectrophotometer is needed. This higher resolution study would determine the following: total absorption and backscattering coefficients; partial absorption and backscattering coefficients of water, phytoplankton, non-algal particulates; and the partial absorption coefficient of CDOM. Obtaining these coefficients would allow for higher accuracy predictions of the light attenuation coefficient, which will model various future scenarios of constituent values (Gallegos & Kenworthy 1996, Gallegos 2001, Kemp et al. 2004, Biber et al. 2008). Sampling over the entire year and in more areas would also be beneficial in understanding the light relationship to chlorophyll, TSS, and CDOM in this system.

CDOM was deemed an important water constituent in determining the light attenuation coefficient in Peconic Bay, doubling the coefficient of determination in the multiple linear regression of the entire bay. Although CDOM did not attenuate light as highly as other model constituents during this sampling period, it is still useful to include in light modeling and important

to attenuation in higher concentrations (Branco & Kremer 2005, Biber et al. 2008). For instance, CDOM was found to be the dominant absorber of light in Quantuck Bay (Shinnecock Bay, Long Island, NY) during a brown tide event in 2004 (Etheridge & Roesler 2004). While a brown tide event has not occurred in Peconic Bay since 1995, this does not exclude the possibility of a future occurrence, especially while there are still blooms occurring in nearby estuaries (Gobler & Sunda 2012, Tettelbach et al. 2015). Sampling should be performed in creeks and close to freshwater influences to obtain a broader scope of CDOM absorbance and possible effects of CDOM on light attenuation, especially if modeling a freshwater influenced system. Running samples on the Turner fluorometer is much easier and less expensive than running on the spectrophotometer (Rochelle-Newall et al. 2014). The correlation curve produced by this study will be useful in converting between absorbance and fluorescence. More measurements, especially from areas higher in CDOM absorbance, should be added to the curve to increase accuracy. In addition, it would be beneficial to include measurements from different seasons where concentrations may be higher than those sampled in the summer and contribute more to light attenuation (Organelli et al. 2014).

A threshold evaluation determined the cut-off value and strength of the relationship between sufficient light and presence of *Z. marina*. The light threshold was determined as *Z. marina* absence under 11 days of 22.5% PLW and *Z. marina* presence over 11 days of 22.5% PLW. The value 22.5% light through water, the best predictor of *Z. marina* in Peconic Bay based on light, was well within the hypothesized range of *Z. marina* light requirements, 10–30% (Dennison et al. 1993, Dixon & Leverone 1995, Batiuk et al. 2000, Kemp et al. 2004, Kenworthy et al. 2014). Plotting percent light to bottom points throughout Peconic Bay revealed that light was not the only factor limiting *Z. marina* presence within the estuary — 38% of random points were misclassified as having present *Z. marina* when it was absent. The area of Peconic Bay that should hold *Z. marina* according to the light threshold of 11 days over PLW of 22.5% is 50.32 km^2, but *Z. marina* only occupies 1.46 km^2 (2.90% of the total area). The majority of this sufficient light area is west of Shelter Island (35.36km^2), outside of theoretical temperature requirements (Pickerell & Schott 2017). East of Shelter Island, *Z. marina* occupied only 9.3% of the predicted area. Expansion into these areas by *Z. marina* is possible, but other factors such as temperature, wave action, current, and sediment properties, may be preventing this (Batiuk et al. 2000, Kenworthy et al. 2014, Uhrin & Turner 2018). Temperature is an important factor to the west of Shelter Island and results in higher light requirements (Pickerell & Schott 2015, Zimmerman et al.

2015). Developing a model that considers both temperature and light will be important for this estuary.

Determining *Z. marina* presence based on light alone yielded inaccurate results. Incorporating other factors into a habitat suitability model should be considered as many of these factors vary concurrently. For example, higher temperatures require higher light levels to offset heightened metabolic rates (Zimmerman et al. 1989, Hammer et al. 2018). Temperature and light should continue to be monitored in this system, especially with warming waters. Creating a bio-optical model with measured inherent and apparent optical properties will establish an accurate model of light attenuation based on past and future model parameters. Minimally, agencies should monitor throughout all seasons for chlorophyll, total suspended solids, and CDOM. While *Z. marina* will adapt to certain environmental stressors, alleviating light stress through water quality management is essential for *Z. marina* populations. Taking measures to increase water clarity could save local species from extirpation due to climate change and allow the seagrass to survive and thrive in this estuary.

LITERATURE CITED

Abdelrhman MA (2016) Modeling water clarity and light quality in oceans. J Mar Sci Eng 4:80.

Abdelrhman MA (2017) Quantifying contributions to light attenuation in estuaries and coastal embayments: Application to Narragansett Bay, Rhode Island. Estuaries and Coasts 40:994–1012.

Arar EJ, Collins GB (1997) In vitro determination of chlorophyll a and pheophytin in marine and freshwater algae by fluoroescence. Method 445.0. National Exposure Research Laboratory, US EPA, Cincinnati.

Baker KS, Smith RC (1981) Optical properties of the clearest natural waters (200–800 nm). Appl Opt 20:177.

Batiuk RA, Bergstrom PW, Kemp WM, Koch EW, Murray L, Stevenson JC, Bartleson R, Carter V, Rybicki NB, Landwehr JM, Gallegos CL, Karrh L, Naylor M, Wilcox DJ, Moore KA, Ailstock S, Teichberg M (2000) Chesapeake Bay submerged aquatic vegetation water quality and habitat-based requirements and restoration targets: A second technical synthesis.CBP/TRS 245/00. EPA 903-R-00-014. U.S. EPA, Chesapeake Bay Program, Annapolis, Maryland.

Biber PD, Gallegos CL, Kenworthy WJ (2008) Calibration of a bio-optical model in the North River, North Carolina (Albemarle-Pamlico Sound): A tool to evaluate water quality impacts on seagrasses. Estuaries and Coasts 31:177–191.

Biber PD, Paerl HW, Gallegos CL, Kenworthy WJ, Fonseca MS (2005) Evaluating indicators of seagrass stress to light. Estuar Indic:193–209.

Boynton WR, Kemp WM, Keefe CW (1982) A comparative analysis of nutrients and other factors influencing estuarine phytoplankton production. Academic Press, New York, NY, USA.

Branco AB (2007) Empirical methods for the prediction of optical properties in shallow estuaries, Ph.D. thesis, Univ. of Conn., Groton, Conn.

Branco AB, Kremer JN (2005) The relative importance of chlorophyll and Colored Dissolved Organic Matter (CDOM) to the prediction of the diffuse attenuation coefficient in shallow estuaries. Estuaries 28:643–652.

Carroll JM, Peterson BJ, Bonal D, Weinstock A, Smith CF, Tettelbach ST (2010) Comparative survival of bay scallops in eelgrass and the introduced alga, *Codium fragile*, in a New York estuary. Mar Biol 157:249–259.

Carruthers TJB, Longstaff BJ, Dennison WC, Abal EG, Aioi K (2001) Measurement of light penetration in relation to seagrass. In: *Global Seagrass Research Methods*. Elsevier Science, p 369–392

Dennison WC, Alberte RS (1985) Role of daily light period in the depth distribution of *Zostera marina* (eelgrass). Mar Ecol Prog Ser 25:51–61.

Dennison WC, Marshall GJ, Wigand C (1989) Effect of "brown tide" shading on eelgrass (*Zostera marina* L.) distributions. In: *In E. M. Cosper, V.M. Bricelj, and E.J. Carpenter (eds.), Novel Phytoplankton Blooms: Causes and Impacts of Recurrent Brown Tides and other Unusual Blooms. Lecture Notes on Coastal and Estuarine Studies. Springer-Verlag, New York.* p 675–692

Dennison WC, Orth RJ, Moore KA, Stevenson JC, Carter V, Kollar S, Bergstrom PW, Batiuk RA (1993) Assessing water quality with submersed aquatic vegetation. Bioscience 43:86–94.

Dixon JL, Osburn CL, Paerl HW, Peierls BL (2014) Seasonal changes in estuarine dissolved organic matter due to variable flushing time and wind-driven mixing events. Estuar Coast Shelf Sci 151:210–220.

Dixon L, Leverone JR (1995) Light Requirements of *Thalassia testudinum* in Tampa Bay, Florida. Final Rept. SW Florida Water Management District, Mote Marine Lab Tech Rept, vol. 425.

Etheridge SM, Roesler CS (2004) Temporal variations in phytoplankton, particulates, and colored dissolved organic material based on optical properties during a Long Island brown tide compared to an adjacent embayment. Harmful Algae 3:331–342.

Fourqurean JW, Duarte CM, Kennedy H, Marbà N, Holmer M, Mateo MA, Apostolaki ET, Kendrick GA, Krause-Jensen D, McGlathery KJ, Serrano O (2012) Seagrass ecosystems as a globally significant carbon stock. Nat Geosci 5:505–509.

Fox J, Weisberg S, Price B (2020) Package 'car'. 1–149.

Gallegos CL (2001) Calculating optical water quality targets to restore and protect submersed aquatic vegetation: Overcoming problems in partitioning the diffuse attenuation coefficient for photosynthetically active radiation. Estuar Res Fed Estuaries 381:381–397.

Gallegos CL, Kenworthy WJ (1996) Seagrass depth limits in the Indian River Lagoon (Florida, U.S.A.): Application of an optical water quality model. Estuar Coast Shelf Sci 42:267–288.

Gobler CJ, Sunda WG (2012) Ecosystem disruptive algal blooms of the brown tide species, *Aureococcus anophagefferens* and *Aureoumbra lagunensis*. Harmful Algae 14:36–45.

Greening H, Janicki AJ, Sherwood ET, Pribble R, Johansson JOR (2014) Ecosystem responses to long-term nutrient management in an urban estuary: Tampa Bay, Florida, USA. Estuar Coast Shelf Sci 151:1–16.

Greiner JT, McGlathery KJ, Gunnell J, McKee BA (2013) Seagrass restoration enhances 'Blue Carbon' sequestration in coastal waters. PLoS One 8:1–8.

Hammer KJ, Borum J, Hasler-Sheetal H, Shields EC, Sand-Jensen K, Moore KA (2018) High temperatures cause reduced growth, plant death and metabolic changes in eelgrass *Zostera marina*. Mar Ecol Prog Ser 604:121–132.

Hardy CD (1976) A preliminary description of the Peconic Bay Estuary. Marine Sciences Research Center, State University of New York at Stony Brook. Special Report 3. Stony Brook.

Hijmans RJ (2019) Package 'raster': Geographic data analysis and modeling with raster data. R package version 3.0-7.

Hijmans RJ, Phillips S, Leathwick J, Maintainer JE (2017) Package 'dismo'- species distribution modeling. R package version 1.1-4.

Hoge FE, Vodacek A, Blough N V. (1993) Inherent optical properties of the ocean: Retrieval of the absorption coefficient of chromophoric dissolved organic matter from fluorescence measurements. Limnol Oceanogr 38:1394–1402.

Hughes BB, Eby R, Van Dyke E, Tinker MT, Marks CI, Johnson KS, Wasson K (2013) Recovery of a top predator mediates negative eutrophic effects on seagrass. Proc Natl Acad Sci U S A 110:15313–15318.

James G, Witten D, Hastie T, Tibshirani R (2013) An introduction to statistical learning with applications in R. Springer, New York, NY, USA.

Jordan TE, Correll DL, Miklas J, Weller DE (1991) Long-term trends in estuarine nutrients and chlorophyll, and short- term effects of variation in watershed discharge. Mar Ecol Prog Ser 75:121–132.

Kemp WM, Batiuk RA, Bartleson R, Bergstrom PW, Carter V, Gallegos CL, Hunley W, Karrh L, Koch EW, Landwehr JM, Moore KA, Murray L, Naylor M, Rybicki NB, Stevenson JC, Wilcox DJ (2004) Habitat requirements for submerged aquatic vegetation in Chesapeake Bay: Water quality, light regime, and physical-chemical factors. Estuaries 27:363–377.

Kenworthy WJ, Gallegos CL, Costello C, Field D, di Carlo G (2014) Dependence of eelgrass (*Zostera marina*) light requirements on sediment organic matter in Massachusetts coastal bays: Implications for remediation and restoration. Mar Pollut Bull 83:446–457.

Koch EW (2001) Beyond light: Physical, geological, and geochemical parameters as possible submersed aquatic vegetation habitat requirements. Estuaries 24:1–17.

Koch EW (1999) Sediment resuspension in a shallow *Thalassia testudinum* banks ex Konig bed. Aquat Bot 65:269–280.

Krause-Jensen D, Carstensen J, Nielsen SL, Dalsgaard T, Christensen PB, Fossing H, Rasmussen MB (2011) Sea bottom characteristics affect depth limits of eelgrass *Zostera marina*. Mar Ecol Prog Ser 425:91–102.

Lavery PS, Mateo MÁ, Serrano O, Rozaimi M (2013) Variability in the carbon storage of seagrass habitats and its implications for global estimates of Blue Carbon ecosystem service. PLoS One 8:73748.

Lefcheck JS, Orth RJ, Dennison WC, Wilcox DJ, Murphy RR, Keisman J, Gurbisz C, Hannam M, Brooke Landry J, Moore KA, Patrick CJ, Testa J, Weller DE, Batiuk RA (2018) Long-term nutrient reductions lead to the unprecedented recovery of a temperate coastal region. Proc Natl Acad Sci U S A 115:3658–3662.

Lloyd S (2014) Nitrogen load modeling to forty-three subwatersheds of the Peconic Estuary. The Nature Conservancy. Final Report.

NYS Seagrass Taskforce (2009) Final Report of the New York State Seagrass Task Force: Recommendations to the New York State Governor and Legislature. 1–69.

Organelli E, Bricaud A, Antoine D, Matsuoka A (2014) Seasonal dynamics of light absorption by chromophoric dissolved organic matter (CDOM) in the NW Mediterranean Sea (BOUSSOLE site). Deep Res Part I Oceanogr Res Pap 91:72–85.

Orth RJ, Carruthers TJB, Dennison WC, Duarte CM, Fourqurean JW, Heck KL, Hughes RA, Kendrick GA, Kenworthy WJ, Olyarnik S, Short FT, Waycott M, Williams SL (2006) A global crisis for seagrass ecosystems. Bioscience 56:987–996.

Pickerell C, Schott S (2015) Peconic Estuary Program 2015 long-term eelgrass (*Zostera marina*) monitoring program. Marine Program Cornell Cooperative Extension prepared for the Peconic Estuary Program. Report 16.

Pickerell C, Schott S (2017) Peconic Estuary Program 2016 long-term eelgrass (*Zostera marina*) monitoring program. Marine Program Cornell Cooperative Extension prepared for the Peconic Estuary Program. Report 17.

Reynolds LK, Waycott M, McGlathery KJ, Orth RJ (2016) Ecosystem services returned through seagrass restoration. Restor Ecol 24:583–588.

Rochelle-Newall E, Hulot FD, Janeau JL, Merroune A (2014) CDOM fluorescence as a proxy of DOC concentration in natural waters: A comparison of four contrasting tropical systems. Environ Monit Assess 186:589–596.

Schaefer S (2017) Peconic Estuary State of the Bay. Peconic Estuary Program.

Short FT, Muehlstein LK, Porter D (1987) Eelgrass wasting disease: Cause and recurrence of a marine epidemic. Biol Bull 173:557–562.

Stevenson JC, Staver LW, Staver KW (1993) Water quality associated with survival of submersed aquatic vegetation along an estuarine gradient. Estuaries 16:346–361.

Tettelbach ST, Peterson BJ, Carroll JM, Furman BT, Hughes SWT, Havelin J, Europe JR, Bonal DM, Weinstock AJ, Smith CF (2015) Aspiring to an altered stable state: Rebuilding of bay scallop populations and fisheries following intensive restoration. Mar Ecol Prog Ser 529:121–136.

Thayer GW (1974) Identity and regulation of nutrients limiting phytoplankton production in the shallow estuaries near Beaufort, N.C. Oecologia 14:75–92.

Uhrin A V., Turner MG (2018) Physical drivers of seagrass spatial configuration: the role of thresholds. Landsc Ecol 33:2253–2272.

USEPA (1999) Total Suspended Solids (TSS) EPA Method 160.2 (Gravimetric, Dried at 103-105 E C). US Environmental Protection Agency, Washington, DC.

Ward LG, Michael Kemp W, Boynton WR (1984) The influence of waves and seagrass communities on suspended particulates in an estuarine embayment. Mar Geol 59:85–103.

Zimmerman RC, Hill VJ, Gallegos CL (2015) Predicting effects of ocean warming, acidification, and water quality on Chesapeake region eelgrass. Limnol Oceanogr 60:1781–1804.

Zimmerman RC, Smith RD, Alberte RS (1989) Thermal acclimation and whole-plant carbon balance in *Zostera marina* L. (eelgrass). J Exp Mar Bio Ecol 130:93–109.

FIGURES

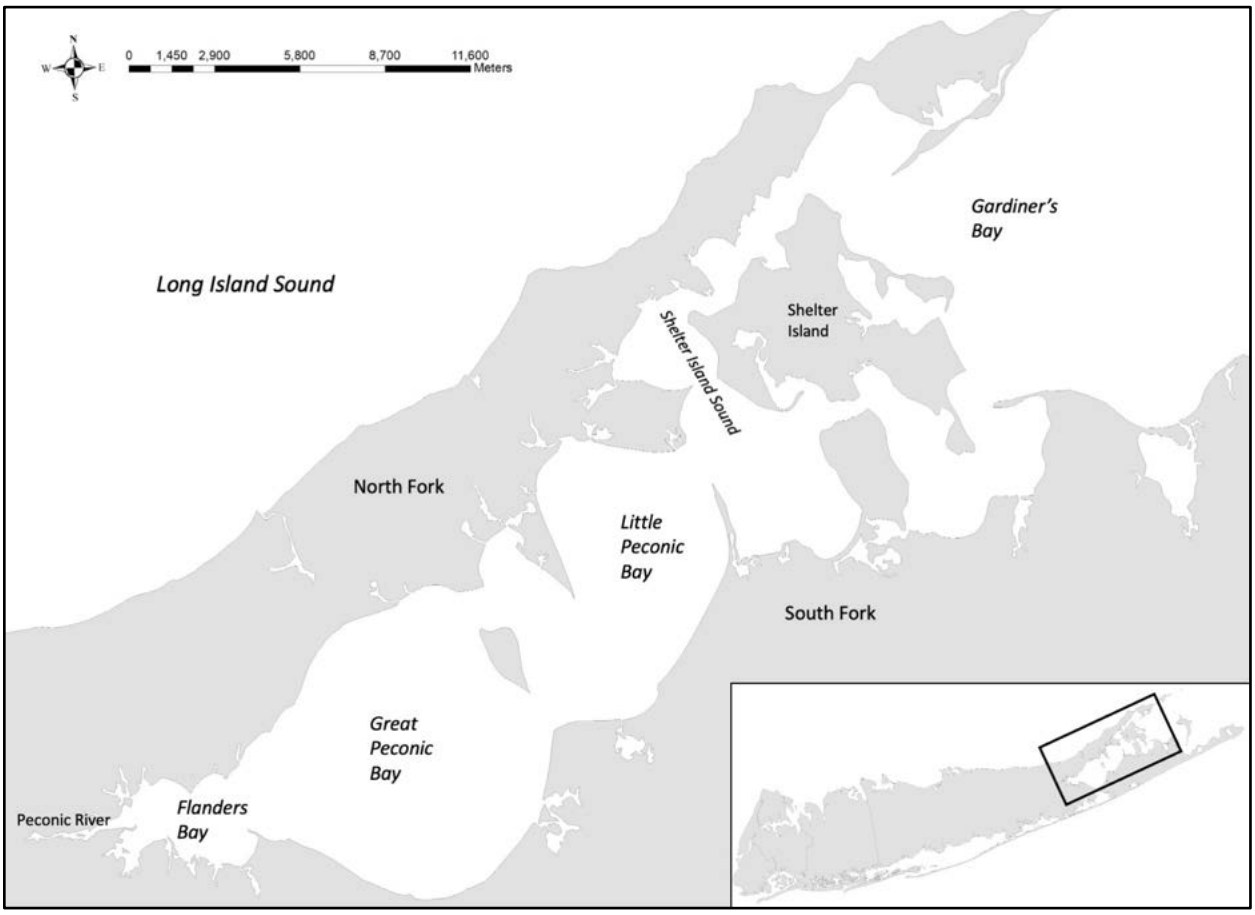

Figure 1: Peconic Bay, Long Island, NY.

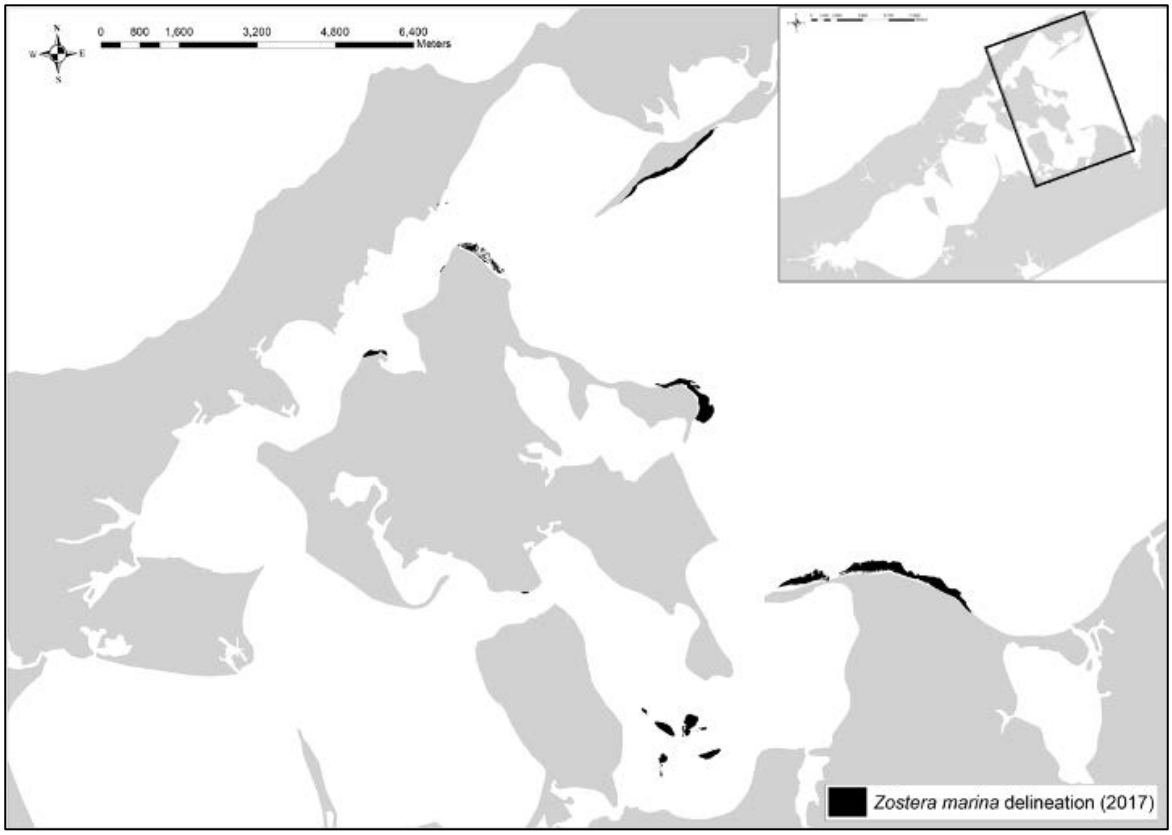

Figure 2: *Z. marina* extent in Peconic Bay delineated from 2017 orthoimagery.

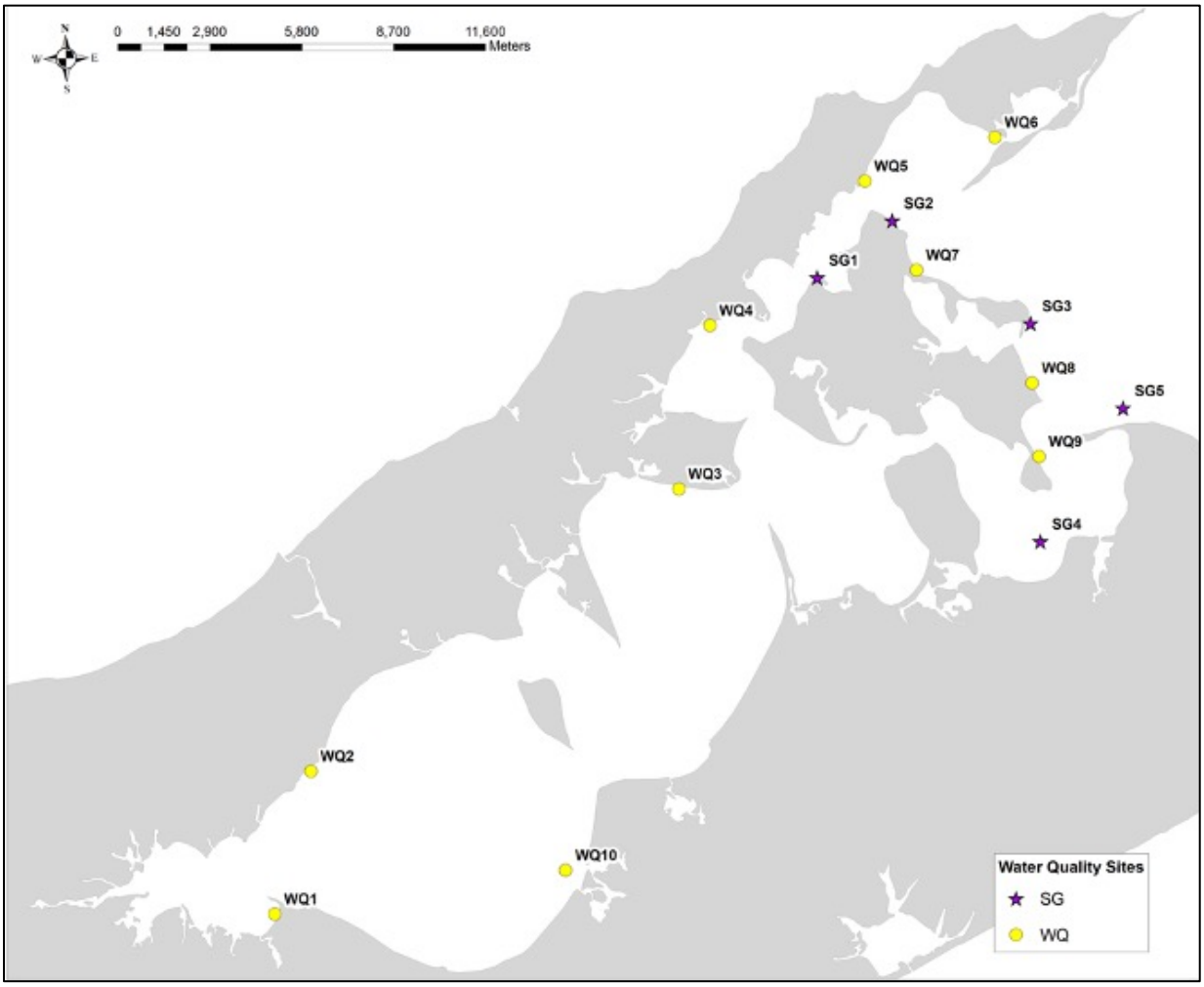

Figure 3: Water quality sampling locations in Peconic Bay for 2017 and 2018. Type indicates whether sampling occurred at *Z. marina* (SG) or non- *Z. marina* (WQ) sites.

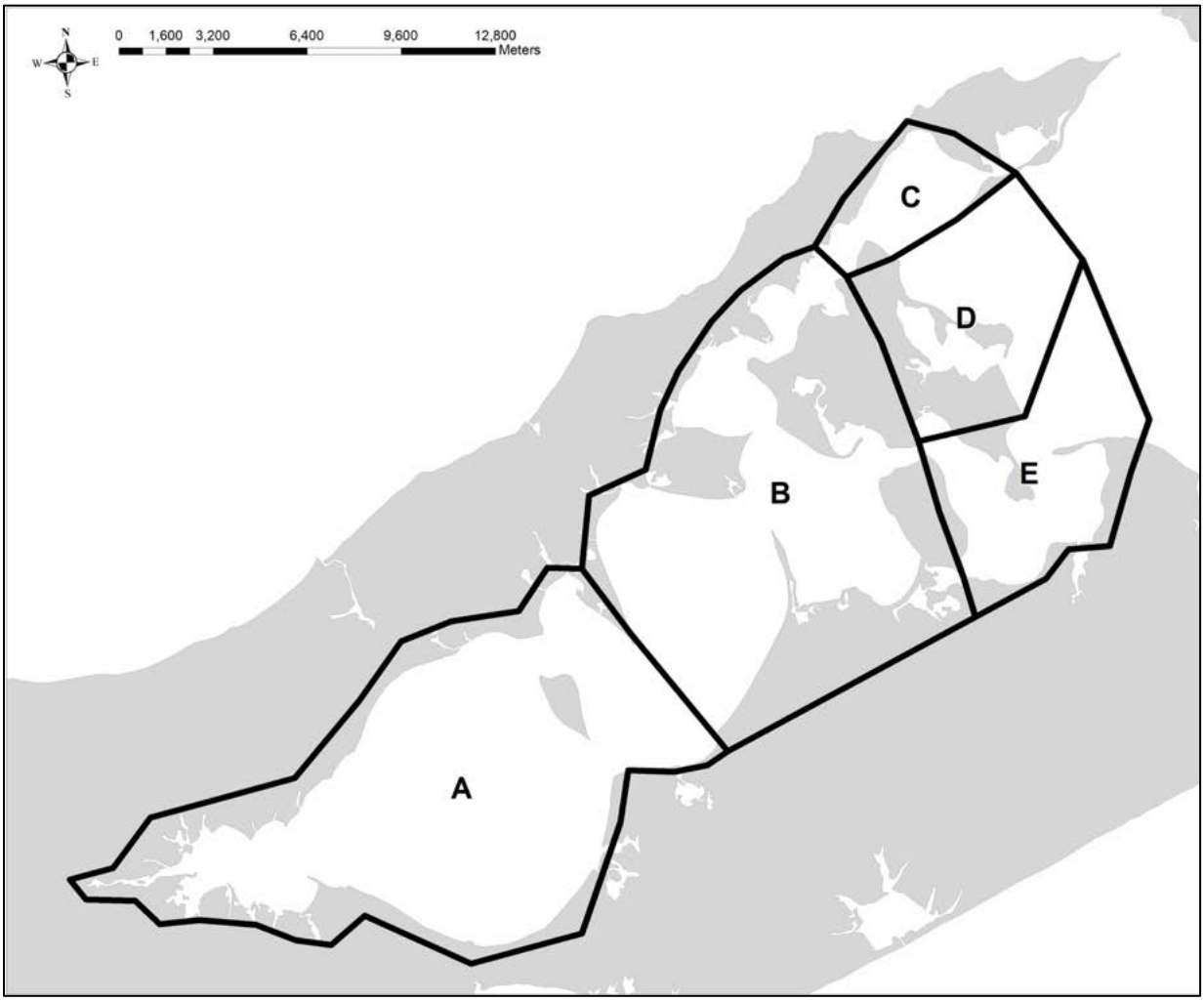

Figure 4: Grouping designations (A-E) for water quality sampling locations in Peconic Bay for 2017 and 2018.

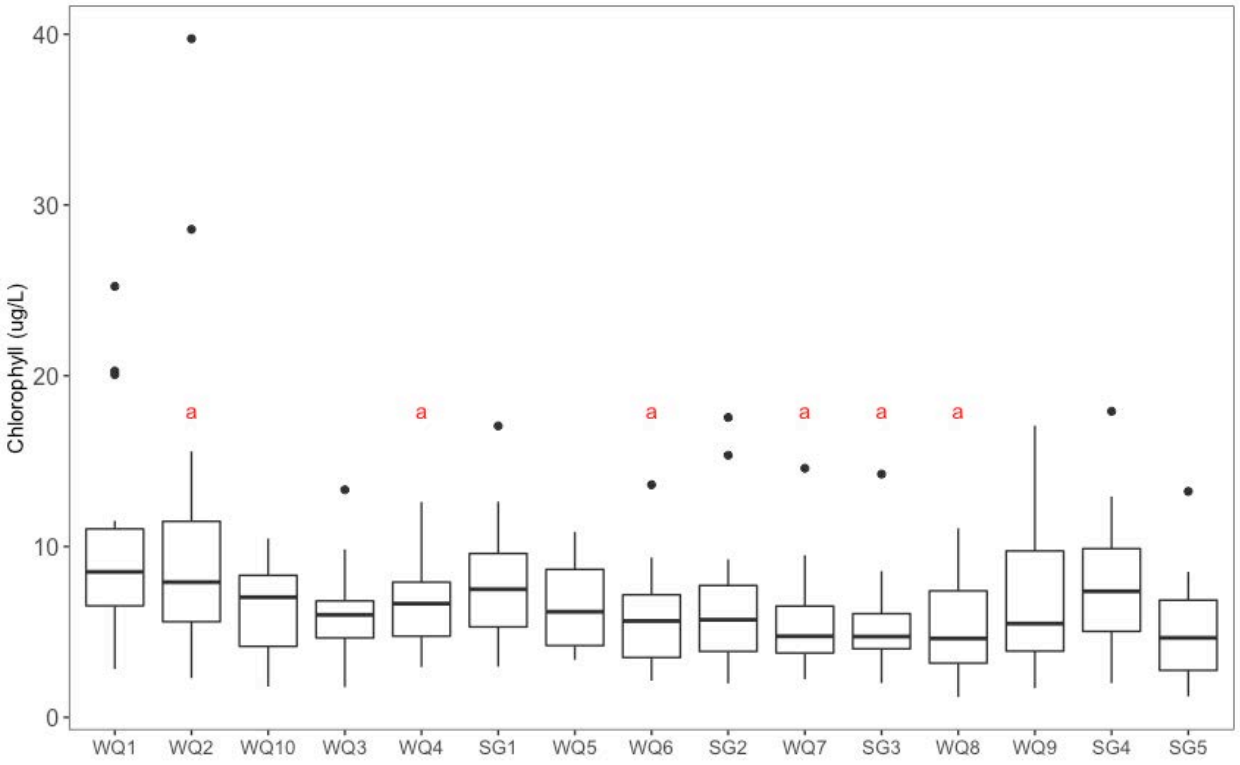

Figure 5: Boxplot of chlorophyll concentrations (µg/L) at individual sites. ANOVA was run to determine significance between sites (F-value=2.565, df=14) followed by a Tukey HSD test. Red "a" denotes a significant difference in concentrations between that site and WQ2.

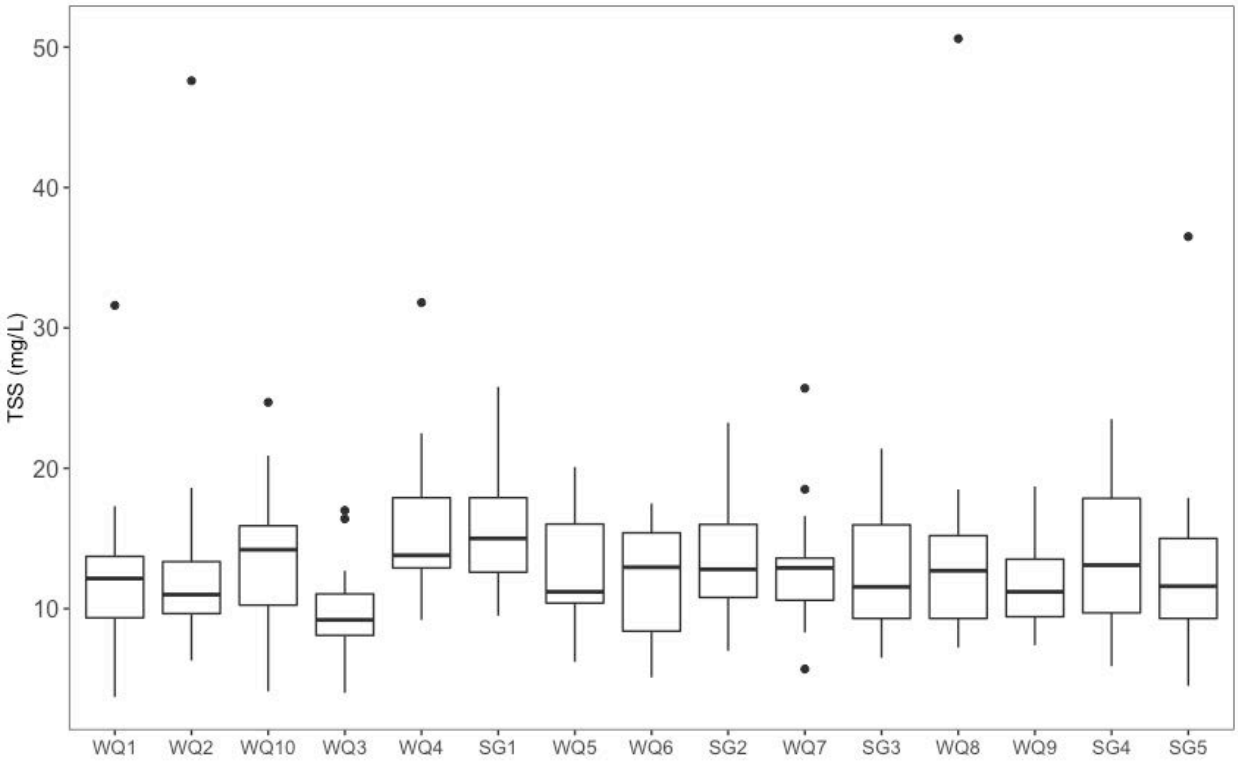

Figure 6: Boxplot of TSS concentrations (mg/L) at individual sites. ANOVA was run to determine significance between sites (F-value=1.064, df=14).

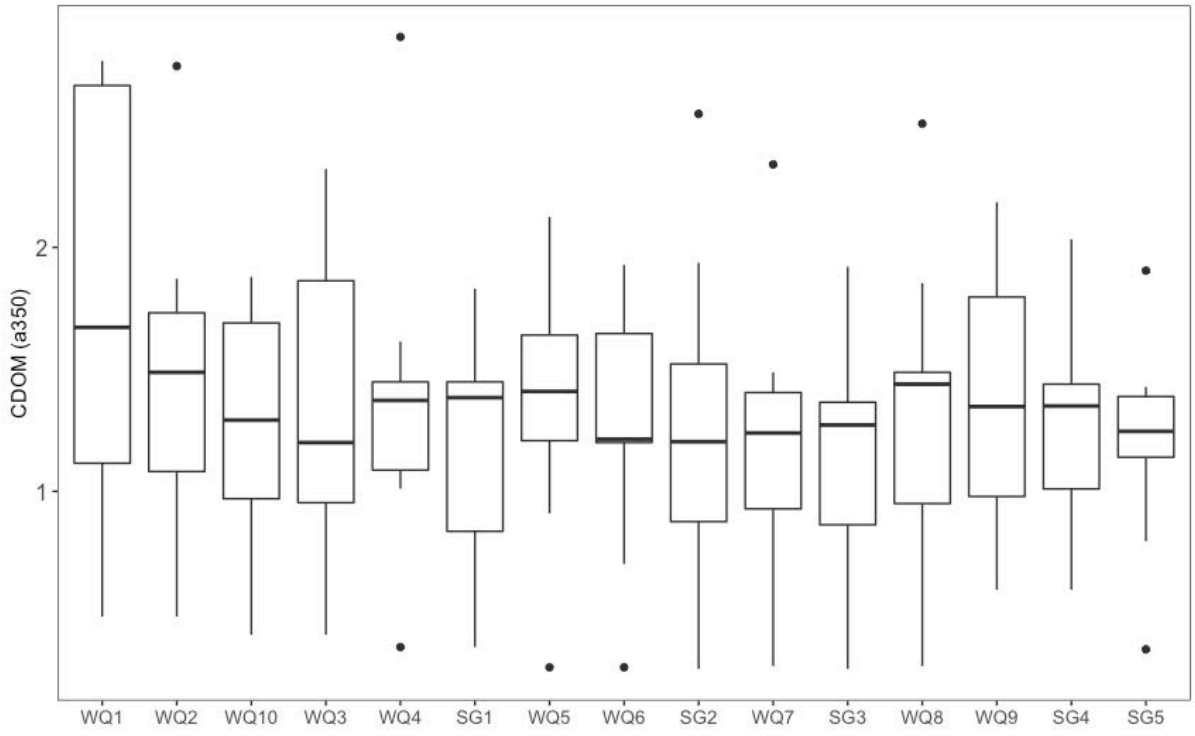

Figure 7: Boxplot of CDOM absorptions at 350nm (m^{-1}) at individual sites. ANOVA was run to determine significance between sites (F-value=0.55, df=14).

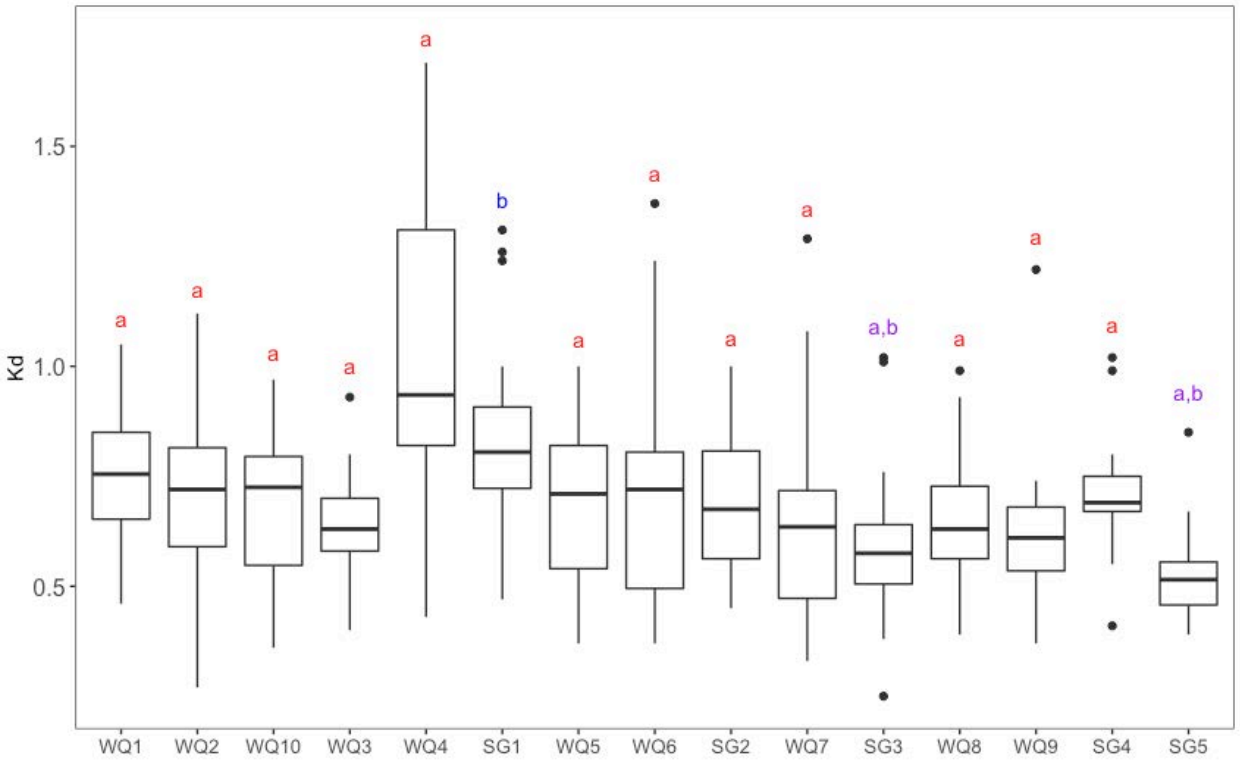

Figure 8: Boxplot of K_d (m^{-1}) at individual sites. ANOVA was run to determine significance between sites (F-value=5.542, df=14) followed by a Tukey HSD test. Red "a" denotes a significant difference in concentrations between that site and WQ4, blue "b" between SG1 and that site, and purple "a, b" denotes statistical differences between that site and WQ4 and SG1.

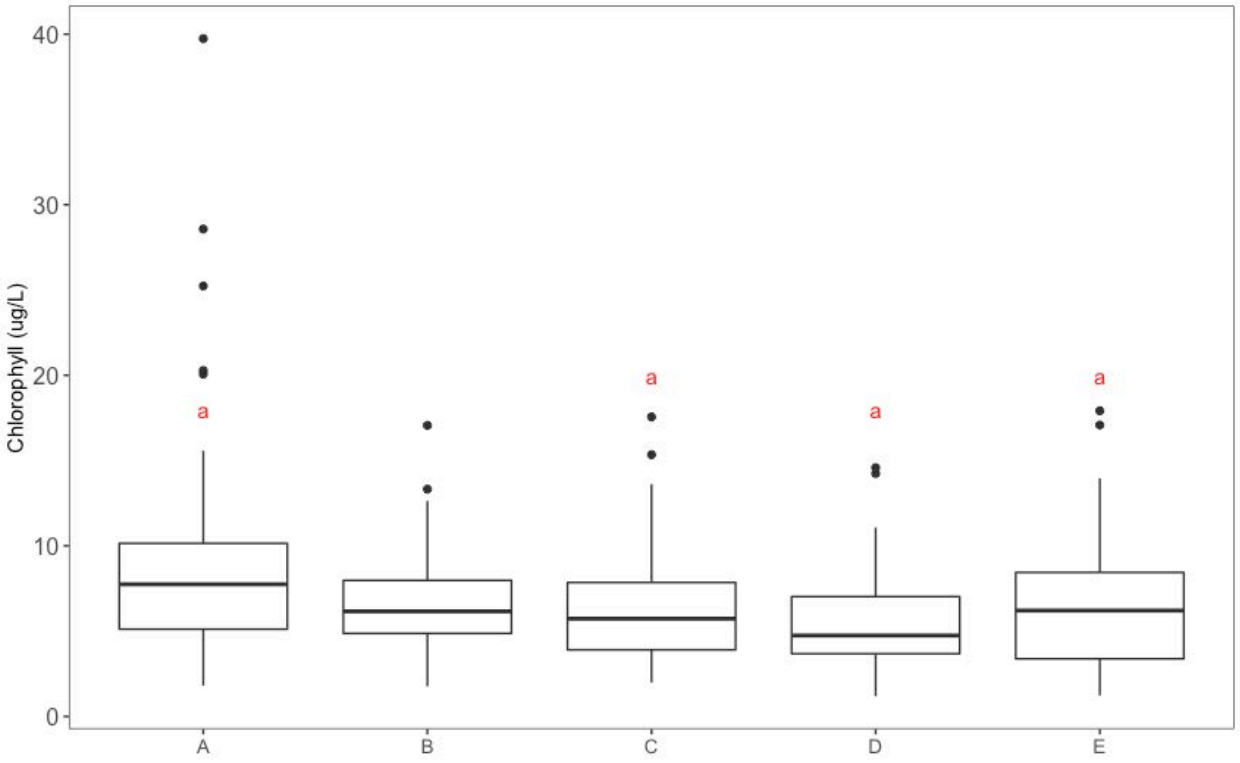

Figure 9: Boxplot of chlorophyll concentrations (µg/L) for each region. ANOVA was run to determine significance between sites (F-value=4.965, df=4) followed by a Tukey HSD test. Red "a" denotes a significant difference in concentrations between that region and region A.

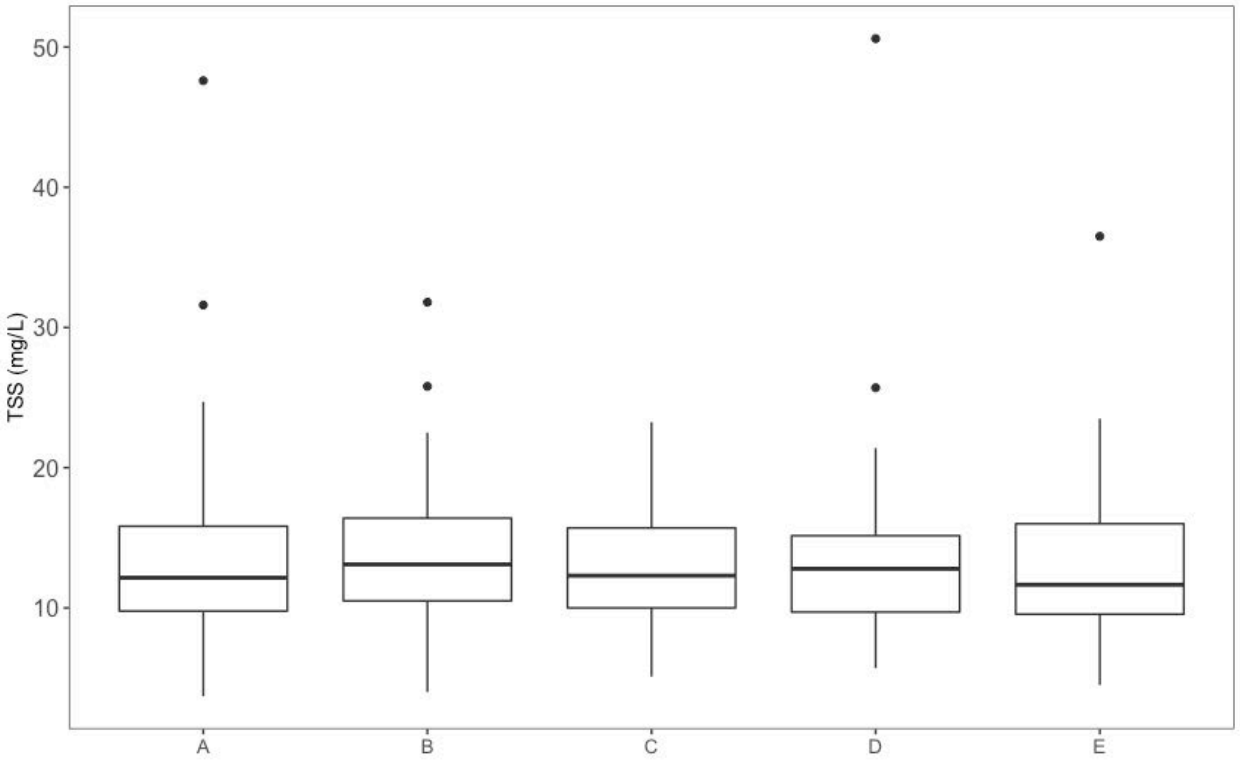

Figure 10: Boxplot of TSS concentrations (mg/L) for each region. ANOVA was run to determine significance between sites (F-value=0.239, df=4).

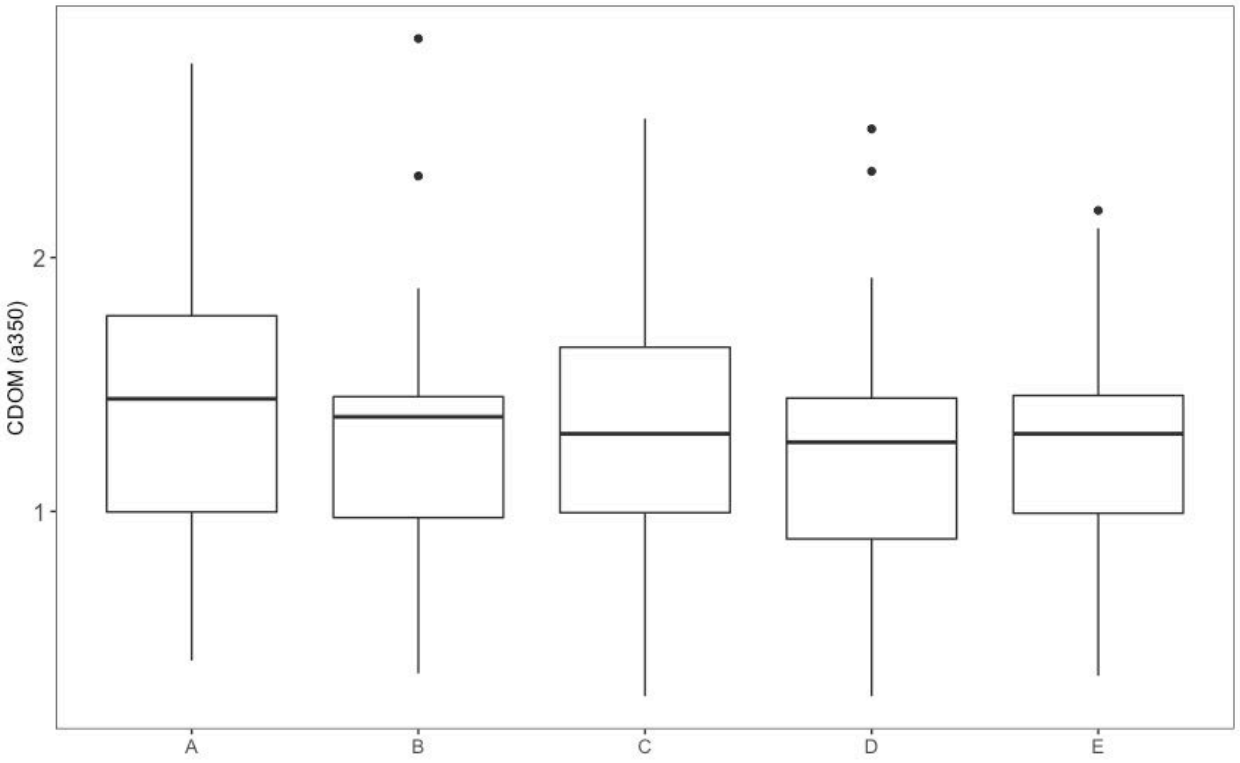

Figure 11: Boxplot of CDOM absorptions at 350nm (m^{-1}) for each region. ANOVA was run to determine significance between sites (F-value=0.85, df=4).

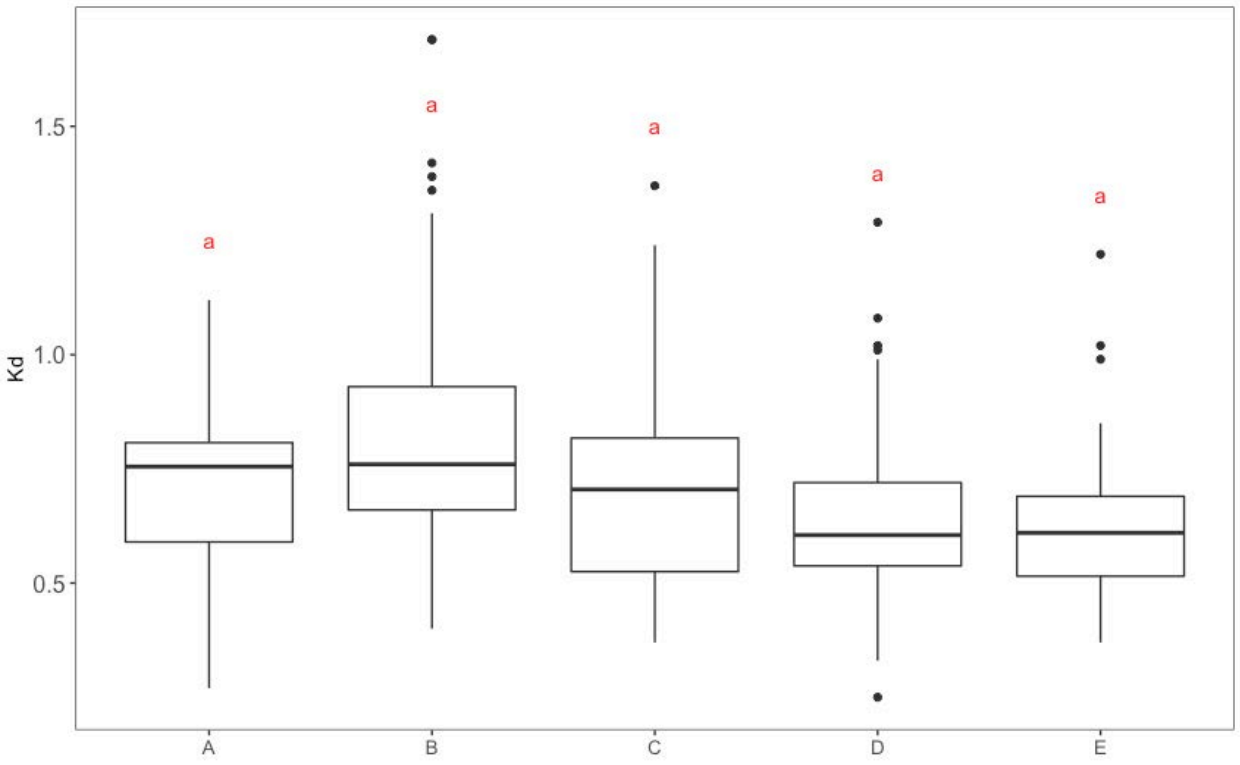

Figure 12: Boxplot of K_d (m^{-1}) for each region. ANOVA was run to determine significance between sites (F-value=8.187, df=4) followed by a Tukey HSD test. Red "a" denotes a significant difference in concentrations between that region and region B.

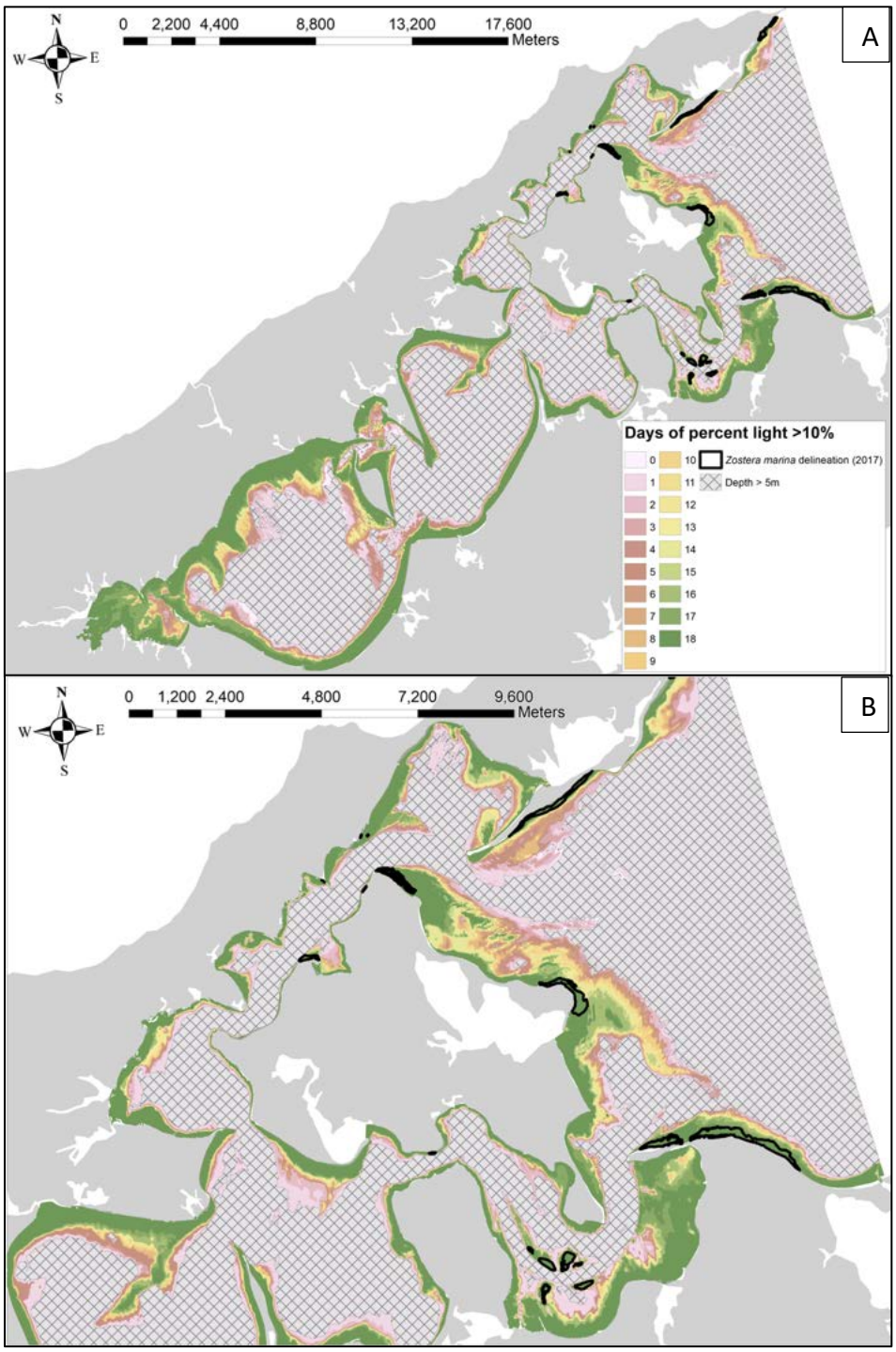

Figure 13: Days over PLW > 10% calculated from K_d and bathymetry. Depths > 5m were excluded (hash) due to low light levels and no *Z. marina* growing deeper than 4.5m at MLW. (A) All of Peconic Bay, (B) close-up.

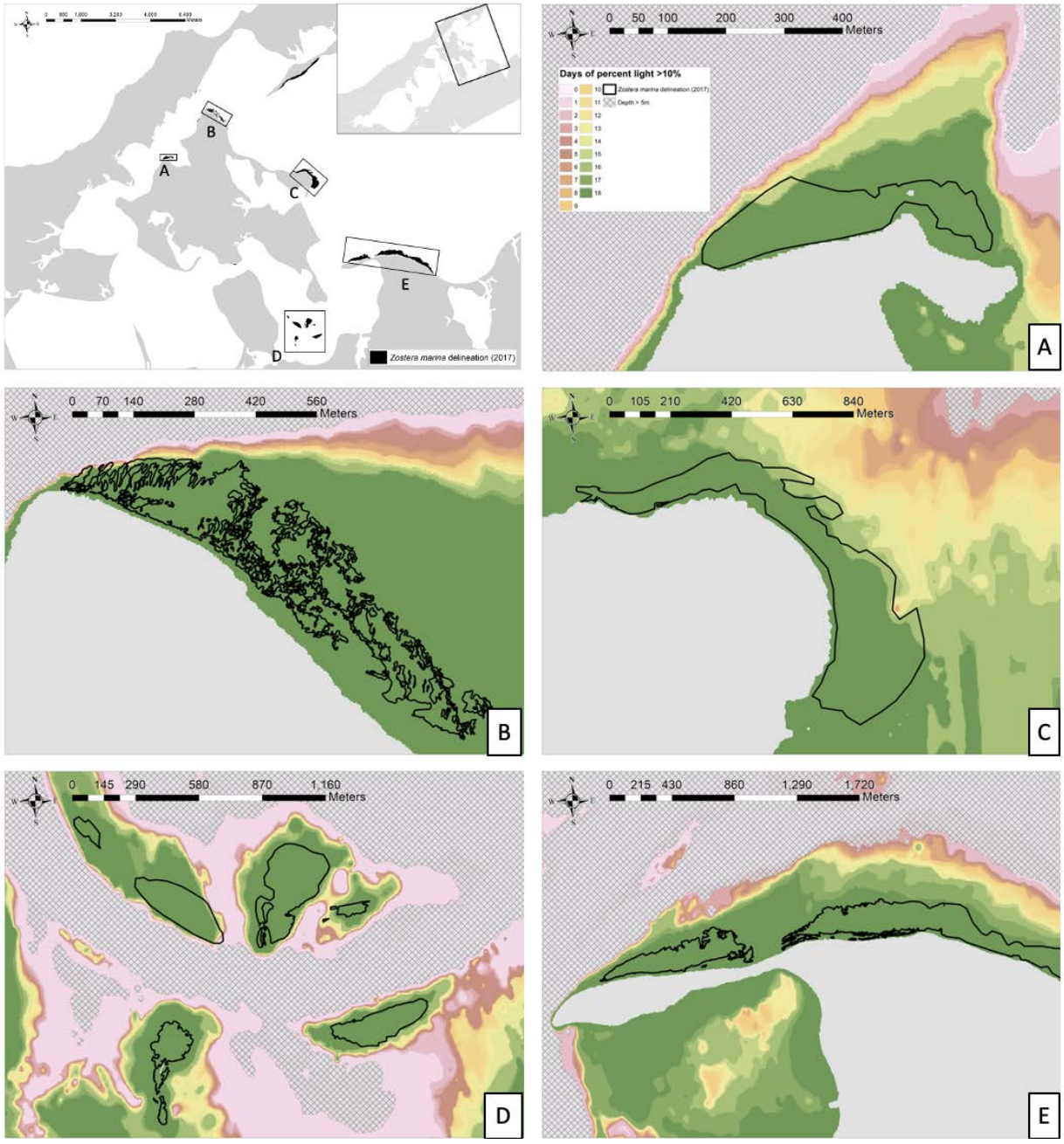

Figure 14: Days over PLW > 10% at *Z. marina* beds, (A) SG1, (B) SG2, (C) SG3, (D) SG4, (E) SG5, calculated from K_d and bathymetry. Depths > 5m were excluded (hash) due to low light levels and no *Z. marina* growing deeper than 4.5m at MLW.

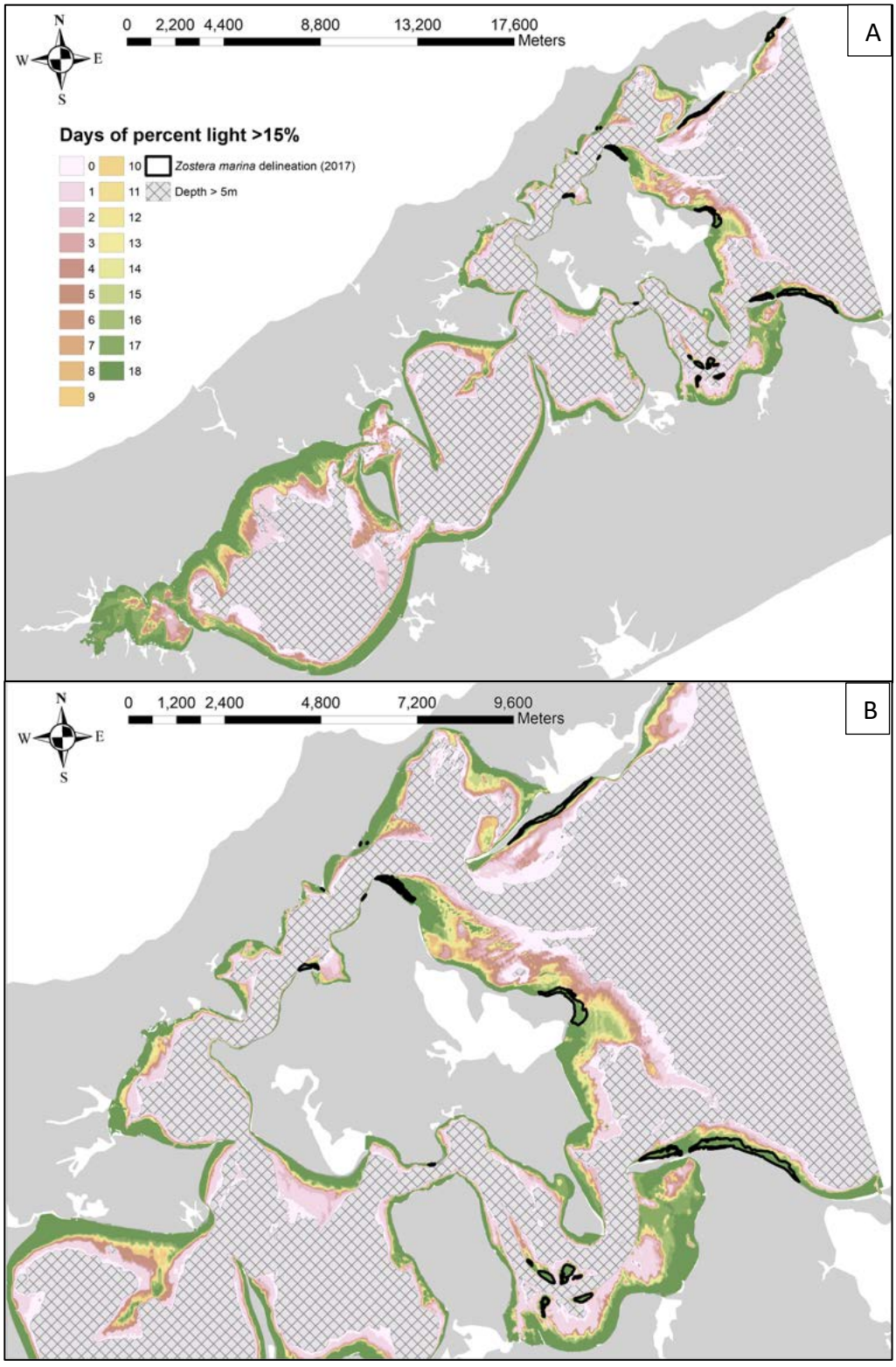

Figure 15: Days over PLW > 15% calculated from K_d and bathymetry. Depths > 5m were excluded (hash) due to low light levels and no *Z. marina* growing deeper than 4.5m at MLW. (A) All of Peconic Bay, (B) close-up.

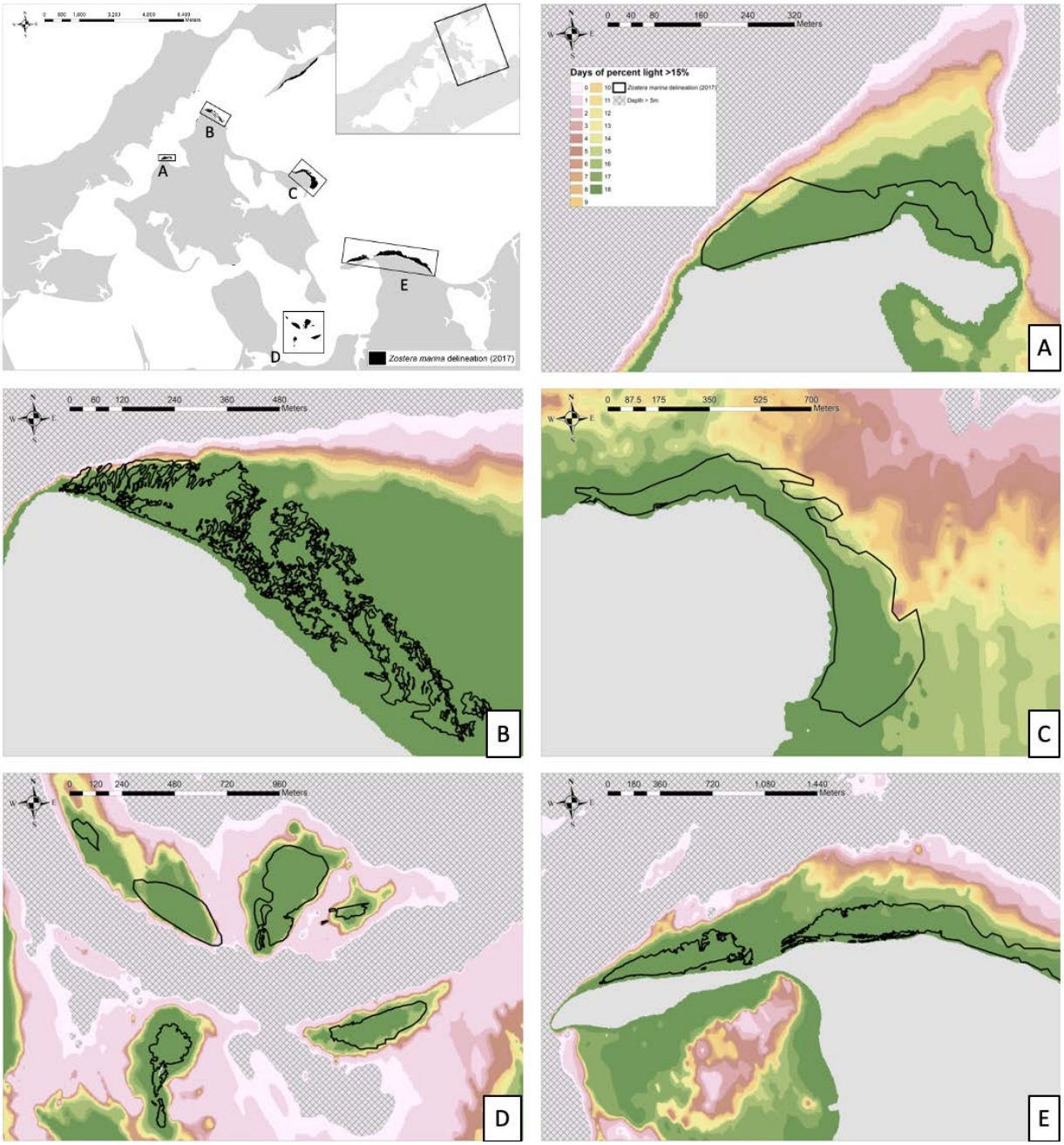

Figure 16: Days over PLW > 15% at *Z. marina* beds, (A) SG1, (B) SG2, (C) SG3, (D) SG4, (E) SG5, calculated from K_d and bathymetry. Depths > 5m were excluded (hash) due to low light levels and no *Z. marina* growing deeper than 4.5m at MLW.

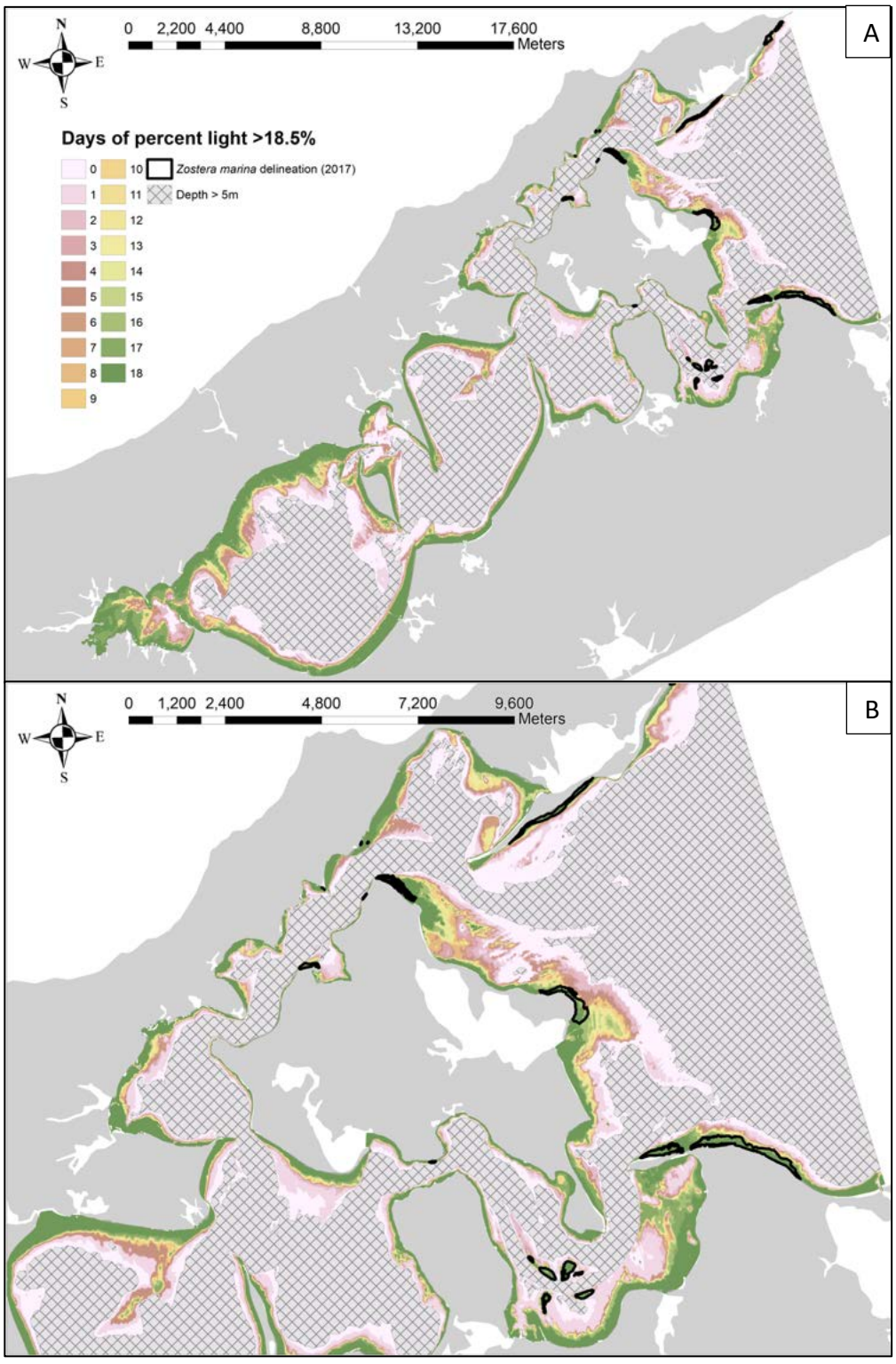

Figure 17: Days over PLW > 18.5% calculated from K_d and bathymetry. Depths > 5m were excluded (hash) due to low light levels and no *Z. marina* growing deeper than 4.5m at MLW. (A) All of Peconic Bay, (B) close-up.

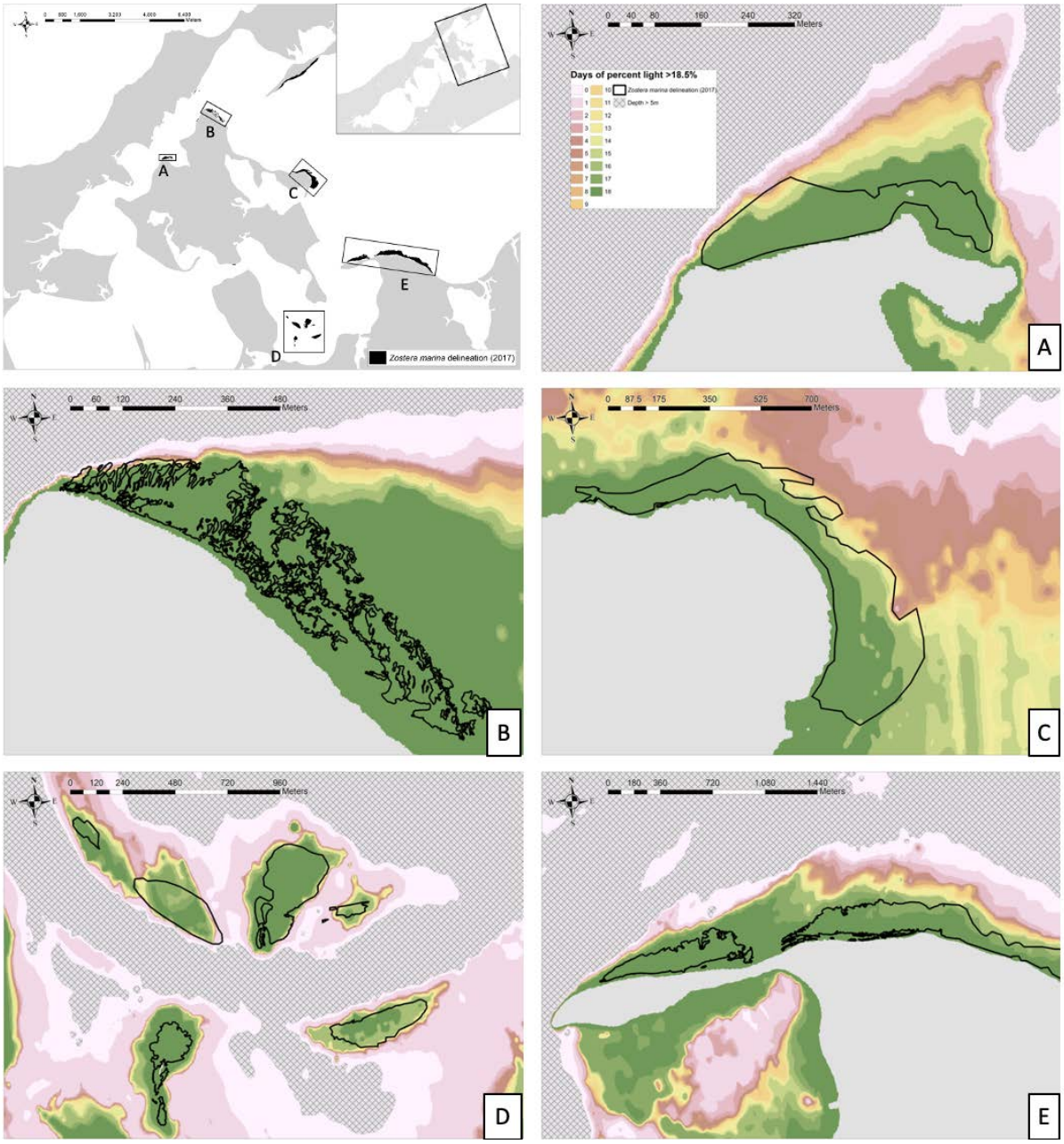

Figure 18: Days over PLW > 18.5% at *Z. marina* beds, (A) SG1, (B) SG2, (C) SG3, (D) SG4, (E) SG5, calculated from K_d and bathymetry. Depths > 5m were excluded (hash) due to low light levels and no *Z. marina* growing deeper than 4.5m at MLW.

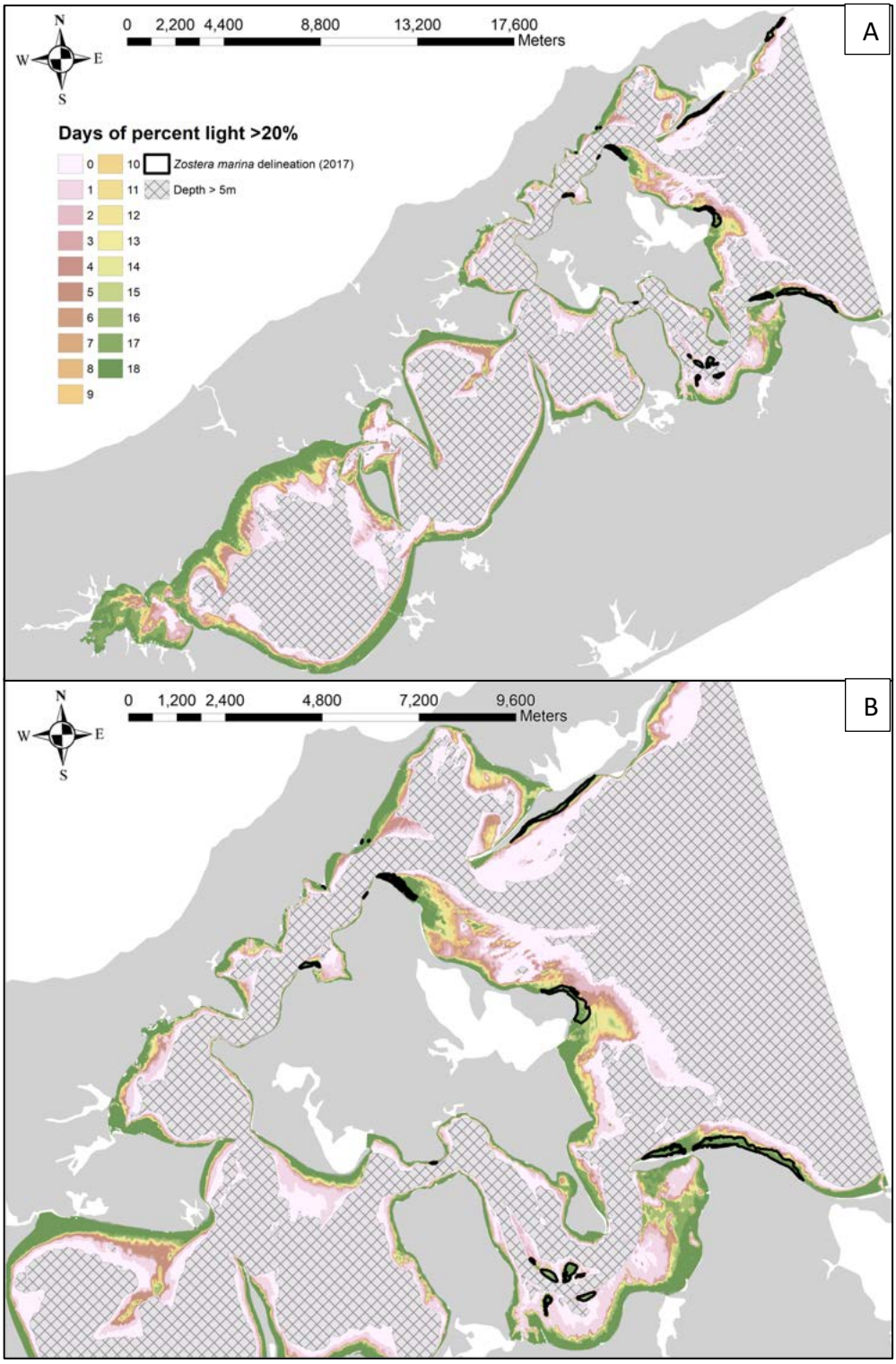

Figure 19: Days over PLW > 20% calculated from K_d and bathymetry. Depths > 5m were excluded (hash) due to low light levels and no *Z. marina* growing deeper than 4.5m at MLW. (A) All of Peconic Bay, (B) close-up.

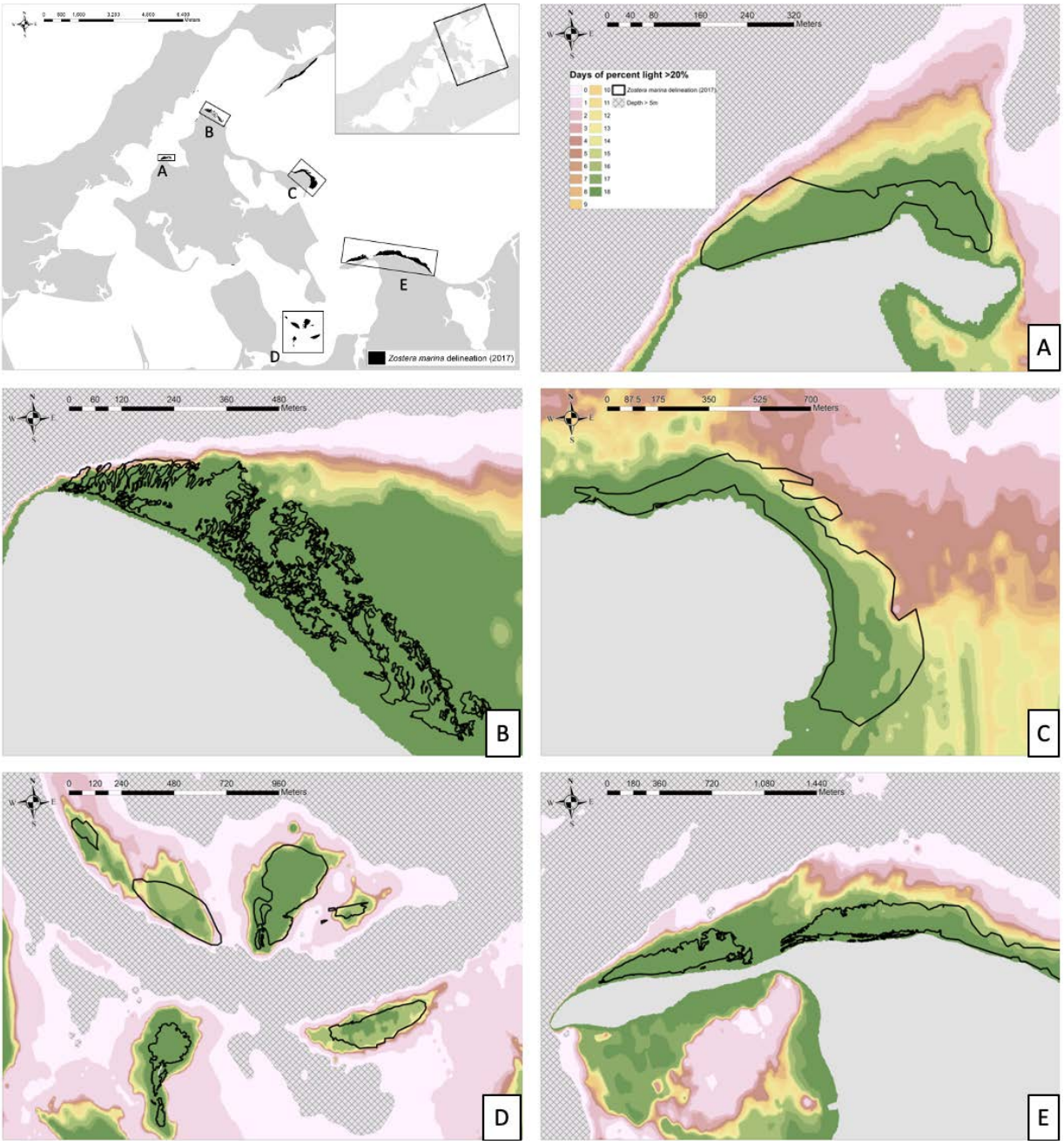

Figure 20: Days over PLW > 20% at *Z. marina* beds, (A) SG1, (B) SG2, (C) SG3, (D) SG4, (E) SG5, calculated from K_d and bathymetry. Depths > 5m were excluded (hash) due to low light levels and no *Z. marina* growing deeper than 4.5m at MLW.

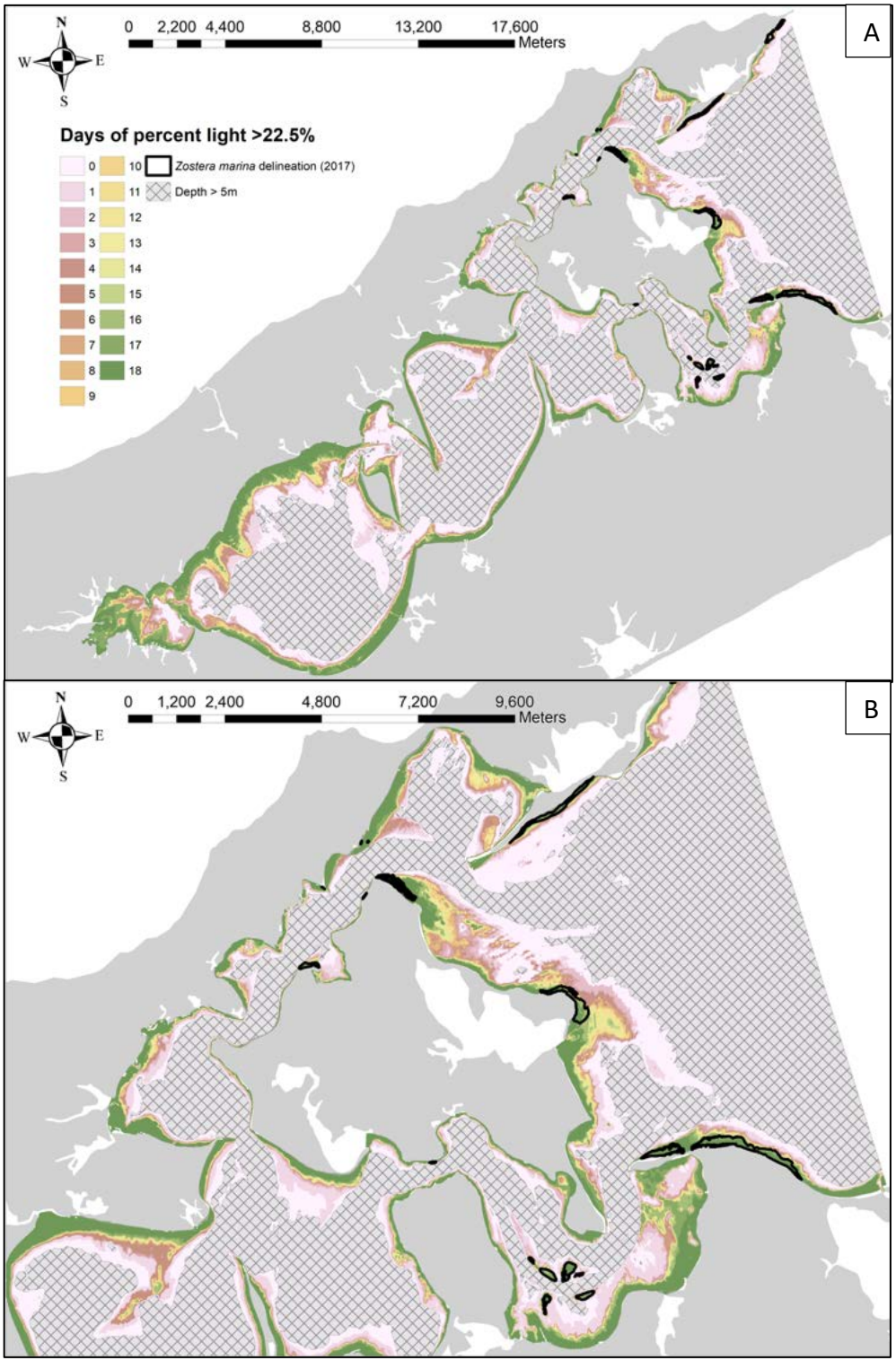

Figure 21: Days over PLW > 22.5% calculated from K_d and bathymetry. Depths > 5m were excluded (hash) due to low light levels and no *Z. marina* growing deeper than 4.5m at MLW. (A) All of Peconic Bay, (B) close-up.

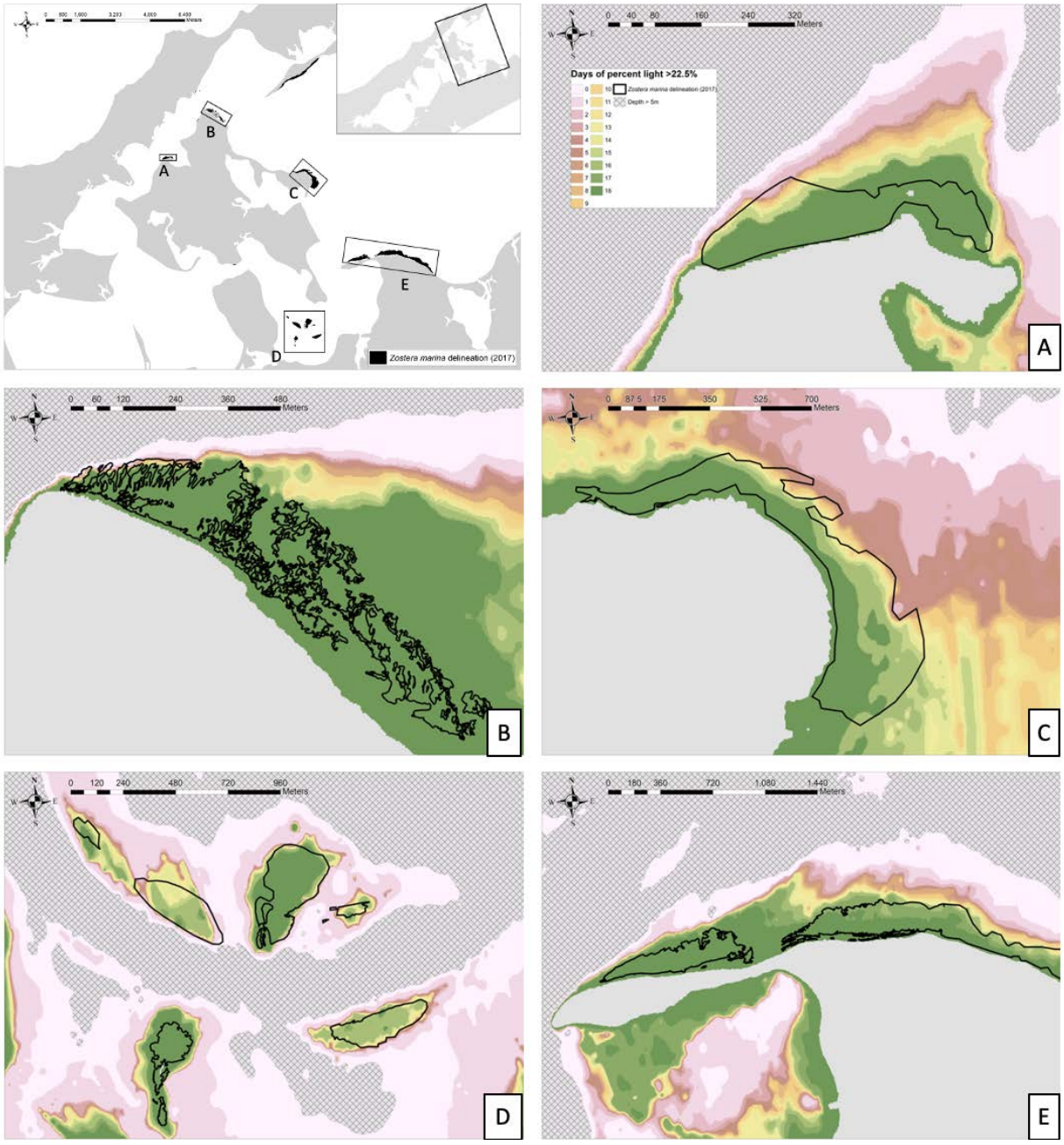

Figure 22: Days over PLW > 22.5% at *Z. marina* beds, (A) SG1, (B) SG2, (C) SG3, (D) SG4, (E) SG5, calculated from K_d and bathymetry. Depths > 5m were excluded (hash) due to low light levels and no *Z. marina* growing deeper than 4.5m at MLW.

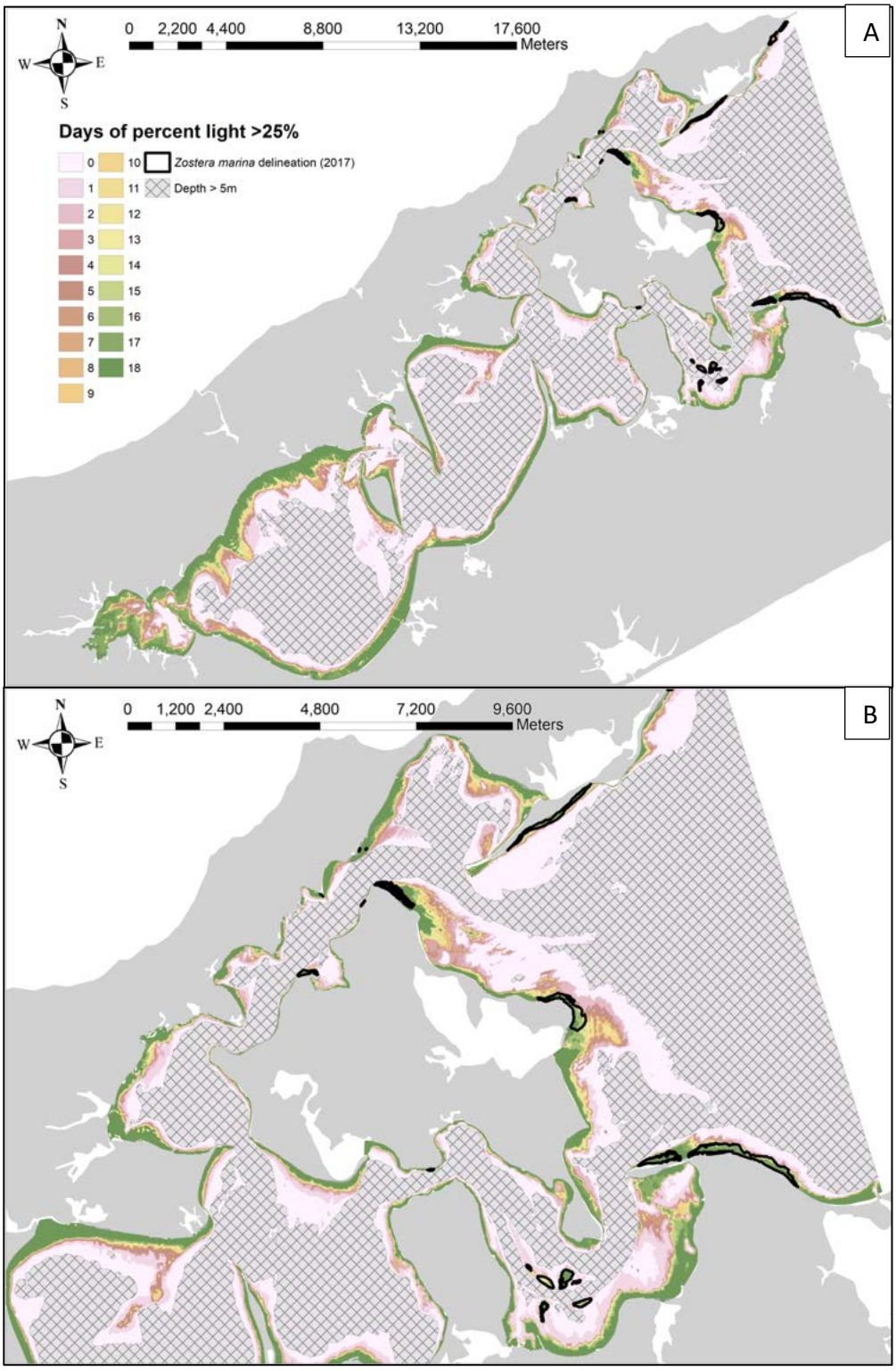

Figure 23: Days over PLW > 25% calculated from K_d and bathymetry. Depths > 5m were excluded (hash) due to low light levels and no *Z. marina* growing deeper than 4.5m at MLW. (A) All of Peconic Bay, (B) close-up.

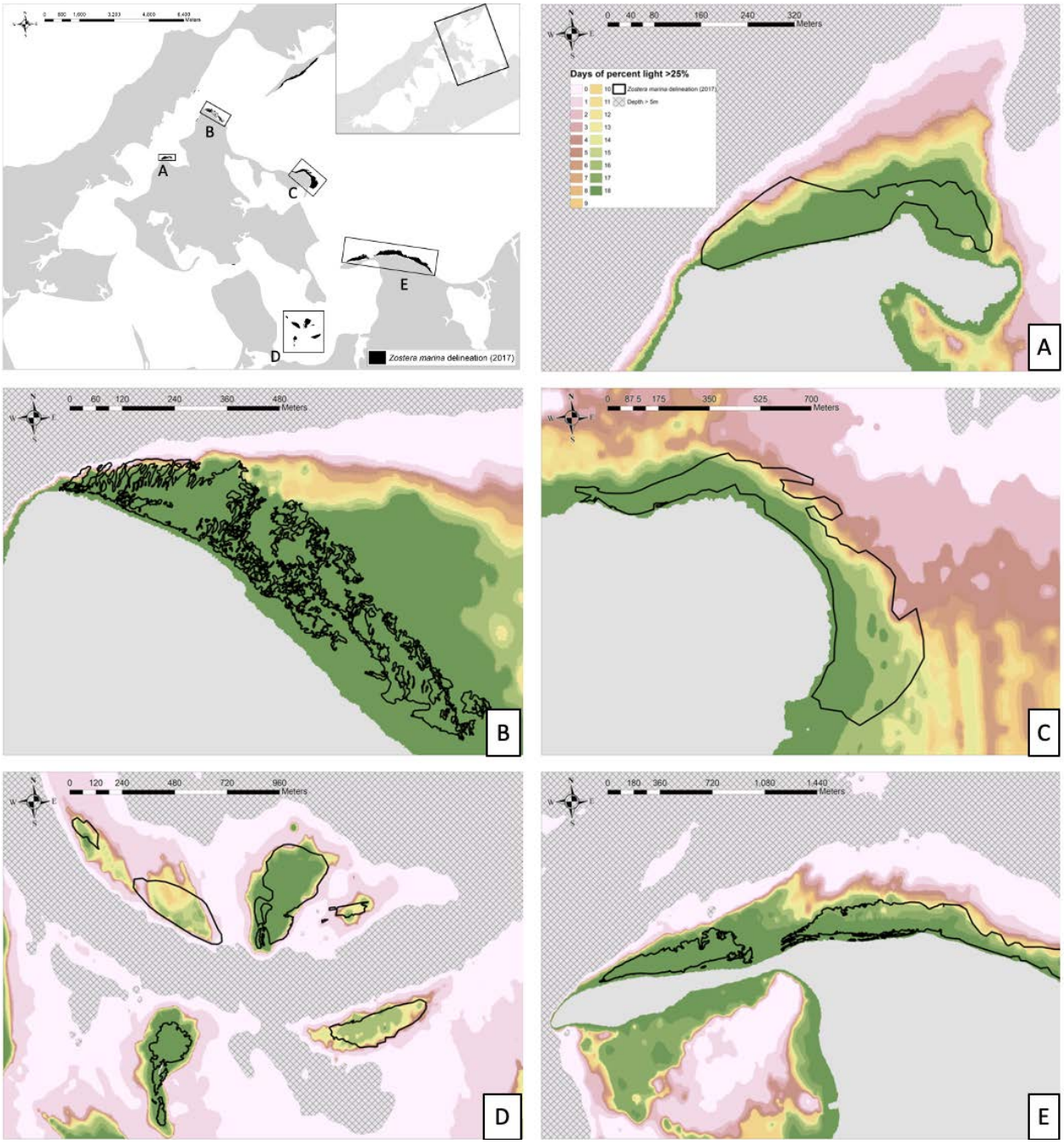

Figure 24: Days over PLW > 25% at *Z. marina* beds, (A) SG1, (B) SG2, (C) SG3, (D) SG4, (E) SG5, calculated from K_d and bathymetry. Depths > 5m were excluded (hash) due to low light levels and no *Z. marina* growing deeper than 4.5m at MLW.

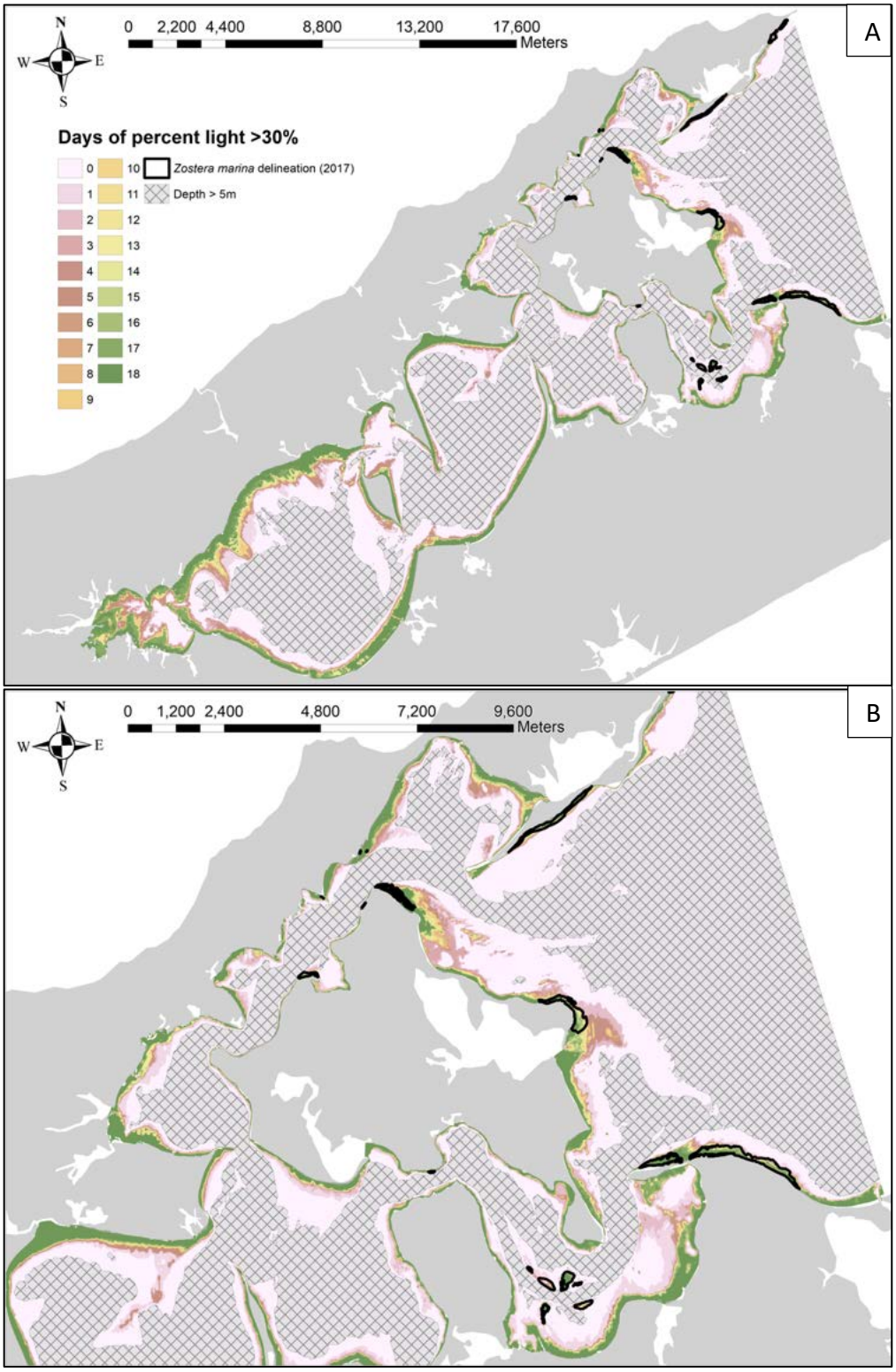

Figure 25: Days over PLW > 30% calculated from K_d and bathymetry. Depths > 5m were excluded (hash) due to low light levels and no *Z. marina* growing deeper than 4.5m at MLW. (A) All of Peconic Bay, (B) close-up.

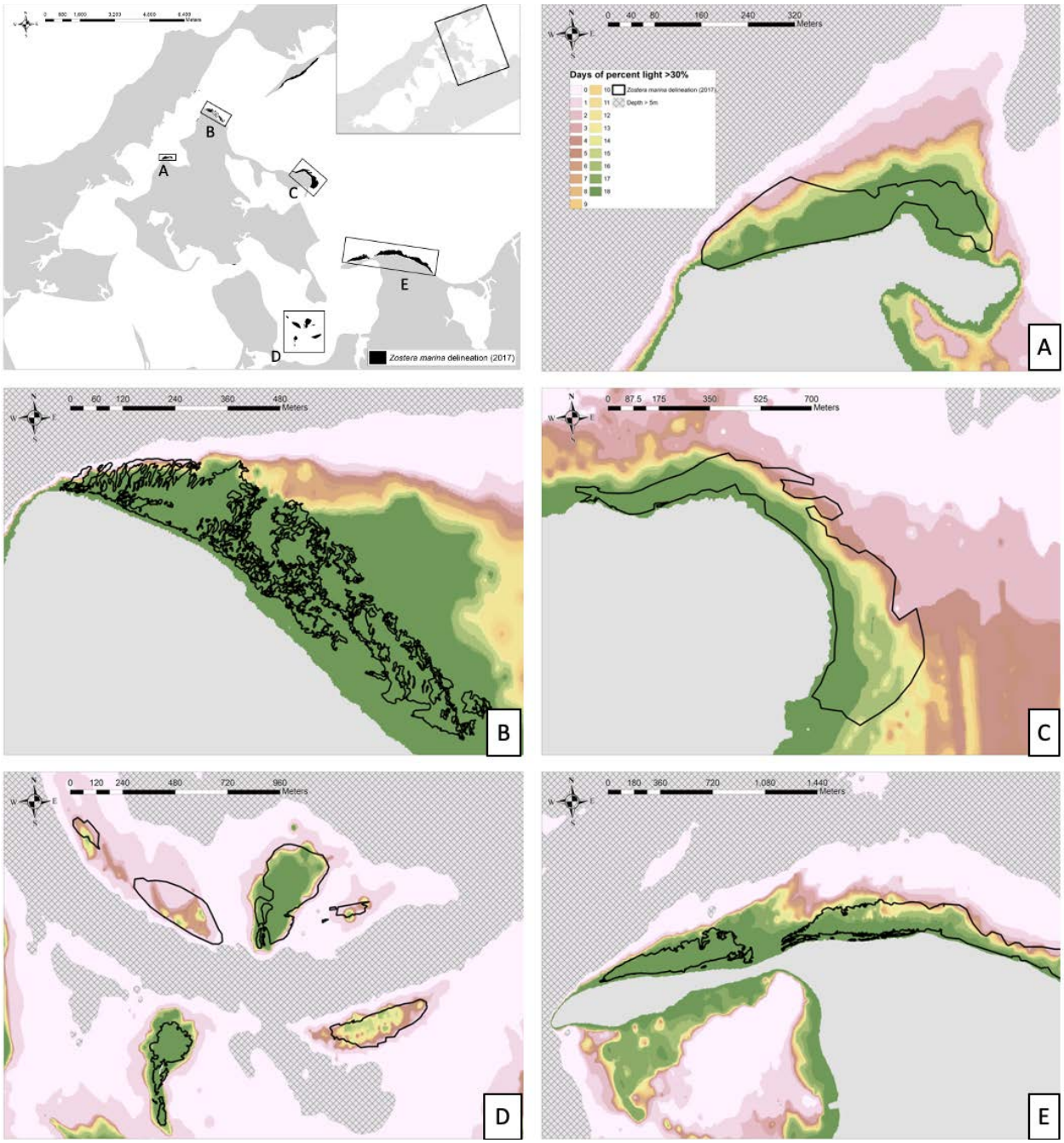

Figure 26: Days over PLW > 30% at *Z. marina*, (A) SG1, (B) SG2, (C) SG3, (D) SG4, (E) SG5, calculated from K_d and bathymetry. Depths > 5m were excluded (hash) due to low light levels and no *Z. marina* growing deeper than 4.5m at MLW.

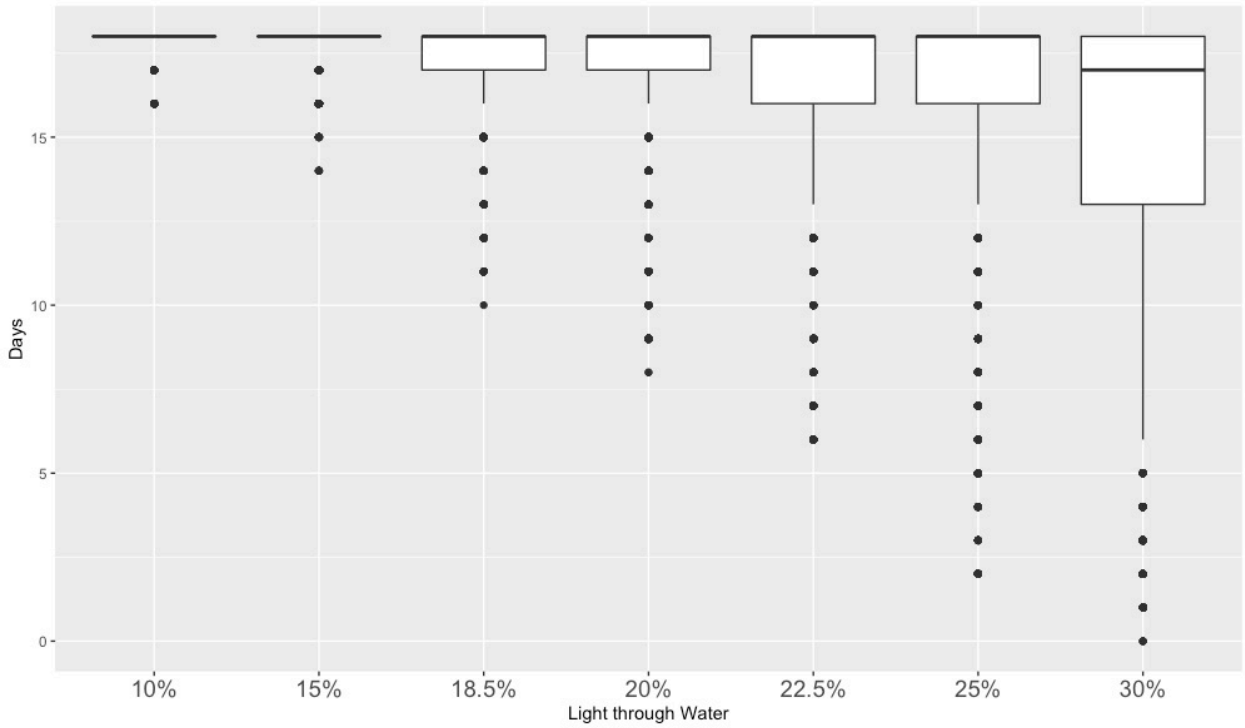

Figure 27: Days over each threshold of percent light through water (PLW) for points with *Z. marina* (5,000) in Peconic Bay.

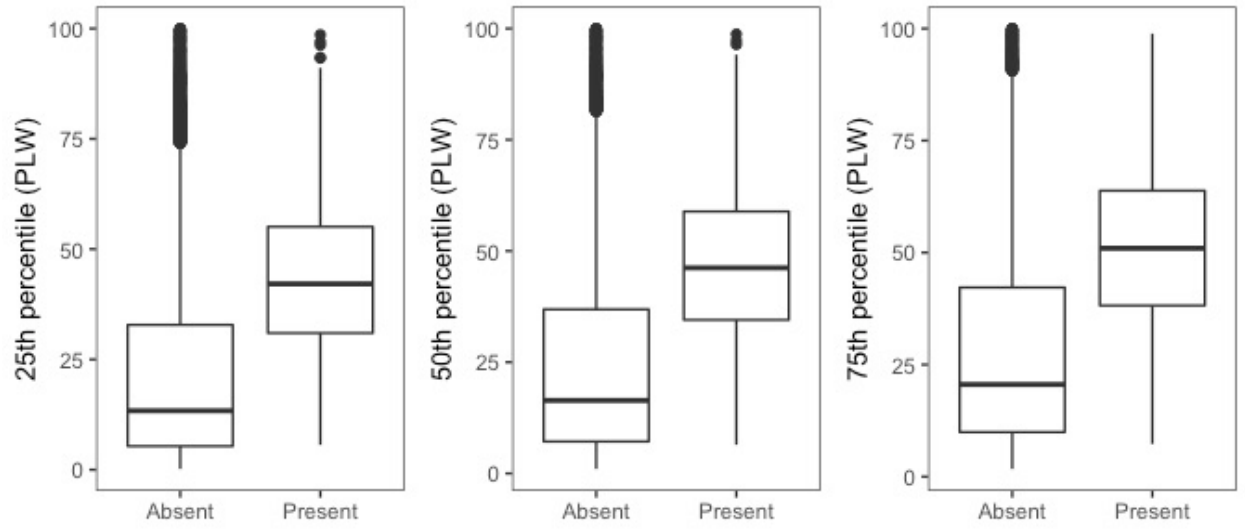

Figure 28: Median, 25th and 75th percentile PLW values for present (5,000) and absent (45,000) *Z. marina* points in Peconic Bay.

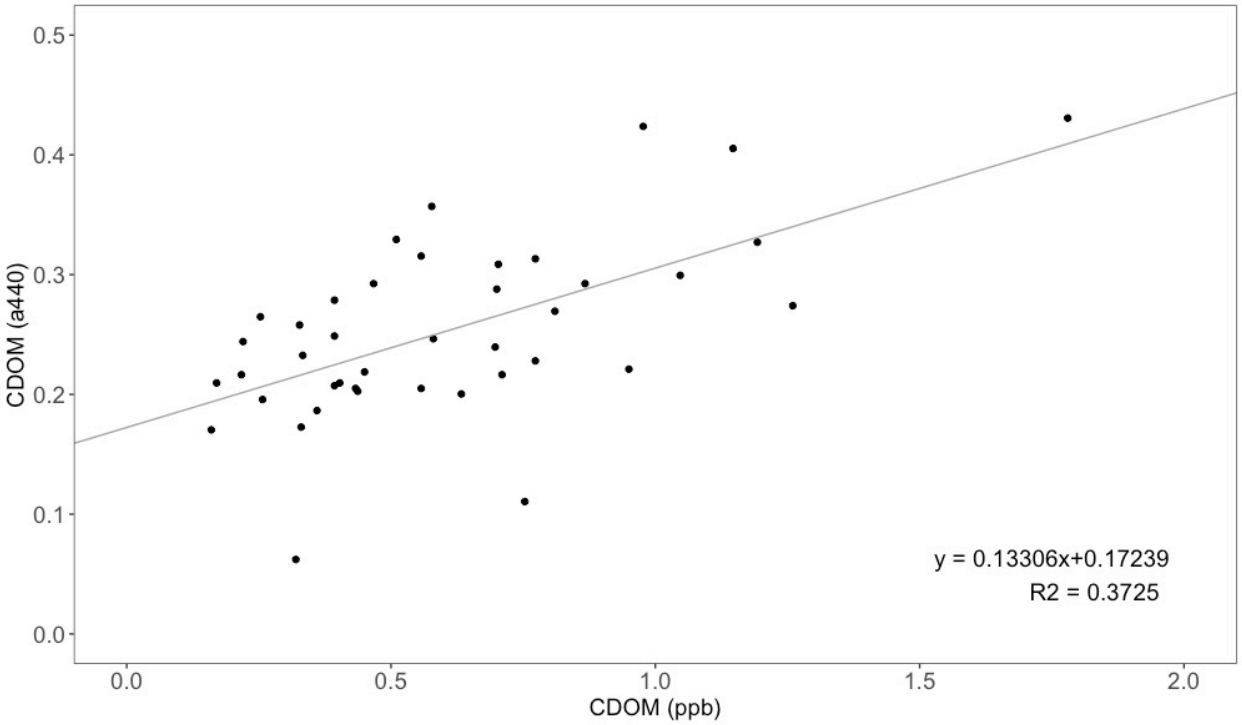

Figure 29: Peconic Bay CDOM fluorometric (ppb) and CDOM spectrophotometric (a_{440}) measurements from three sampling days at every water quality site ($p < 0.001$).

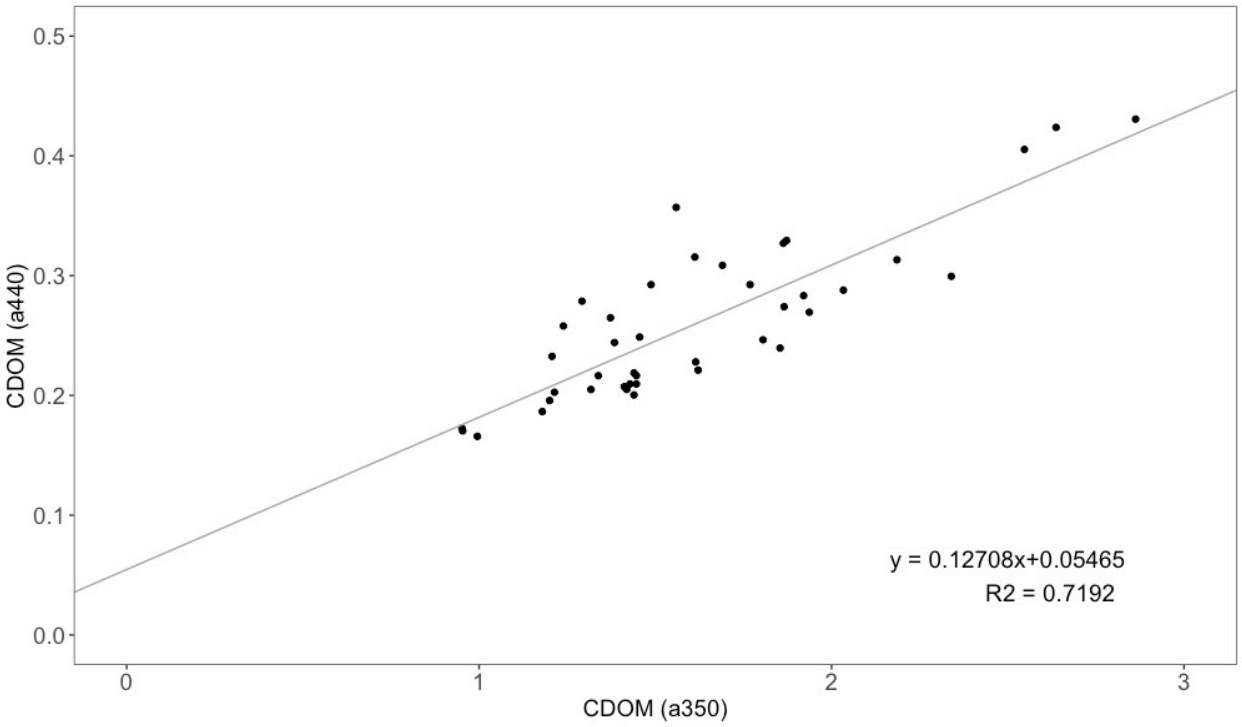

Figure 30: Peconic Bay CDOM spectrophotometric measurements at 440nm (a_{440}) and 350nm (a_{350}) from three sampling days at every water quality site ($p < 0.001$).

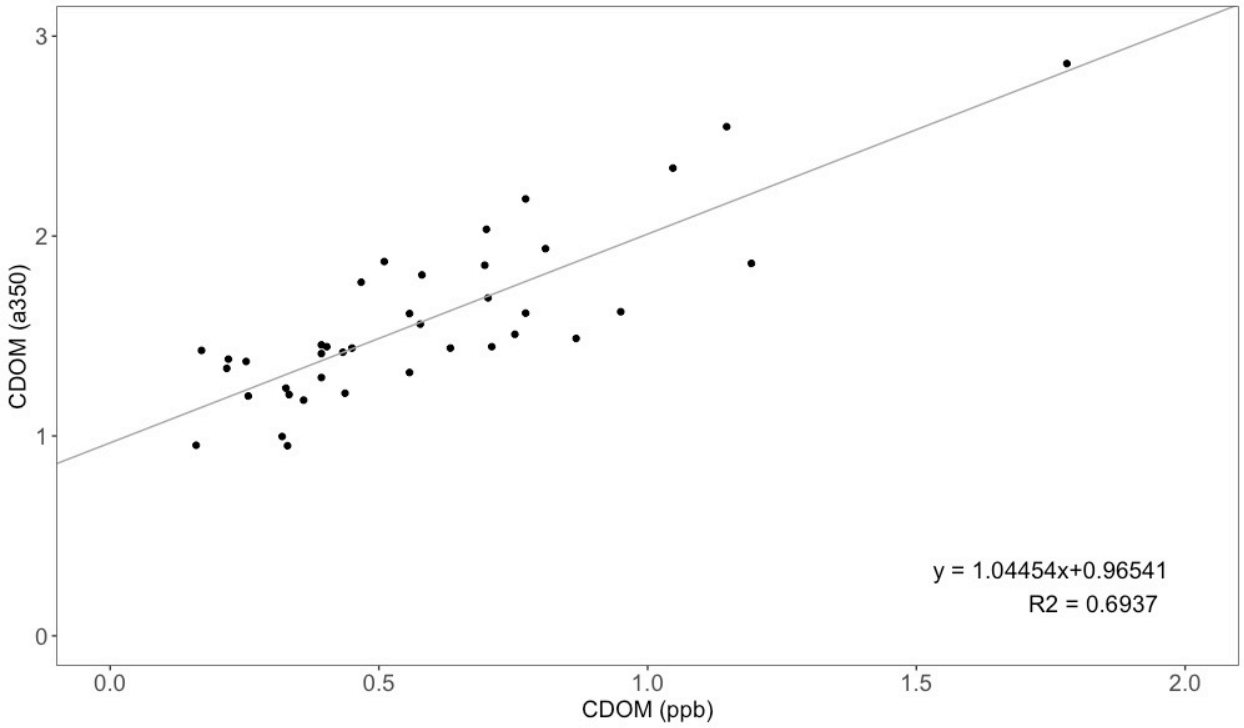

Figure 31: Peconic Bay CDOM spectrophotometric (a_{350}) and CDOM fluorometric (ppb) measurements from three sampling days at every water quality site ($p < 0.001$).

TABLES

Table 1: Site minimum, median, and maximum for chlorophyll-a (µg/L), TSS (mg/L), CDOM (a_{350}), and K_d (m^{-1}).

Site		Chl-a	TSS	CDOM	Kd
SG1	Median	7.50	15.00	1.384	0.81
	Min	2.97	9.5	0.362	0.47
	Max	17.07	25.8	1.831	1.31
SG2	Median	5.72	12.8	1.203	0.68
	Min	1.99	7.0	0.272	0.46
	Max	17.56	23.25	2.547	1.00
SG3	Median	4.73	11.55	1.272	0.58
	Min	2.01	6.5	0.272	0.25
	Max	14.245	21.4	1.921	1.02
SG4	Median	7.38	13.1	1.350	0.69
	Min	2.01	5.9	0.597	0.41
	Max	17.92	23.5	2.034	1.02
SG5	Median	4.66	11.6	1.246	0.52
	Min	1.23	4.5	0.352	0.39
	Max	13.23	36.5	1.905	0.85
WQ1	Median	8.52	12.15	1.672	0.76
	Min	2.83	3.7	0.486	0.46
	Max	25.24	31.6	2.764	1.05
WQ2	Median	7.92	11.0	1.488	0.72
	Min	2.30	6.3	0.486	0.27
	Max	39.74	47.6	2.742	1.12
WQ3	Median	6.0	9.2	1.12	0.63
	Min	1.77	4	0.412	0.4
	Max	13.33	17.0	2.321	0.93
WQ4	Median	6.66	13.8	1.373	0.94
	Min	2.95	9.2	0.362	0.43
	Max	12.62	31.8	2.863	1.69
WQ5	Median	6.18	11.2	1.409	0.71
	Min	3.37	6.2	0.279	0.43
	Max	10.87	20.1	2.124	1.0
WQ6	Median	5.64	12.95	1.214	0.72
	Min	2.15	5.1	0.279	0.37
	Max	13.62	17.5	1.928	1.37
WQ7	Median	4.75	12.9	1.239	0.635
	Min	2.24	5.7	0.283	0.33
	Max	14.59	25.7	2.34	1.29
WQ8	Median	4.62	12.7	1.439	0.63
	Min	1.19	7.22	0.283	0.39
	Max	11.08	50.6	2.507	0.99
WQ9	Median	5.49	11.2	1.35	0.61
	Min	1.71	7.4	0.597	0.37
	Max	17.09	18.7	2.186	1.22
WQ10	Median	7.03	14.2	1.292	0.725
	Min	1.81	4.1	0.412	0.36
	Max	10.48	24.7	1.879	0.97

Table 2: Grouped minimum, median, and maximum for chlorophyll-a (µg/L), TSS (mg/L), CDOM (a_{350}), and K_d (m^{-1})

Group		Chl-a	TSS	CDOM	K_d
A	Median	7.75	12.15	1.44	0.76
	Min	1.81	3.7	0.41	0.27
	Max	39.74	47.6	2.76	1.12
	N	48	47	26	51
B	Median	6.16	13.1	1.37	0.76
	Min	1.77	4.0	0.36	0.40
	Max	17.07	31.8	2.86	1.69
	N	50	49	27	53
C	Median	5.73	12.3	1.31	0.71
	Min	1.99	5.1	0.27	0.37
	Max	17.56	23.25	1.55	1.37
	N	50	49	29	50
D	Median	4.75	12.79	1.27	0.61
	Min	1.19	5.7	0.27	0.25
	Max	14.59	50.6	2.51	1.29
	N	50	50	26	52
E	Median	6.21	11.65	1.31	0.61
	Min	1.23	4.5	0.35	0.37
	Max	17.92	36.5	2.19	1.22
	N	48	48	26	51

Table 3: Interaction between K_d and chlorophyll (μg/L) at each site. Bold p-values indicates significant interactions ($p < 0.05$). The significance (sig) of each parameter is denoted by "." ($p < 0.1$), " * " ($p < 0.05$), " ** " ($p < 0.01$), " *** " ($p < 0.001$).

Site	Df	Intercept	Sig	Chl	Sig	R2	p
SG1	14	0.9983	***	-0.0184		0.0804	0.2871
SG2	14	0.5201	***	0.0288	*	0.3074	**0.0258**
SG3	13	0.6108	***	0.0009		0.0002	0.9640
SG4	12	0.7370	***	-0.0036		0.0090	0.7464
SG5	13	0.5079	***	0.0043		0.0138	0.6763
WQ1	9	0.6613	***	0.0048		0.0532	0.4949
WQ2	13	0.5694	***	0.0112	.	0.2604	0.0520
WQ3	12	0.7168	***	-0.0118		0.0555	0.4176
WQ4	14	1.5346	***	-0.0795	*	0.3373	**0.0183**
WQ5	13	0.7474	***	-0.0117		0.0277	0.5531
WQ6	12	0.5357	**	0.0143		0.0330	0.5342
WQ7	14	0.8020	***	-0.0293		0.0483	0.4135
WQ8	14	0.7077	***	-0.0093		0.0353	0.4860
WQ9	13	0.6080	***	-0.0051		0.0317	0.5253
WQ10	13	0.5491	***	0.0232		0.1605	0.1390

Table 4: Interaction between K_d and TSS (mg/L) at each site. Bold p-values indicates significant interactions ($p < 0.05$). The significance (sig) of each parameter is denoted by "." ($p < 0.1$), " * " ($p < 0.05$), " ** " ($p < 0.01$), " *** " ($p < 0.001$).

Site	Df	Intercept	Sig	TSS	Sig	R^2	p-value
SG1	15	0.7594	**	0.0059		0.0127	0.6665
SG2	14	0.6357	***	0.0053		0.0212	0.5903
SG3	11	0.5382	***	0.0023		0.0126	0.7147
SG4	12	0.5289	***	0.0066		0.0671	0.3713
SG5	13	0.5380	***	-0.0016		0.0120	0.6981
WQ1	11	0.6575	***	0.0051		0.0587	0.4251
WQ2	11	0.1132		0.0536	***	0.7864	**0.0001**
WQ3	11	0.4394	***	0.0176	.	0.2503	0.0817
WQ4	15	0.5955	*	0.0294	.	0.1990	0.0727
WQ5	13	0.7276	***	-0.0057		0.0209	0.6071
WQ6	12	0.3471		0.0313		0.1912	0.1179
WQ7	15	0.5860	*	0.0061		0.0110	0.6883
WQ8	13	0.6662	***	-0.0015		0.0136	0.6787
WQ9	11	0.4596	**	0.0093		0.0855	0.3325
WQ10	15	0.5094	**	0.0116		0.1092	0.1951

Table 5: Interaction between K_d and CDOM (a_{350}) at each site. Bold p-values indicates significant interactions ($p < 0.05$). The significance (sig) of each parameter is denoted by "." ($p < 0.1$), " * " ($p < 0.05$), " ** " ($p < 0.01$), " *** " ($p < 0.001$).

Site	Df	Intercept	Sig	CDOM	Sig	R2	p
SG1	7	0.9690	**	-0.1612		0.1654	0.2774
SG2	8	0.3552	.	0.2108	.	0.3407	0.0765
SG3	6	0.5659	**	-0.0130		0.0027	0.9031
SG4	7	0.7997	*	-0.0724		0.0252	0.6833
SG5	7	0.4629	***	0.0264		0.0349	0.6306
WQ1	6	0.5091	**	0.0800		0.3115	0.1505
WQ2	7	0.5067		0.1175	.	0.0778	0.4672
WQ3	7	0.7926	**	-0.1276		0.1859	0.2466
WQ4	6	0.2162		0.4855		0.2816	0.1760
WQ5	8	1.2694	***	-0.4139	*	0.5721	**0.0114**
WQ6	6	1.6237	**	-0.6700	*	0.6043	**0.0232**
WQ7	5	0.9783	**	-0.3175		0.4420	0.1032
WQ8	5	1.1768	***	-0.3167	***	0.9367	**0.0003**
WQ9	8	0.6350	**	-0.0374		0.0287	0.6397
WQ10	7	0.6024	.	0.0644		0.0179	0.7313

Table 6: Interaction between K_d and chlorophyll (µg/L) for each spatial group. Bold p-values indicates significant interactions ($p < 0.05$). The significance (sig) of each parameter is denoted by "." ($p < 0.1$), " * " ($p < 0.05$), " ** " ($p < 0.01$), " ***" ($p < 0.001$).

Group	Df	Intercept	Sig	Chlorophyll	Sig	R2	p
A	42	0.6165	***	0.0084	*	0.1128	**0.0258**
B	46	1.0236	***	-0.0246	.	0.0598	0.0939
C	43	0.5815	***	0.0134	.	0.0672	0.0854
D	44	0.6793	***	-0.0102		0.0204	0.3434
E	43	0.5636	***	0.0045		0.0234	0.3155

Table 7: Interaction between K_d and TSS (mg/L) for each spatial group. Bold p-values indicates significant interactions ($p < 0.05$). The significance (sig) of each parameter is denoted by "." ($p < 0.1$), " * " ($p < 0.05$), " ** " ($p < 0.01$), " *** " ($p < 0.001$).

Group	Df	Intercept	Sig	TSS	Sig	R2	p
A	42	0.5842	***	0.0091	*	0.1400	**0.0143**
B	46	0.4660	***	0.0279	***	0.2237	**0.0007**
C	43	0.5830	***	0.0084		0.0300	0.2551
D	41	0.5265	***	0.0058		0.0325	0.2473
E	41	0.4860	***	0.0083	.	0.0791	0.0677

Table 8: Interaction between K_d and CDOM (a_{350}) for each spatial group. Bold p-values indicates significant interactions ($p < 0.05$). The significance (sig) of each parameter is denoted by "." ($p < 0.1$), " * " ($p < 0.05$), " ** " ($p < 0.01$), " *** " ($p < 0.001$).

Group	Df	Intercept	Sig	CDOM	Sig	R2	p
A	23	0.5678	***	0.0723		0.0559	0.2449
B	21	0.8268	***	-0.0853		0.0351	0.3921
C	21	1.0181	***	-0.2676	*	0.2194	**0.0242**
D	24	0.6667	***	-0.0649		0.0626	0.2178
E	26	0.6403	***	-0.0335		0.0113	0.5902

Table 9: Interaction between K_d and each parameter for all of Peconic Bay. Bold p-values indicates significant interactions ($p < 0.05$). The significance (sig) of each parameter is denoted by "." ($p < 0.1$), " * " ($p < 0.05$), " ** " ($p < 0.01$), " *** " ($p < 0.001$).

Parameter	Df	Intercept	Sig	Parameter slope	Sig	R2	p
TSS	225	0.5400	***	0.0120	***	0.0632	**0.0001**
Chlorophyll	227	0.6455	***	0.0048		0.0100	0.1368
CDOM	131	0.6196	***	0.0169		0.0023	0.5863

Table 10: Multiple linear regression (K_d ~ TSS + Chlorophyll + CDOM) at each sampling site. Bold p-values indicates significant interactions ($p < 0.05$). The significance (sig) of each parameter is denoted by "." ($p < 0.1$), " * " ($p < 0.05$), " ** " ($p < 0.01$), " *** " ($p < 0.001$).

Site	Df	Intercept	Sig	TSS	Sig	Chlorophyll	Sig	CDOM	Sig	R^2	p
SG1	4	0.5039		0.0174		-0.0057		-0.0242		0.5338	0.3373
SG2	6	0.3159		0.0142		0.0213		-0.0072		0.6200	0.1014
SG3	4	0.5518		0.0149		0.0076		-0.1732	*	0.5344	0.3365
SG4	5	0.7075		0.0116		-0.0053		-0.0945		0.1227	0.8698
SG5	4	0.4624	**	0.0000	.	-0.0150		0.0562		0.6661	0.1841
WQ1	3	0.4605	.	-0.0132		0.0099		0.1051		0.6372	0.3276
WQ2	5	-0.3024	.	0.0664	**	-0.0019		0.1438	*	0.9425	**0.0016**
WQ3	4	0.5305	*	0.0423	*	-0.0311	.	-0.1024		0.8334	**0.0491**
WQ4	3	1.2422	***	-0.0298	*	-0.1555	***	0.7058	**	0.9882	**0.0022**
WQ5	4	1.8072	***	-0.0621	*	0.0647	*	-0.4932	**	0.9607	**0.0029**
WQ6	3	0.7301	**	-0.0013		-0.0931	**	0.1889		0.9707	**0.0085**
WQ7	3	0.7301	**	-0.0013		-0.0931	**	0.1889	.	0.9707	**0.0085**
WQ8	3	1.1125	***	0.0045		-0.0089		-0.2784	**	0.9826	**0.0039**
WQ9	4	0.5082	*	0.0134		-0.0537	.	0.0953		0.7429	0.1128
WQ10	5	0.5973		0.0123		-0.0069		-0.0191		0.1480	0.8318

Table 11: Multiple linear regression (K_d ~ TSS + Chlorophyll + CDOM) for each spatial group, and all of Peconic Bay. Bold p-values indicates significant interactions ($p < 0.05$). The significance (sig) of each parameter is denoted by "." ($p < 0.1$), " * " ($p < 0.05$), " ** " ($p < 0.01$), " *** " ($p < 0.001$).

Group	Df	Intercept	Sig	TSS	Sig	Chlorophyll	Sig	CDOM	Sig	R^2	p
A	21	0.3113	*	0.0182	*	0.0064	.	0.3011		0.4431	**0.0057**
B	19	0.6118	***	0.0378	***	-0.0312	***	-0.5946	*	0.6125	**0.0036**
C	21	0.9962	***	0.0002		0.0036	*	-1.6858	**	0.3076	**0.0483**
D	22	0.6160	***	0.0198	***	-0.0068		-0.9909	***	0.6016	**0.0001**
E	23	0.3293	***	0.0095		0.0041		0.3350	*	0.3089	**0.0340**
All	125	0.3225	***	0.0210	***	0.0010		0.2031		0.2473	**$8.901e^{-8}$**

Table 12: Multiple linear regression (K_d ~ TSS + Chlorophyll) at each sampling site. Bold p-values indicates significant interactions ($p < 0.05$). The significance (sig) of each parameter is denoted by "." ($p < 0.1$), " * " ($p < 0.05$), " ** " ($p < 0.01$), " *** " ($p < 0.001$).

Site	Df	Intercept	Sig	TSS	Sig	Chlorophyll	Sig	R^2	p
SG1	11	0.6695	.	0.0229		-0.0203		0.2125	0.2687
SG2	11	0.5407	**	-0.0022		0.0346	*	0.4656	**0.0319**
SG3	8	0.4333	**	0.0096		-0.0010		0.1943	0.4214
SG4	11	0.4295	***	0.0258	**	-0.0110		0.4995	**0.0222**
SG5	10	0.4743	***	0.0021		-0.0006		0.0169	0.9184
WQ1	8	0.6817	**	-0.0023		0.0053		0.0564	0.7926
WQ2	10	0.0386		0.0674	***	-0.0068	.	0.8403	**0.0001**
WQ3	10	0.4914	***	0.0328	*	-0.0277		0.3851	0.0879
WQ4	12	0.9647	**	0.0368	**	-0.0753	**	0.6429	**0.0021**
WQ5	10	0.8804	***	0.0067		-0.0454	*	0.3923	0.0829
WQ6	10	0.1814		0.0599	*	-0.0362		0.4675	**0.0428**
WQ7	13	0.4917		0.0223		-0.0175		0.0621	0.6593
WQ8	12	0.5128	**	0.0121		-0.0053		0.1426	0.3972
WQ9	10	0.7436	***	-0.0115		-0.0018		0.1254	0.5116
WQ10	13	0.5288	**	0.0077		0.0029		0.0574	0.6808

Table 13: Multiple linear regression (K_d ~ TSS + Chlorophyll) for each spatial group, and all of Peconic Bay. Bold p-values indicates significant interactions ($p < 0.05$). The significance (sig) of each parameter is denoted by "." ($p < 0.1$), " * " ($p < 0.05$), " ** " ($p < 0.01$), " *** " ($p < 0.001$).

Group	Df	Intercept	Sig	TSS	Sig	Chlorophyll	Sig	R^2	p
A	37	0.4914	***	0.0108	.	0.0072	*	0.2009	**0.0158**
B	37	0.4543	***	0.0438	***	-0.0320	**	0.6048	**$3.0e^{-8}$**
C	38	0.5945	***	-0.0006		0.0119		0.0554	0.3386
D	40	0.5595	***	0.0080		-0.0065		0.0309	0.5343
E	39	0.4260	***	0.0146	*	-0.0004		0.1504	**0.0416**
All	213	0.4581	***	0.0187	***	0.0001		0.1221	**$9.4e^{-7}$**

Table 14: Evaluation of PLW threshold values for determining *Z. marina* presence/absence in Peconic Bay. Value indicates the cut-off of presence or absence of *Z. marina* s found by maximizing the TPR (true positive rate) and TNR (true negative rate) in the evaluate function (R, 'dismo'). FPR and FNR are the false positive and negative rates, respectively.

Percent Light through Water	Correlation	Value	TPR	TNR	FPR	FNR
10	0.2641	18	0.9696	0.5910	0.4090	0.304
15	0.3090	18	0.8736	0.6776	0.3224	0.126
18.5	0.3307	15	0.9570	0.6096	0.3904	0.0430
20	0.3376	14	0.9570	0.6147	0.3853	0.0430
22.5	**0.3439**	**11**	**0.9640**	**0.6186**	**0.3814**	**0.0360**
25	0.3419	10	0.9440	0.6441	0.3559	0.0560
30	0.3267	6	0.8938	0.6551	0.3449	0.1062
25th percentile	0.2953	21.61	0.9434	0.6390	0.3610	0.0566
50th percentile	0.3031	24.76	0.9520	0.6330	0.3670	0.0480
75th percentile	0.2978	26.30	0.9670	0.5838	0.4162	0.0330
Depth (m)	0.2847	-2.27	0.0572	0.4266	0.5734	0.9428

Chapter 2

INTRODUCTION

Seagrasses are an integral—but declining—habitat type in coastal ecosystems. Seagrasses provide many ecosystem functions: nursery habitats for juvenile fishes, refuge and foraging habitat for many finfishes and shellfish, and coastal food web enhancement (Thayer & Stuart 1974, Jenkins et al. 1997, Heck et al. 2008, Beck et al. 2018). As an ecosystem engineer, seagrasses cycle nutrients, reduce wave attenuation and currents, stabilize sediments, and sequester carbon (Costanza & D'Arge 1997, Orth et al. 2006, Bos et al. 2007, Fourqurean et al. 2012, Reynolds et al. 2016). Successful application of habitat suitability models elsewhere in the U.S. through improvements in water quality allowed for successful restoration of seagrasses in the Indian River Lagoon, Tampa Bay, Chesapeake Bay, and coastal Virginia (Reynolds et al. 2016, Greening et al. 2014). Restored eelgrass (*Zostera marina*)—within 10 years of seeding—sequestered carbon and removed nitrogen at the same rate as established beds. Additionally, restored beds increased species diversity and ecosystem services comparable to pre-loss levels (Greiner et al. 2013, Reynolds et al. 2016). *Zostera marina*, a temperate species, grows in the Northeast Atlantic from North Carolina to the Arctic Circle (Krause-Jensen & Duarte 2014). Anthropogenic stressors, including light reduction and temperature increases, appear to explain a 1.4% average yearly decline in coverage (Short et al. 2011, Lefcheck et al. 2017). Rapidly warming temperatures and subsequent northward shift of *Z. marina* are predicted to result in complete extirpation in Long Island Sound by 2100 (Wilson & Lotze 2019).

Peconic Bay, designated as one of the "Estuaries of National Significance" by the United States Environmental Protection Agency (US EPA), lies between the eastern North and South "Forks" of Long Island, New York, USA. Comprised of five smaller bays with increasing residence times and shallower depths moving westward, *Z. marina* is found only in the eastern most two bays (Hardy 1976, Pickerell & Schott 2017). Widespread loss of *Z. marina* occurred during the 1930s from the wasting disease *Labyrinthula zosterae*, and then decades later in the 1980s from several brown tide events (Short et al. 1987, Dennison et al. 1989). Restoration efforts west of Shelter Island have failed (Pickerell & Schott 2017). *Zostera marina* coverage declined ~35% from 2000 to 2015 in Peconic Bay despite no brown tide blooms for the 25 years to present (Schott 2015, Tettelbach et al. 2015). Established in 2006, the New York State (NYS) Seagrass Taskforce evaluated potential causes of *Z. marina* declines in Long Island waters. They concluded

that declines were from insufficient light levels and noted the vulnerability of *Z. marina* in Peconic Bay to hardened shorelines and rising temperatures due to climate change (NYS Seagrass Taskforce 2009).

Properties of habitat suitability for Z. marina

The creation of a bio-optical model to predict light attenuation will advance the establishment of nutrient management thresholds for water quality targets in Peconic Bay (NYS Seagrass Taskforce 2009). High nutrient loading causes algal and epiphyte blooms, blocking light from reaching seagrass leaves (Neckles et al. 1993, Short et al. 1995). Seagrasses with high belowground biomass such as *Z. marina* also have higher light requirements, due to the added high oxygen demand of below-ground root and rhizome structures (Dennison et al. 1993, Nielsen et al. 2002). Depending on temperature and sediment composition, *Zostera marina* requires a minimum of ~10–30% surface light attenuating to depth (Dennison et al. 1993, Batiuk et al. 2000, Kemp et al. 2004, Moore et al. 2012, Kenworthy et al. 2014). Higher temperatures and organic matter increase the photosynthetic demand which heightens light requirements (Koch & Erskine 2001, Moore 2004). Failure to meet photosynthetic demand results in depleted carbon reserves and reduced pumping of oxygen to the rhizosphere (Dennison & Alberte 1985, Dennison 1987, Goodman et al. 1995, Greve et al. 2003, Pulido & Borum 2010, McPherson et al. 2015, Moreno-Marín et al. 2018, Gao et al. 2019). Extended duration of these metabolic imbalances results in mortality (Goodman et al. 1995, Kenworthy et al. 2014). Improvements to water quality increase the light availability to *Z. marina* by reducing light attenuation by phytoplankton and epiphytes, which may offset stresses associated with high water temperatures (Staehr & Borum 2011).

Higher water temperatures increase the metabolic rate of *Z. marina*, which increases the respiration rate and photosynthetic demand. Optimal temperatures for *Z. marina* are between 10 and 25 ºC: prolonged exposure (30+ days) above 25 ºC induces stress, and short-term exposure between 27 and 30 ºC can cause mortality (Zimmerman et al. 1989). Water temperature in Long Island Sound (Long Island, NY, USA) increased 0.03 ºC annually since 1948, coincident with an increase in "summer days" (days over 21 ºC; Rice et al. 2014). A greater occurrence of extreme temperature events (over 28 ºC) and an increase by 22 "summer days" in the Chesapeake Bay region since the 1950's is known to have negatively affected *Z. marina* populations: at its southern

extent in the North Atlantic, *Z. marina* exhibits a modified phenology with earlier summer peaks in biomass (Shields et al. 2018). In response to extreme heat stress, some Pacific populations exhibit an annual lifecycle, relying on seeds to replace the previous year's coverage (Santamaría-Gallegos et al. 2000). Therefore, studies on response and adaptations of *Z. marina* populations in Peconic Bay to rising temperatures and its interactions with other factors, such as light and sediment—are warranted.

Sediment properties influence where *Z. marina* exists, however, *Z. marina* also changes the composition of the sediment. Organic matter accumulation occurs due to either increased deposition of fine particles in the slowing of the current by seagrass canopies or reduced photosynthesis from light limitation (Grady 1981, Kemp et al. 1984, Newell et al. 1986). Net negative production causes a reduction in oxygen pumping into the sediments by the plant and reduced aerobic microbial decomposition, leading to an accumulation of organic matter in the sediments over time (Goodman et al. 1995, Lee & Dunton 1996). High organic matter accumulations—whether naturally or from light reduction—lead to an increased light requirement (Kenworthy & Fonseca 1996, Kenworthy et al. 2014). When roots do not release enough oxygen to compensate for high organic matter under light limited conditions, hydrogen sulfide will diffuse into the rhizomes (Pregnall et al. 1984, Smith et al. 1988, Lee & Dunton 1996). Hydrogen sulfide, an end-product of anaerobic respiration, causes seagrass mortality at high concentrations (>400 μM porewater; Dennison & Alberte 1985, Goodman et al. 1995). Therefore, both the reduction in physical flow or light limitation can increase organic matter content and concentrations of hydrogen sulfide in the sediment of seagrasses. (Goodman et al. 1995, Pérez et al. 2007, Krause-Jensen et al. 2011, Kenworthy et al. 2014).

Alterations in sediment composition may also occur as a result of modifications to natural shorelines and high wind events (Douglas & Rippey 2000, Miles et al. 2001). Hardened shorelines reflect waves and can cause a long-shore current, increasing sediment re-suspension and movement (Miles et al. 2001). The altered water movement and increased suspended sediments caused by hardened shorelines result in increased light attenuation and physical damage to roots and rhizomes (Patrick et al. 2016, Landry & Golden 2018, Currin 2019). Landry & Golden (2016) found that SAV (submerged aquatic vegetation) adjacent to hardened shorelines had significantly reduced species diversity, evenness, and percent cover when compared to natural shorelines. They also noted the threat of sea level rise to SAV adjacent to hardened shorelines, a process they termed

"squeezing", which prevents the landward migration of seagrasses between the hardened shoreline and deepening water. In Peconic Bay, hardened shorelines increased by 130% from 2003 to 2016, potentially spurred by Hurricane Sandy in 2014 (Peconic Estuary Program unpublished data). Additionally, Patrick et al. (2016) identified bulkheads as the most deleterious type of hardened shoreline to seagrasses in Chesapeake Bay: bulkhead length in Peconic Bay increased by 170% between 2003 and 2016. Hardened shorelines intensify the detrimental effects of wind induced waves and boat action on seagrass (Patrick et al. 2016).

Relative wave exposure (RWE) is determined from wind speed, fetch, and depth (Fonseca & Malhotra 2007). High wind exposure and tidal currents degrade seagrass bed edges, suspend sediments, bury plants, and expose roots (Patriquin 1975, Kirkman & Kuo 1990, Fonseca & Bell 1998, Batiuk et al. 2000, van Katwijk & Hermus 2000, Frederiksen et al. 2004). Uhrin & Turner (2018) found a change point threshold value between 679 and 774 J m^{-1} (RWE) for *Z. marina* in Chesapeake Bay (Uhrin & Turner 2018). Prior to this study, the interaction between RWE and Z. *marina* has not been evaluated in Peconic Bay. Modeling *Z. marina* habitat suitability in Peconic Bay incorporated light, temperature, sediment characteristics, hardened shorelines, and wave exposure, as well as possible interactions between variables.

Modeling current and future distributions

Species distribution modeling (SDM) predicts the geographic range of species from correlation of species with environmental parameters (Elith & Leathwick 2009). SDM's have increased in complexity and frequency of use in the marine environment, especially over the past 10 years (Robinson et al. 2017). Popular machine-learning SDM's previously used to predict the presence of seagrass species include Maxent, generalized additive models (GAMs), boosted regression trees (BRT), and random forest models, among others (Valle et al. 2013, Folmer et al. 2016, Effrosynidis et al. 2018, Wilson & Lotze 2019). Classification and regression trees (CART) predict outcomes based on several variables, with some variables used more than once. For example, *Z. marina* survives at a range of thresholds: high water temperature typically yields a high light requirement, but lower temperatures lessen the light requirement. A CART models a 'tree' of binary outcome values ('present' or 'absent') based on combinations of variables determined by the model (De'Ath & Fabricius 2000). A random forest classification model uses

a “forest” of CARTs to decrease error and correlation as well as increase accuracy (James et al. 2013). This random forest model predicts present and absent values for cells to create a habitat suitability model in Peconic Bay for *Z. marina*.

The aim of this study was to better understand the factors governing *Z. marina* distribution in Peconic Bay. First, we used random forest modeling with light, temperature, sediment, wind, and hardened shoreline variables to create a model of distribution—a habitat suitability model. Second, via recursive feature elimination, we calculated feature importance of variables that determined *Z. marina* distribution in Peconic Bay. We hypothesized light would be a limiting factor of distribution in Peconic Bay, followed by temperature, wind, sediment, and hardened shorelines. We aimed to create thresholds of survival based off outputs from the random forest modeling. Of these variables, only light could be addressed from a management perspective. We also created a restoration potential model that established areas of high probability for restoration success. Lastly, using the habitat suitability model, we modeled future scenarios of temperature and sea level rise to predict areas at risk to habitat loss. Peconic Bay represented an understudied water body regarding factors influencing *Z. marina* habitat suitability. As such, successful modeling of survival thresholds and habitat suitability improved future restoration efficacy of *Z. marina* in this estuary.

METHODS

Study Area

The study area encompassed most of Peconic Bay: from Flanders Bay to western Gardiner's Bay (Figure 1). Peconic Bay receives little freshwater influence from riverine sources. Freshwater input originates mainly from submarine groundwater discharge and results in estuarine salinity similar to oceanic salinity (Hardy 1976, Soren 1978, Barusich et al. 2012). Two seagrasses, *Z. marina* and *Ruppia maritima,* currently exist in Long Island waters. The predominant seagrass, *Z. marina*, inhabited the clearer, cooler, oceanic influenced waters east of Shelter Island. Conversely, and not included in this study, *R. maritima* occupied turbid, warm, shallow creeks throughout the estuary (Cashin Associates 1996). Peconic Bay, divided for this study into west and east of Shelter Island, was determined by *Z. marina* absence (western) and presence (eastern).

Characterized by warmer temperatures, longer residence time, and shallower bathymetry, western Peconic Bay currently lacks any *Z. marina*, completely lost prior to 1988 (Hardy 1976, Dennison et al. 1989). Occasionally, *Z. marina* flourishes west of Shelter Island in locations heavily influenced by groundwater, such as in Bullhead Bay, Southampton, NY (Pickerell & Schott 2017). Excluding areas with known groundwater influence from this study avoided possible confounding factors. Eastern Peconic Bay, defined by cooler temperatures attributed to deeper depths and higher oceanic flushing, contains the remaining *Z. marina* population (Hardy 1976). *Zostera marina* in the study area inhabited 0.001–4.53 m at mean low water (MLW) and 0.96–5.48 m at mean high water (MHW, Figure 2). A mask called the "ideal bathymetry layer" constrained the analysis to a depth interval of 0–5 m (MLW), focusing on depths of *Z. marina* found in the study area (Figure 3). Subject to ice-scouring, shallow areas—typically 0.5 m or less and exposed to wave action—may prevent *Z. marina* growth (Duarte & Kalff 1990). Additionally, *Z. marina* at depths greater than 5 m may experience light limitation, typically resulting in a distinct "deep edge" of beds existing along depth gradients (Krause-Jensen et al. 2003).

Field Sampling

Water quality sampling was performed in Peconic Bay at 15 sites (Figure 4) from May–October in 2017 and 2018 every two weeks. Fifteen water quality sampling sites were determined by choosing five areas with extant *Z. marina* (denoted as "SG") and ten areas without extant *Z. marina* (denoted as "WQ"). The ten "WQ" sites—without current *Z. marina*—were chosen from areas with previous coverage of *Z. marina* that has since been lost. Photosynthetically active radiation (PAR) light measurements were taken using a Li-COR 1400 handheld console equipped with a deck and underwater quantum sensor: the light attenuation coefficient (K_d) was determined using the Beer-Lambert exponential decay function (Carruthers et al. 2001). At the deep edge for "SG" sites and at 1–1.5 m MLW for "WQ" sites, HOBO pendant temperature loggers took measurements every 15 minutes from June through October at all stations. The deep edge of *Z. marina* beds was estimated with aerial imagery, ground-truthed using SCUBA, and mapped with GPS. Sediment cores of 5.25-cm diameter and 10-cm depth were taken annually to determine percent organic matter (POM) and grain size at each site in 2018 and 2019. At sites with extant *Z. marina*, sediment coring occurred both in and out (0.25 m from deep edge) of the bed. Sediment was dried and sieved into two grain size classes, larger and smaller than fine-grained (<63 µm, silt and clay) sediment (Poppe et al. 2000). Sediment was combusted and reweighed for total matter loss to determine POM (Schumacher 2002).

Raster Layers

For all rasters: cell size was 3 m^2 on edge; interpolation between points was performed with inverse distance weighting (IDW); and clipped to the "study area". All spatial functions were performed in ArcGIS v.10.6, unless otherwise noted. This study area excluded interior harbors and creeks which may not respond to the same factors as the bay proper, e.g. groundwater influence. Vegetation in most of these areas has not been surveyed since 1994 (Cashin Associates 1996).

Bathymetry data was obtained from the NOAA NCEI 2014 Hurricane Sandy DEM (LIDAR; horizontal and vertical resolution of 10 cm). Bathymetry was transformed from NAVD88 to MLW using the NOAA vertical datum converter, VDatum v.4.0.1 (Figure 5, NOAA 2019). *Zostera marina* in the study area covered 1.46 km^2. Delineation of *Z. marina* using

National Agriculture Imagery Program (NAIP) orthoimagery from 2017 was compared with ground-truthed delineation of 2014 imagery by Cornell Cooperative Extension of Suffolk County imagery for accuracy (Figure 2; Schott 2015). *Zostera marina* presence (value = 1) or absence (value = 0) was determined for all cells in the study area.

K_d values were interpolated between sampling sites. Percent light through water—the amount of surface light reaching the bottom of the water column—was calculated using the raster calculator with Equation 1 (Batiuk et al. 2000):

$$PLW = 100 * exp^{-K_d * Z}$$

where Z was depth (m) at MLW. PLW was calculated for all days sampled (18 days; Figure 6). Application of PLW "threshold" values at 10, 15, 18.5, 20, 22.5, 25, and 30%—chosen based on literature recommendation—created seven light layers for analysis (Dennison et al. 1993, Dixon & Leverone 1995, Batiuk et al. 2000, Kemp et al. 2004). Raster cells were reclassified using the 'raster' R package (Hijmans 2019). Cells in each PLW threshold layer received either a 0 (under) or 1 (over) for every day sampled resulting in a score of 0–18. For example, a cell with a PLW value under 22.5% received a 0 and a cell over 22.5% received a 1 (using the threshold of 22.5% PLW for one day of sampling). Each reclassified cell contained a 0 or 1 for an individual sampling day and threshold (126 layers). Adding together resultant days of reclassified cells at each threshold produced seven layers with values between 0 and 18. Three additional layers—Q1 (first quartile), Q2 (median), and Q3 (third quartile) of PLW values (0–100%) for all sampling days, computed with the 'raster' package in R—were also used to compare light in this analysis (Hijmans 2019).

Temperature data was calculated from HOBO dataloggers deployed in summer of 2018, the warmest, and "highest" heat stress of the four summers sampled (2016–2019, Figure 7). A jitter function was applied to the data to lessen erroneous measurements and smooth temperature values using the 'zoo' R package (Zeileis & Grothendieck 2005). A moving average of 5 data points—1.25 hours or 30 minutes on either side of a temperature measurement—was calculated for every measurement. Cumulative and sequential hours over designated "stressful" temperatures were determined for each recovered HOBO. Temperatures over 25, 27, and 30 ºC represent the low, intermediate, and high heat stress for *Z. marina*, respectively. Cumulative temperatures over 25–30 ºC (at every 1 ºC) were calculated to determine total heat stress during the summer with the 'dplyr' package in R (Wickham et al. 2020). Additionally, sequential temperatures over 25 and

27 ºC were calculated to determine the longest period of time spent above the low and intermediate heat stress with the 'rle' function in R (R Core Team 2018). Temperatures over 30 ºC were infrequent during the sampling period, and as such, excluded from sequential data. The highest cumulative hours over 30 ºC was 15 hours at the westernmost site. The cumulative and sequential hour layers were interpolated between sites (Figure 8).

The Peconic Estuary Program provided unpublished hardened shoreline and bulkhead shapefiles. The shoreline of the study area was 26% armored as of 2016. Euclidian distance and direction determined the straight-line distance and direction of all cells to hardened shorelines and bulkheads (Figure 8). Relative wave exposure (RWE) values were computed using the NOAA Wave Exposure Model, WEMo v.5.0 (Fonseca & Malhotra 2007). Inputs to the model included: bathymetry at MLW; wind data in 2018 (entire year, top 20% wind speeds) from the East Hampton airport (Station ID: WBAN: 64761); shoreline from the NOAA shoreline data explorer (CUSP); and 280 random points within the ideal bathymetry layer. Highest stress from waves occurred at MLW. Computed RWE values at the random points were then interpolated throughout the bay (Figure 9).

Random points established within the ideal bathymetry layer (45,000 points) and *Z. marina* delineations (5,000 points) comprised a 50,000-point shapefile. Using the 'raster' R package, 25 variable (post-interpolation) values were extracted to each point in the shapefile: depth, days over 10, 15, 18.5, 20, 22.5, 25, and 30% percent light through water (PLW), 25, 50, 75th IQR of PLW, relative wave exposure, hours over 25, 26, 27, 28, 29, and 30 ºC, sequential hours over 25 and 27 ºC, distance and direction to hardened shoreline, distance and direction to bulkhead shoreline, and *Z. marina* presence (Figure 10; Hijmans 2019).

Presence/Absence Classification

The 50,000 random points were run through a random forest classification with the 'randomForest' R package to predict presence or absence of *Z. marina* using 24 variables (Figure 10; Liaw & Wiener 2002). Random forest classification is a machine learning algorithm that can use many correlated variables—particularly important with the light and temperature variables in this model. Random forest classification creates a model of high accuracy and low correlation between trees by using 'out-of-bag' (OOB) bootstrap sampling of values and feature randomness.

'Out-of-bag' bootstrap sampling of values reduces model error (a third of random values removed with replacement from each tree) creating a "unique" tree and outcome each time. Feature randomness within each tree (limiting number of variables at each node split) reduces correlation between trees. The number of variables used at each split is equal to the square root of the number of predictor variables which allows for different set of variables to be "tried" at each split (Breiman 2001).

The random point shapefile was split into a training set of 37, 500 points and test set of 12,500 points, maintaining a 10% "presence" of *Z. marina* points in each set using 'caTools' package in R (Tuszynski 2019). The random forest function ran first without removal of any features, with unlimited max nodes and 500 trees. However, since several features were co-varying, determining the most important features within groups (light, temperature, hardened shorelines) led to a stronger model by decreasing correlation between trees. Principal component analysis (PCA, scaled and centered) confirmed variable groupings. Feature importance—ranking features based on the increase or decrease of model accuracy through removal of that feature—was used to determine which features to keep in the model with recursive feature elimination in R package 'caret' (Wing & Kuhn 2019). Additionally, the number of nodes on trees was limited to make it more manageable for interpretation and sharing. Model selection was based on the lowest OOB error estimate within training and test data and evaluation of accuracy, kappa statistic, and AUROC (area under the receiver operating characteristics).

To explore how model predictions would change under different climate projections we subjected the final model to three sea level rise (SLR), five temperature, and 15 combinations of SLR and temperature scenarios. Three predictions of SLR were based on projections for the Long Island region by 2050: low, 0.2 m; medium, 0.4 m; and high, 0.8 m (Horton et al. 2014). Sea level rise scenarios were subtracted from present day bathymetry to create future possible bathymetric layers. Five temperature increase projections were based on a 0.03 ºC/year increase in Long Island Sound: 0.25 ºC (2028); 0.5 ºC (2037); 0.75 ºC (2045); 1 ºC (2053); and 2 ºC (2087; Horton et al. 2014, Rice et al. 2014). Temperature scenarios (0.25–2 ºC) were added to HOBO temperature logger data at every data point; cumulative and sequential hours over all temperature thresholds were re-run. For example, 0.75 ºC was added to all temperature data points in each HOBO file to simulate temperatures predicted by 2045. The model then predicted the effect of combined sea level rise and temperature scenarios (15 models).

RESULTS

Figures 12–18 display values for extracted variables, including: PLW of 22.5, median PLW, hours over 25 ºC, RWE, hardened shorelines, and bulkheads. Shallow depths (Figure 12) and areas with *Z. marina* (Figure 13) had more days of threshold PLW values than deeper depths. Western Peconic Bay had much higher temperatures than eastern Peconic Bay (Figure 14), likely due to reduced oceanic influence west of Shelter Island. A possible cumulative temperature threshold may be ~1000 hours, found at the most western *Z. marina* bed (SG1, Figure 7). Comparison of temperature loggers (in a separate study) in two other bays on Long Island—Great South Bay and Shinnecock Bay—reinforced the idea that *Z. marina* in Peconic Bay experienced lower temperature stress than other eastern bays (Figure 15). RWE was higher on the south shoreline of Peconic Bay and areas exposed to winds from the north (Figure 16). Hardened shorelines accounted for 26% of Peconic Bay shoreline: 70% of the ideal bathymetry layer was within 1,000 m of a hardened shoreline and ~45% of *Z. marina* was within 500 m (Figure 17). Bulkheads comprise 77% of hardened shorelines and 20% of the Peconic Bay shoreline; 32% of *Z. marina* was within 500 m of a bulkhead (Figure 18).

Sampled POM was higher in *Z. marina* than un-vegetated areas, 1.12% ± 0.44 (SD) and 0.47% ± 0.32, respectively (Figure 19). The maximum value for all POM samples was 1.59%, below the low-end literature threshold value of 5% (Koch 2001). Percent silt and clay (fine sediment) was also higher in *Z. marina* (0.52% ± 0.44; un-vegetated 0.41% ± 1.1; Figure 19). High standard deviation in un-vegetated samples results from high percent fine sediment at WQ4 (mean = 3.53%). This location was at the mouth of Hashamomuck Pond (Southold, NY), subject to run-off. Excluding WQ4 reduced mean percent fine sediment to 0.06% ± 0.05 at un-vegetated sites. The highest percent fine sediment sample was 4.35% at WQ4, also below the low-end literature threshold value of 7.2% (Krause-Jensen et al. 2011).

The random points file allowed for comparison of variables between present and absent *Z. marina* points (Figure 20, 21; Table 1). In general, variables at absent points had higher standard deviation when compared to variables at present points (Table 3). When comparing light variables between the two types of points, the mean values of PLW were much higher—typically double—in points with *Z. marina* than without, a similar pattern was found for depth. In contrast, points with *Z. marina* had lower cumulative and sequential hours over the temperature thresholds.

Hardened shorelines and bulkheads were further from points with *Z. marina* than without while RWE was relatively similar between point types.

When run through the random forest package in R with all parameters (Model 1, 24 variables) and unlimited nodes, model OOB error was 0.57%. Model evaluations in Table 1 weighed the number of variables, number of nodes, OOB error rate, true positive rate, true negative rate, false positive rate, false negative rate, accuracy, Cohen's Kappa, and area under the receiving operating curve (ROC). Feature importance (via recursive feature elimination) was determined in decreasing order: RWE, bulkhead distance, bulkhead direction, hardened shoreline distance, hardened shoreline direction, sequential hours over 25 ºC, sequential hours over 27 ºC, cumulative hours over 25 ºC, depth, and hours over 30, 26, 27, 28 ºC. Interestingly, the most important model features did not consider any percent light to bottom variables. Only depth, a correlate with light availability, was retained. PCA confirmed the groupings: light (PLW10–30, 25/50/75th PLW, depth), temperature (cumulative and sequential hours over 25–30 ºC), RWE, and hardened shorelines (distance/direction, bulkheads; Figure 21). To select only one of each variable per grouping—cumulative temperature, sequential temperature, percent light to bottom, and hardened shoreline—the results of RFE determined the most important variable out of the groups: sequential and cumulative hours over 25 ºC, median PLW, and bulkhead direction and distance. Model 3, created from RWE, depth, hours over 25 ºC (sequential and cumulative), median PLW, and bulkhead direction and distance, had an OOB error estimate of 0.58% (Model 3, 7 variables). Removal of the light variable decreased the OOB error to 0.54% (Model 5, 6 variables). The decrease in error from removing light suggested that light was not a main driver of *Z. marina* habitat suitability in Peconic Bay. Model 5 was renamed, "Habitat Suitability Model" (HS Model; Table 1).

Intended for future use by restoration management, the Habitat Suitability Model was modified to limit the number of nodes to 50, creating a more manageable model. Node restraint was also applied to Model 1 and 3. Restraining nodes in Model 1 (24 variables) produced Model 2 with an OOB error of 1.94%. Model 4—or a variation on Model 2 with one variable from each grouping (7 variables)—reduced the OOB error to 1.87%. Removal of the light variable from Model 4 further reduced the error to 1.54% (Table 1): this was called "Restoration Potential Model" (RP Model, Figure 22). The RP Model predicted suitable habitats appropriate for *Z. marina* restoration. Interestingly, the model predicted absence of *Z. marina* in areas between 204

and 254º from a bulkhead, consistent with winter winds from the NE, suggesting an interaction. Locations of false positives and negatives from the dataset were extracted and mapped. False negatives concentrated around northern Shelter Island (Figure 23, 24) and around the deep edges of the *Z. marina* beds throughout Peconic Bay. False positives clustered around *Z. marina* beds at the shallow and deep edges and extended beyond beds at similar depths (Figure 25, 26). In addition, false positives aggregated in four distinct areas (Figure 27), which suggests the possibility of these areas for *Z. marina* restoration.

The HS Model predicted *Z. marina* presence and absence from the random points file in 23 climate change scenarios: (3) sea level rise, (5) temperature increase, and (15) combinations of the SLR and temperature increases. Considering sea level rise alone, the HS model predicted: an increase of 2.8% *Z. marina* present points at low (0.2 m), an increase of 2.4% at medium (0.4 m), and a decrease of 5.2% at high (0.8 m) 2050 projections. This increase in points from low to medium sea level rise reflected landward range expansion, especially in areas of shallow sloping shorelines. However, ideal depth area decreased in every SLR scenario: the highest being a ~14% decrease in ideal depth area by 2100 in the high SLR scenario (Table 2). An average temperature increase of 0.25 ºC decreased *Z. marina* present points by 95%, 0.5 ºC by 99.8%, and an increase to temperatures over 0.75 ºC yielded a decrease in *Z. marina* by 100% (0 present, 50,000 absent points). However, the temperatures used in the model from the summer of 2018 likely did not represent the warmest year for *Z. marina* in this estuary. Additionally, the HS model could not predict the interaction of temperature and *Z. marina* response. Combinations of SLR and temperature also predicted a high decline in *Z. marina*. An average increase of 0.25 ºC with: low SLR decreased *Z. marina* by 95.6%, medium SLR decreased by 97%, and high SLR decreased by 98.3%. An average increase of 0.5 ºC with low and medium SLR decreased *Z. marina* present points by 99.8% and high SLR decreased by 99.7%. An average increase of 0.75 ºC or greater under any SLR scenario would result in 100% absence of *Z. marina* points, suggesting a possible temperature threshold (Table 3). Temperature had a greater effect on *Z. marina* distributions than depth; the temperature threshold in Peconic Bay had not yet been confirmed but warming temperatures will certainly force *Z. marina* to adapt in the future.

DISCUSSION

Seagrasses are declining worldwide; determining the stressors to local populations is vital for their successful management and restoration. Our random forest model determined *Z. marina* habitat suitability in Peconic Bay and identified environmental factors—light, temperature, depth, wind exposure, and hardened shorelines—regulating its distribution. The initial model used 24 variables: ten light, eight temperature, four hardened shorelines, and one each for RWE and depth. Initial models included light because *Z. marina* is known to have high light requirements (~10–30%) and light availability was thought to limit *Z,marina* presence in the bay (Dennison et al. 1993, Nielsen et al. 2002, NYS Seagrass Taskforce 2009). Recursive feature elimination ranked median PLW as the most important light variable: this variable reflected typical light conditions in the bay during the growing season (median PLW for 18 days sampled). The final model achieved highest accuracy by leaving PLW light variables out. However, depth—a large component in determining the percent light reaching the bottom—ranked as an important predicting variable to model. Including the two other bays studied, Peconic Bay had the deepest *Z. marina* beds and clearest water, based on TSS, chlorophyll, and light measurements (Figure 28). If percent light reaching the bottom was the primary driver of *Z. marina* in Peconic Bay, there would be far more expansion into appropriate areas. Percent organic matter below literary threshold values also suggests that at the time of sampling *Z. marina* beds were not light limited (Kenworthy et al. 2014). A more comprehensive study of light in Peconic Bay may reveal higher resolution of light requirements for the *Z. marina* community. And the importance of light requirements may increase at higher temperatures, particularly during heat waves (Zimmerman et al. 2015). Many smaller-scale habitat suitability models for *Z. marina* included a light variable, but larger studies typically used depth, likely because consistent light data over large areas was not available (Batiuk et al. 2000, Valle et al. 2013, Detenbeck & Rego 2015, Folmer et al. 2016). Regardless, it appears that light alone cannot determine habitat suitability—especially in bays where water temperatures frequently exceed 25 ºC.

When determining temperature thresholds for seagrasses, average and maximum temperatures during the growing season are typically used (Valle et al. 2013, Lefcheck et al. 2017, Wilson & Lotze 2019). However, average and maximum temperatures do not consider time spent at stressful temperatures. Cumulative and sequential hours exceeding certain temperature

thresholds better captures the time *Z. marina* endures temperature stress (Eakin et al. 2009, Marbà & Duarte 2010). Cumulative hours represent the total time spent over a certain temperature, whereas sequential hours incorporate the length of time above that temperature. Diurnal oceanic tidal flushing, especially in eastern Peconic Bay, may relieve *Z. marina* stressed by warmer temperatures from the outgoing tide of the western bay (Collier et al. 2017). The most important temperature variable—sequential hours over 25 ºC—ranked sixth in feature importance, behind RWE and all hardened shoreline variables. Cumulative temperature over 25 ºC ranked eighth and highest of the other cumulative temperatures analyzed. Additionally, the higher ranked variables (RWE and hardened shoreline) had a full range of possible values, inclusive over time and space. RWE and hardened shoreline layers were modeled over the entire bay with many more points for interpolation and longer time periods; temperature variables used in this model may not represent the limits of temperature and higher (more limiting) values may increase feature importance. Confirming cumulative and sequential temperature thresholds of this population is imperative given warming temperature trends. Based on model outputs, the thresholds likely stand around 1000 cumulative hours over 25 ºC or an average increase in temperature above 0.75 ºC.

Wave exposure (RWE) is frequently left out of habitat suitability models but was an important local factor in Peconic Bay (Koch 2001, Li et al. 2007). Recently, RWE was used to predict the threshold behavior of *Z. marina* in Chesapeake Bay to wave energy of 675–774 J m^{-1}, where *Z. marina* coverage shifted from continuous to patchy as a result of higher wave exposure within the RWE threshold range (Uhrin & Turner 2018). As the climate warms, higher energy storms may become more common—and with stronger storms comes higher winds. RWE ranked as the most important variable in predicting *Z. marina* presence in Peconic Bay. High wind events from north-northeast winter storms ("Nor'easters") expose areas on the southern shoreline of Peconic Bay, including areas of current *Z. marina* extent. However, wave exposure tends to be more detrimental to shallow communities, and *Z. marina* in Peconic Bay is generally at deeper depths than in other estuaries on Long Island. Hardened shorelines, particularly bulkheads, may attenuate waves back over the *Z, marina* and create additional longshore currents and sediment resuspension (Miles et al. 2001, Patrick et al. 2016). The RP model determined an absence of *Z. marina* when bulkheads were directionally ~200–250 º (SW)—coinciding with strong winter northeast winds from the opposite direction. Bulkheads likely ranked higher in feature importance than hardened shorelines because this structure specifically increases energy, sediment suspension,

and longshore current at the shoreline (Miles et al. 2001). Living shorelines should be considered with current *Z. marina* distributions and applied where appropriate.

The HS and RP models predicted current distributions of *Z. marina* in Peconic Bay from depth, wave exposure, hardened shorelines, and temperature. Mapped locations of false positives and negatives showed that both models performed worst at edges of *Z. marina* beds, which may be due, in part, to inaccurate delineations. Large boulders covered in *sargassum sp.* often surrounded the edges of *Z. marina* beds in Peconic Bay; this made it difficult to distinguish between the two in aerial imagery. CCE ground-truthed the deep edge of several long-term monitoring sites in 2014 (Schott 2015), however, many *Z. marina* beds included in the current study were not validated. The RP model was less accurate (by ~1%) than the HS model but highlighted several areas of clustered false positives. These areas were either on the periphery of existing *Z. marina* beds or at historic edges of beds. Further evaluation of summertime temperatures, tidal currents, and sediment characteristics could inform the restoration potential of these sites.

Predictions of *Z. marina* locations with future climate change scenarios have a degree of uncertainty since the model did not incorporate the possible adaptations of the population to the stressors (Zimmerman et al. 2015, Hammer et al. 2018). Additionally, the environmental constraints of current *Z. marina* populations may not accurately reflect future genetic changes that could allow for survival in lower light (sea level rise) and higher temperature (Ehlers et al. 2008). However, these genetic changes may occur too slowly to keep up with rapidly warming temperatures and lowered light availability (Duarte et al. 2018). By 2050 the Long Island region will experience rising sea levels between 0.2 and 0.8 m (Horton et al. 2014). The model predicts that *Z. marina* will expand into previously shallow areas at the low to medium SLR projections, assuming the seagrass will keep up with increasing water depths. However, this cannot occur with a structure blocking the plant's landward expansion. The large increase in hardened structures over the past 15 years could "squeeze" the landward march of *Z. marina*, as seen in marshes elsewhere (Waycott et al. 2007, Saunders et al. 2013). Decreasing proximity of *Z. marina* to bulkheads may also stress and eliminate that bed entirely. The overall area of ideal depth decreased in every SLR scenario from 0.2–14%: however, a more detailed evaluation of landscape changes are needed.

Analysis of warming scenarios yielded complete extirpation of *Z. marina* in the study area with an increase of 0.75 ºC, not accounting for genetic or physiological responses. Populations of *Z. marina* in two other shallower estuaries on Long Island were more resilient to higher temperatures experienced during the same time period. Furthermore, in at least one *Z. marina* bed in Shinnecock Bay, the summertime strategy was similar to populations at the southern range limit— die-off during periods of high stress and replenish from either the seed bank over the winter (Jarvis et al. 2014, Lefcheck et al. 2017; personal observation). The HS model also did not account for groundwater discharge or an increase in CO_2 availability—which could increase *Z. marina* productivity and resilience (Zimmerman et al. 1991). A model by Rozell & Wong (2010) predicted seaward expansion of the seawater-freshwater interface of groundwater by 23 m seaward around Shelter Island, NY, which could alleviate anticipated temperature stresses. However, this model relied heavily on the assumption of future increased precipitation, without this increase, the groundwater interface will move landward with SLR. Populations of *Z. marina* in creeks and harbors of Peconic Bay experience higher cumulative and sequential temperatures, such as in Bullhead Bay, Coecles Harbor, and Napeague Harbor, than areas in the bay proper (Pickerell & Schott 2017). Groundwater discharge in these areas can mitigate sediment and bottom water temperatures during the stressful summer months, allowing *Z. marina* to persist where it otherwise could not (Barusich et al. 2012, Pickerell & Schott 2017). Yet, groundwater has long been considered detrimental to seagrasses, a potential source of pesticides and nutrients (Valiela et al. 1990, Burkholder et al. 2007, Damien & Pascaline 2013, Kenworthy et al. 2014, Detenbeck & Rego 2015). The net effect of this factor may shift as the climate continues to warm.

Anthropogenic inputs of carbon dioxide to the atmosphere have increased the DIC concentrations in the ocean (Zeebe & Wolf-Gladrow 2001). *Zostera marina* is often carbon limited, deriving 50% of carbon from aqueous CO_2 or, under limited aqueous CO_2 conditions, converting the readily available HCO_3^- to useable carbon (Zimmerman et al. 1995, 1997, Beer & Rehnberg 1997). Zimmerman et. al (2015) modeled projected CO_2 concentrations and temperature with sampled light to demonstrate how increased carbon availability buffered temperature stress in Chesapeake Bay. Increased CO_2 levels in embayments may offset higher metabolic demands from higher temperatures and actually increase *Z. marina* coverage (Palacios & Zimmerman 2007, Zimmerman et al. 2015). Although the models predict *Z. marina* die-off in Peconic Bay due primarily to temperature stress, the model cannot account for genetic adaptations and interaction

with future environmental variables. Reduction in genetic diversity in Peconic Bay was hypothesized as cause for widespread declines despite this bay being cooler than surrounding bays (Ehlers et al. 2008, NYS Seagrass Taskforce 2009). Genetic diversity was not found to be lacking (Peterson et al. 2013), but *Z. marina* at a Shelter Island site was much less resilient to high sediment organic matter and low light than other sites sampled, including Great South Bay (Plaisted et al. 2019). High genetic diversity implies that these populations are utilizing seed dispersal for reproduction and are responding to stressful environmental conditions, typically plants use clonal reproduction in stable environments (Hughes & Stachowicz 2009, Cabaço & Santos 2012).

Utilizing a random forest model to predict areas of *Z. marina* restoration potential was economically efficient and useful for predicting effects of climate change. Understanding the limitations of local populations to controllable variables (light and hardened shorelines) and variables out of management control (temperature and RWE) assists restoration managers in determining areas for remediation, for example: increasing light availability by nutrient reduction or converting a bulkhead into a living shoreline. This model also highlighted frequently overlooked physical factors such as hardened shorelines and RWE that should be considered when deciding on a restoration area. Sea level rise and temperature are inevitable, though the degree and effects are uncertain. Research into the physical drivers of *Z. marina* presence in Peconic Bay should continue to be a research priority, especially in terms of the interaction of temperature with groundwater discharge, increased CO_2 availability, and possible increased habitat with sea level rise.

LITERATURE CITED

Barusich P, Wong T, Wanlass J, Paulsen RJ (2012) Summary and Review of Reports and Data of Monitoring Wells in Peconic Estuary System. Prepared for: Peconic Estuary Program, Suffolk County Department of Health Services.

Batiuk RA, Bergstrom PW, Kemp WM, Koch EW, Murray L, Stevenson JC, Bartleson R, Carter V, Rybicki NB, Landwehr JM, Gallegos CL, Karrh L, Naylor M, Wilcox DJ, Moore KA, Ailstock S, Teichberg M (2000) Chesapeake Bay submerged aquatic vegetation water quality and habitat-based requirements and restoration targets: A second technical synthesis.CBP/TRS 245/00. EPA 903-R-00-014. U.S. EPA, Chesapeake Bay Program, Annapolis, Maryland.

Beck MW, Hagy JD, Le C (2018) Quantifying Seagrass Light Requirements Using an Algorithm to Spatially Resolve Depth of Colonization. Estuaries and Coasts 41:592–610.

Beer S, Rehnberg J (1997) The acquisition of inorganic carbon by the seagrass *Zostera marina*. Aquat Bot 56:277–283.

Bos AR, Bouma TJ, de Kort GLJ, van Katwijk MM (2007) Ecosystem engineering by annual intertidal seagrass beds: Sediment accretion and modification. Estuar Coast Shelf Sci 74:344–348.

Breiman L (2001) Random Forests. Mach Learn 45:5–32.

Burkholder JAM, Tomasko DA, Touchette BW (2007) Seagrasses and eutrophication. J Exp Mar Bio Ecol 350:46–72.

Cabaço S, Santos R (2012) Seagrass reproductive effort as an ecological indicator of disturbance. Ecol Indic 23:116–122.

Carruthers TJB, Longstaff BJ, Dennison WC, Abal EG, Aioi K (2001) Measurement of light penetration in relation to seagrass. In: *Global Seagrass Research Methods*. Elsevier Science, p 369–392

Cashin Associates (1996) Peconic Estuary Submerged Aquatic Vegetation Study. Prepared for: Suffolk County Department of Health Services, Division of Environmental Quality. Riverhead, NY.

Collier CJ, Ow YX, Langlois L, Uthicke S, Johansson CL, O'Brien KR, Hrebien V, Adams MP (2017) Optimum temperatures for net primary productivity of three tropical seagrass species. Front Plant Sci 8:1–14.

Costanza R, D'Arge R (1997) The value of the world's ecosystem services and natural capital. Nature 387:253–260.

Currin CA (2019) Living Shorelines for Coastal Resilience. In: *Coastal Wetlands*. Elsevier B.V., p 1023–1053

Damien A, Pascaline H (2013) Herbicide Impact on Seagrass Communities. Herbic - Curr Res Case Stud Use.

De'Ath G, Fabricius KE (2000) Classification and regression trees: A powerful yet simple technique for ecological data analysis. Ecology 81:3178–3192.

Dennison WC (1987) Effects of light on seagrass photosynthesis, growth and depth distribution. Aquat Bot 27:15–26.

Dennison WC, Alberte RS (1985) Role of daily light period in the depth distribution of *Zostera marina* (eelgrass). Mar Ecol Prog Ser 25:51–61.

Dennison WC, Marshall GJ, Wigand C (1989) Effect of "brown tide" shading on eelgrass (*Zostera marina* L.) distributions. In: *In E. M. Cosper, V.M. Bricelj, and E.J. Carpenter (eds.), Novel Phytoplankton Blooms: Causes and Impacts of Recurrent Brown Tides and other Unusual Blooms. Lecture Notes on Coastal and Estuarine Studies. Springer-Verlag, New York.* p 675–692

Dennison WC, Orth RJ, Moore KA, Stevenson JC, Carter V, Kollar S, Bergstrom PW, Batiuk RA (1993) Assessing water quality with submersed aquatic vegetation. Bioscience 43:86–94.

Detenbeck NE, Rego S (2015) Predictive Seagrass Habitat Model. Natl Heal Evironmental Eff Res Lab US EPA.

Dixon L, Leverone JR (1995) Light Requirements of *Thalassia testudinum* in Tampa Bay, Florida. Final Rept. SW Florida Water Management District, Mote Marine Lab Tech Rept, vol. 425.

Douglas RW, Rippey B (2000) The random redistribution of sediment by wind in a lake. Limnol Oceanogr 45:686–694.

Duarte B, Martins I, Rosa R, Matos AR, Roleda MY, Reusch TBH, Engelen AH, Serrão EA, Pearson GA, Marques JC, Caçador I, Duarte CM, Jueterbock A (2018) Climate change impacts on seagrass meadows and macroalgal forests: An integrative perspective on acclimation and adaptation potential. Front Mar Sci 5.

Duarte CM, Kalff J (1990) Patterns in the submerged macrophyte biomass of lakes and the importance of the scale of analysis in the interpretation. Can J Fish Aquat Sci 47:357–363.

Eakin CM, Lough JM, Heron SF (2009) Climate Variability and Change: Monitoring Data and Evidence for Increased Coral Bleaching Stress. In: *Coral Bleaching: Patterns, processes, causes and consequences*. Van Oppen M, Lough JM (eds) Berlin: Springer, p 41–67

Effrosynidis D, Arampatzis A, Sylaios G (2018) Seagrass detection in the mediterranean: A supervised learning approach. Ecol Inform 48:158–170.

Ehlers A, Worm B, Reusch TBH (2008) Importance of genetic diversity in eelgrass *Zostera marina* for its resilience to global warming. Mar Ecol Prog Ser 355:1–7.

Elith J, Leathwick JR (2009) Species Distribution Models: Ecological Explanation and Prediction Across Space and Time. Annu Rev Ecol Evol Syst 40:677–697.

Folmer EO, van Beusekom JEE, Dolch T, Gräwe U, van Katwijk MM, Kolbe K, Philippart CJM (2016) Consensus forecasting of intertidal seagrass habitat in the Wadden Sea. J Appl Ecol 53:1800–1813.

Fonseca MS, Bell SS (1998) Influence of physical setting on seagrass landscapes near Beaufort, North Carolina, USA. Mar Ecol Prog Ser 171:109–121.

Fonseca MS, Malhotra A (2007) WEMo (Wave Exposure Model): formulation, procedures and validation.

Fourqurean JW, Duarte CM, Kennedy H, Marbà N, Holmer M, Mateo MA, Apostolaki ET, Kendrick GA, Krause-Jensen D, McGlathery KJ, Serrano O (2012) Seagrass ecosystems as a globally significant carbon stock. Nat Geosci 5:505–509.

Frederiksen M, Krause-Jensen D, Holmer M, Laursen JS (2004) Spatial and temporal variation in eelgrass (*Zostera marina*) landscapes: Influence of physical setting. Aquat Bot 78:147–165.

Gao Y, Jiang Z, Du M, Fang J, Jiang W, Fang J (2019) Photosynthetic and metabolic responses of eelgrass *Zostera marina* L. to short-term high-temperature exposure. J Oceanol Limnol 37:199–209.

Goodman JL, Moore KA, Dennison WC (1995) Photosynthetic responses of eelgrass (*Zostera marina* L.) to light and sediment sulfide in a shallow barrier island lagoon. Aquat Bot 50:37–47.

Grady JR (1981) Properties of sea grass and sand flat sediments from the intertidal zone of St. Andrew Bay, Florida. Estuaries 4:335–344.

Greiner JT, McGlathery KJ, Gunnell J, McKee BA (2013) Seagrass restoration enhances 'Blue Carbon' sequestration in coastal waters. PLoS One 8:1–8.

Greve TM, Borum J, Pedersen O (2003) Meristematic oxygen variability in eelgrass (*Zostera marina*). Limnol Oceanogr 48:210–216.

Hammer KJ, Borum J, Hasler-Sheetal H, Shields EC, Sand-Jensen K, Moore KA (2018) High temperatures cause reduced growth, plant death and metabolic changes in eelgrass *Zostera marina*. Mar Ecol Prog Ser 604:121–132.

Hardy CD (1976) A preliminary description of the Peconic Bay Estuary. Marine Sciences Research Center, State University of New York at Stony Brook. Special Report 3. Stony Brook.

Heck KL, Carruthers TJB, Duarte CM, Randall Hughes A, Kendrick G, Orth RJ, Williams SW (2008) Trophic transfers from seagrass meadows subsidize diverse marine and terrestrial consumers. Ecosystems 11:1198–1210.

Hijmans RJ (2019) Raster: Geographic Data Analysis and Modeling.

Horton R, Bader D, Rosenzweig C, DeGaetano A, Solecki W (2014) Climate Change in New York State: Updating the 2011 ClimAID Climate Risk Information. New York State Energy Research and Development Authority (NYSERDA), Albany, New York.

Hughes AR, Stachowicz JJ (2009) Ecological impacts of genotypic diversity in the clonal seagrass *Zostera marina*. Ecology 90:1412–1419.

James G, Witten D, Hastie T, Tibshirani R (2013) An introduction to statistical learning with applications in R. Springer, New York, NY, USA.

Jarvis JC, Brush MJ, Moore KA (2014) Modeling loss and recovery of *Zostera marina* beds in the Chesapeake Bay: The role of seedlings and seed-bank viability. Aquat Bot 113:32–45.

Jenkins GP, May HMA, Wheatley MJ, Holloway MG (1997) Comparison of fish assemblages associated with seagrass and adjacent unvegetated habitats of Port Phillip Bay and Corner Inlet, Victoria, Australia, with emphasis on commercial species. Estuar Coast Shelf Sci 44:569–588.

van Katwijk MM, Hermus DCR (2000) Effects of water dynamics on *Zostera marina*: Transplantation experiments in the intertidal Dutch Wadden Sea. Mar Ecol Prog Ser 208:107–118.

Kemp WM, Batiuk RA, Bartleson R, Bergstrom PW, Carter V, Gallegos CL, Hunley W, Karrh L, Koch EW, Landwehr JM, Moore KA, Murray L, Naylor M, Rybicki NB, Stevenson JC, Wilcox DJ (2004) Habitat requirements for submerged aquatic vegetation in Chesapeake Bay: Water quality, light regime, and physical-chemical factors. Estuaries 27:363–377.

Kemp WM, Boynton WR, Twilley RR, Stevenson JC, Ward LG (1984) Influences of submerged vascular plants on ecological processes in upper Chesapeake Bay. In: *The Estuary As a Filter*. Academic Press, p 367–394

Kenworthy WJ, Fonseca MS (1996) Light requirements of seagrasses *Halodule wrightii* and *Syringodium filiforme* derived from the relationship between diffuse light attenuation and maximum depth distribution. Estuaries 19:740–750.

Kenworthy WJ, Gallegos CL, Costello C, Field D, di Carlo G (2014) Dependence of eelgrass (*Zostera marina*) light requirements on sediment organic matter in Massachusetts coastal bays: Implications for remediation and restoration. Mar Pollut Bull 83:446–457.

Kirkman H, Kuo J (1990) Pattern and process in southern Western Australian seagrasses. Aquat Bot 37:367–382.

Koch EW (2001) Beyond light: Physical, geological, and geochemical parameters as possible submersed aquatic vegetation habitat requirements. Estuaries 24:1–17.

Koch MS, Erskine JM (2001) Sulfide as a phytotoxin to the tropical seagrass *Thalassia testudinum*: Interactions with light, salinity and temperature. J Exp Mar Bio Ecol 266:81–95.

Krause-Jensen D, Carstensen J, Nielsen SL, Dalsgaard T, Christensen PB, Fossing H, Rasmussen MB (2011) Sea bottom characteristics affect depth limits of eelgrass *Zostera marina*. Mar Ecol Prog Ser 425:91–102.

Krause-Jensen D, Duarte CM (2014) Expansion of vegetated coastal ecosystems in the future Arctic. Front Mar Sci 1:1–10.

Krause-Jensen D, Pedersen MF, Jensen C (2003) Regulation of eelgrass (*Zostera marina*) cover along depth gradients in Danish coastal waters. Estuaries 26:866–877.

Landry JB, Golden RR (2018) In Situ Effects of Shoreline Type and Watershed Land Use on Submerged Aquatic Vegetation Habitat Quality in the Chesapeake and Mid-Atlantic Coastal Bays. Estuaries and Coasts 41:101–113.

Lee KS, Dunton KH (1996) Production and carbon reserve dynamics of the seagrass *Thalassia testudinum* in Corpus Christi Bay, Texas, USA. Mar Ecol Prog Ser 143:201–210.

Lefcheck JS, Wilcox DJ, Murphy RR, Marion SR, Orth RJ (2017) Multiple stressors threaten the imperiled coastal foundation species eelgrass (*Zostera marina*) in Chesapeake Bay, USA. Glob Chang Biol 23:3474–3483.

Li X, Weller DE, Gallegos CL, Jordan TE, Kim HC (2007) Effects of watershed and estuarine characteristics on the abundance of submerged aquatic vegetation in Chesapeake bay subestuaries. Estuaries and Coasts 30:840–854.

Liaw A, Wiener M (2002) Classification and Regression by randomForest. R News 2:18–22.

Marbà N, Duarte CM (2010) Mediterranean warming triggers seagrass (*Posidonia oceanica*) shoot mortality. Glob Chang Biol 16:2366–2375.

McPherson ML, Zimmerman RC, Hill VJ (2015) Predicting carbon isotope discrimination in eelgrass (*Zostera marina* L.) from the environmental parameters—light, flow, and [DIC]. Limnol Oceanogr 60:1875–1889.

Miles JR, Russell PE, Huntley DA (2001) Field measurements of sediment dynamics in front of a seawall. J Coast Res 17:195–206.

Moore KA (2004) Influence of Seagrasses on Water Quality in Shallow Regions of the Lower Chesapeake Bay. J Coast Res 45:162–178.

Moore KA, Shields EC, Parrish DB, Orth RJ (2012) Eelgrass survival in two contrasting systems: Role of turbidity and summer water temperatures. Mar Ecol Prog Ser 448:247–258.

Moreno-Marín F, Brun FG, Pedersen MF (2018) Additive response to multiple environmental stressors in the seagrass *Zostera marina* L. Limnol Oceanogr 63:1528–1544.

Neckles HA, Wetzel RL, Orth RJ (1993) Relative effects of nutrient enrichment and grazing on epiphyte-macrophyte (*Zostera marina* L.) dynamics. Oecologia 93:285–295.

Newell SY, Fell JW, Miller C (1986) Deposition and Decomposition of Turtlegrass Leaves. Int Rev der gesamten Hydrobiol und Hydrogr 71:363–369.

Nielsen SL, Sand-Jensen K, Borum J, Geertz-Hansen O (2002) Depth colonization of eelgrass (*Zostera marina*) and macroalgae as determined by water transparency in Danish coastal waters. Estuaries 25:1025–1032.

NOAA (2019) NOAA/NOS VDatum 4.0.1: Vertical Datums Transformation.

NYS Seagrass Taskforce (2009) Final Report of the New York State Seagrass Task Force: Recommendations to the New York State Governor and Legislature. 1–69.

Orth RJ, Carruthers TJB, Dennison WC, Duarte CM, Fourqurean JW, Heck KL, Hughes RA, Kendrick GA, Kenworthy WJ, Olyarnik S, Short FT, Waycott M, Williams SL (2006) A global crisis for seagrass ecosystems. Bioscience 56:987–996.

Palacios SL, Zimmerman RC (2007) Response of eelgrass *Zostera marina* to CO2 enrichment: Possible impacts of climate change and potential for remediation of coastal habitats. Mar Ecol Prog Ser 344:1–13.

Patrick CJ, Weller DE, Ryder M (2016) The Relationship Between Shoreline Armoring and Adjacent Submerged Aquatic Vegetation in Chesapeake Bay and Nearby Atlantic Coastal Bays. Estuaries and Coasts 39:158–170.

Patriquin DG (1975) 'Migration' of blowouts in seagrass beds at Barbados and Carriacou, West Indies, and its ecological and geological implications. Aquat Bot 1:163–189.

Pérez M, Invers O, Ruiz JM, Frederiksen MS, Holmer M (2007) Physiological responses of the seagrass *Posidonia oceanica* to elevated organic matter content in sediments: An experimental assessment. J Exp Mar Bio Ecol 344:149–160.

Peterson BJ, Bricker E, Brisbin SJ, Furman BT, Stubler AD, Carroll JM, Berry DL, Gobler CJ, Calladine A, Waycott M (2013) Genetic diversity and gene flow in *Zostera marina* populations surrounding Long Island, New York, USA: No evidence of inbreeding, genetic degradation or population isolation. Aquat Bot 110:61–66.

Pickerell C, Schott S (2017) Peconic Estuary Program 2016 long-term eelgrass (*Zostera marina*) monitoring program. Marine Program Cornell Cooperative Extension prepared for the Peconic Estuary Program. Report 17.

Plaisted HK, Novak AB, Weigel S, Klein AS, Short FT (2019) Eelgrass Genetic Diversity Influences Resilience to Stresses Associated with Eutrophication. Estuaries and Coasts.

Poppe LJ, Eliason AH, Fredericks JJ, Rendigs RR, Blackwood D, Polloni CF (2000) Grain-size analysis of marine sediments: Methodology and data processing. In: U.S. Geological Survey East Coast sediment analysis: Procedures, database, and geo-referenced displays. U.S. Geological Survey Open File Report 00-358.

Pregnall AM, Smith RD, Kursar TA, Alberte RS (1984) Metabolic adaptation of *Zostera marina* (eelgrass) to diurnal periods of root anoxia. Mar Biol 83:141–147.

Pulido C, Borum J (2010) Eelgrass (*Zostera marina*) tolerance to anoxia. J Exp Mar Bio Ecol 385:8–13.

R Core Team (2018) R: A Language and Environment for Statistical Computing.

Reynolds LK, Waycott M, McGlathery KJ, Orth RJ (2016) Ecosystem services returned through seagrass restoration. Restor Ecol 24:583–588.

Rice E, Dam HG, Stewart G (2014) Impact of Climate Change on Estuarine Zooplankton: Surface Water Warming in Long Island Sound Is Associated with Changes in Copepod Size and Community Structure. Estuaries and Coasts 38:13–23.

Robinson NM, Nelson WA, Costello MJ, Sutherland JE, Lundquist CJ (2017) A systematic review of marine-based Species Distribution Models (SDMs) with recommendations for best practice. Front Mar Sci 4:1–11.

Rozell DJ, Wong T fong (2010) Effects of climate change on groundwater resources at Shelter Island, New York State, USA. Hydrogeol J 18:1657–1665.

Santamaría-Gallegos NA, Sánchez-Lizaso JL, Félix-Pico EF (2000) Phenology and growth cycle of annual subtidal eelgrass in a subtropical locality. Aquat Bot 66:329–339.

Saunders MI, Leon J, Phinn SR, Callaghan DP, O'Brien KR, Roelfsema CM, Lovelock CE, Lyons MB, Mumby PJ (2013) Coastal retreat and improved water quality mitigate losses of seagrass from sea level rise. Glob Chang Biol 19:2569–2583.

Schott S (2015) Peconic Estuary Eelgrass (*Zostera marina*) Aerial Survey Ground-Truthing Report. Peconic Estuary Program.

Schumacher BA (2002) Methods for the determination of total organic carbon (TOC) in soils and sediments. US Environ Prot Agency, Washingt DC:1–25.

Shields EC, Moore K, Parrish D (2018) Adaptations by *Zostera marina* Dominated Seagrass Meadows in Response to Water Quality and Climate Forcing. Diversity 10:125.

Short FT, Burdick DM, Kaldy JE (1995) Mesocosm experiments quantify the effects of eutrophication on eelgrass, *Zostera marina*. Limnol Oceanogr 40:740–749.

Short FT, Muehlstein LK, Porter D (1987) Eelgrass wasting disease: Cause and recurrence of a marine epidemic. Biol Bull 173:557–562.

Short FT, Polidoro B, Livingstone SR, Carpenter KE, Bandeira S, Bujang JS, Calumpong HP, Carruthers TJB, Coles RG, Dennison WC, Erftemeijer PLA, Fortes MD, Freeman AS, Jagtap TG, Kamal AHM, Kendrick GA, Judson Kenworthy W, La Nafie YA, Nasution IM, Orth RJ, Prathep A, Sanciangco JC, Tussenbroek B van, Vergara SG, Waycott M, Zieman JC (2011) Extinction risk assessment of the world's seagrass species. Biol Conserv 144:1961–1971.

Smith RD, Pregnall AM, Alberte RS (1988) Effects of anaerobiosis on root metabolism of *Zostera marina* (eelgrass): Implications for survival in reducing sediments. Mar Biol 98:131–141.

Soren J (1978) Hydrogeologic conditions in the town of Shelter Island, Suffolk County, Long Island, New York. U.S. Geological Survey. Water-Resources Investigations 77-77.

Staehr PA, Borum J (2011) Seasonal acclimation in metabolism reduces light requirements of eelgrass (*Zostera marina*). J Exp Mar Bio Ecol 407:139–146.

Tettelbach ST, Peterson BJ, Carroll JM, Furman BT, Hughes SWT, Havelin J, Europe JR, Bonal DM, Weinstock AJ, Smith CF (2015) Aspiring to an altered stable state: Rebuilding of bay scallop populations and fisheries following intensive restoration. Mar Ecol Prog Ser 529:121–136.

Thayer GW, Stuart HH (1974) The bay scallop makes its bed of seagrass. Mar Fish Rev 36:27–30.

Tuszynski J (2019) CaTools: Tools: moving window statistics, GIF, Base64, ROC AUC, etc.

Uhrin A V., Turner MG (2018) Physical drivers of seagrass spatial configuration: the role of thresholds. Landsc Ecol 33:2253–2272.

Valiela I, Costa J, Foreman K, Teal JM, Howes B, Aubrey D (1990) Transport of groundwater-borne nutrients from watersheds and their effects on coastal waters. Biogeochemistry 10:177–197.

Valle M, van Katwijk MM, de Jong DJ, Bouma TJ, Schipper AM, Chust G, Benito BM, Garmendia JM, Borja Á (2013) Comparing the performance of species distribution models of *Zostera marina*: Implications for conservation. J Sea Res 83:56–64.

Waycott M, Collier C, Mcmahon K, Ralph P, Mckenzie L, Udy J, Grech A (2007) Vulnerability of seagrasses in the Great Barrier Reef to climate change. In: *Climate Change and the Great Barrier Reef, Great Barrier Reef Marine Park Authority and Australian Greenhouse Office*. Johnson JE, Marhall PA (eds) p 193–236

Wickham H, François R, Henry L, Müller K (2020) Dplyr: A Grammar of Data Manipulation.

Wilson KL, Lotze HK (2019) Climate change projections reveal range shifts of eelgrass *Zostera marina* in the Northwest Atlantic. Mar Ecol Prog Ser 620:47–62.

Wing J, Kuhn M (2019) Caret: Classification and Regression Training.

Zeebe RE, Wolf-Gladrow D (2001) CO_2 in seawater: Equilibrium, kinetics, isotopes. Elsevier Science, Amserdam.

Zeileis A, Grothendieck G (2005) Zoo: S3 Infrastructure for Regular and Irregular Time Series. J Stat Softw 14:1–27.

Zimmerman RC, Hill VJ, Gallegos CL (2015) Predicting effects of ocean warming, acidification, and water quality on Chesapeake region eelgrass. Limnol Oceanogr 60:1781–1804.

Zimmerman RC, Kohrs DG, Steller DL, Alberte RS (1997) Impacts of CO2 enrichment on productivity and light requirements of eelgrass. Plant Physiol 115:599–607.

Zimmerman RC, Reguzzoni JL, Alberte RS (1995) Eelgrass (*Zostera marina* L.) transplants in San Francisco Bay: Role of light availability on metabolism, growth and survival. Aquat Bot 51:67–86.

Zimmerman RC, Reguzzoni JL, Wyllie-Echeverria S, Josselyn M, Alberte RS (1991) Assessment of environmental suitability for growth of *Zostera marina* L. (eelgrass) in San Francisco Bay. Aquat Bot 39:353–366.

Zimmerman RC, Smith RD, Alberte RS (1989) Thermal acclimation and whole-plant carbon balance in *Zostera marina* L. (eelgrass). J Exp Mar Bio Ecol 130:93–109.

FIGURES

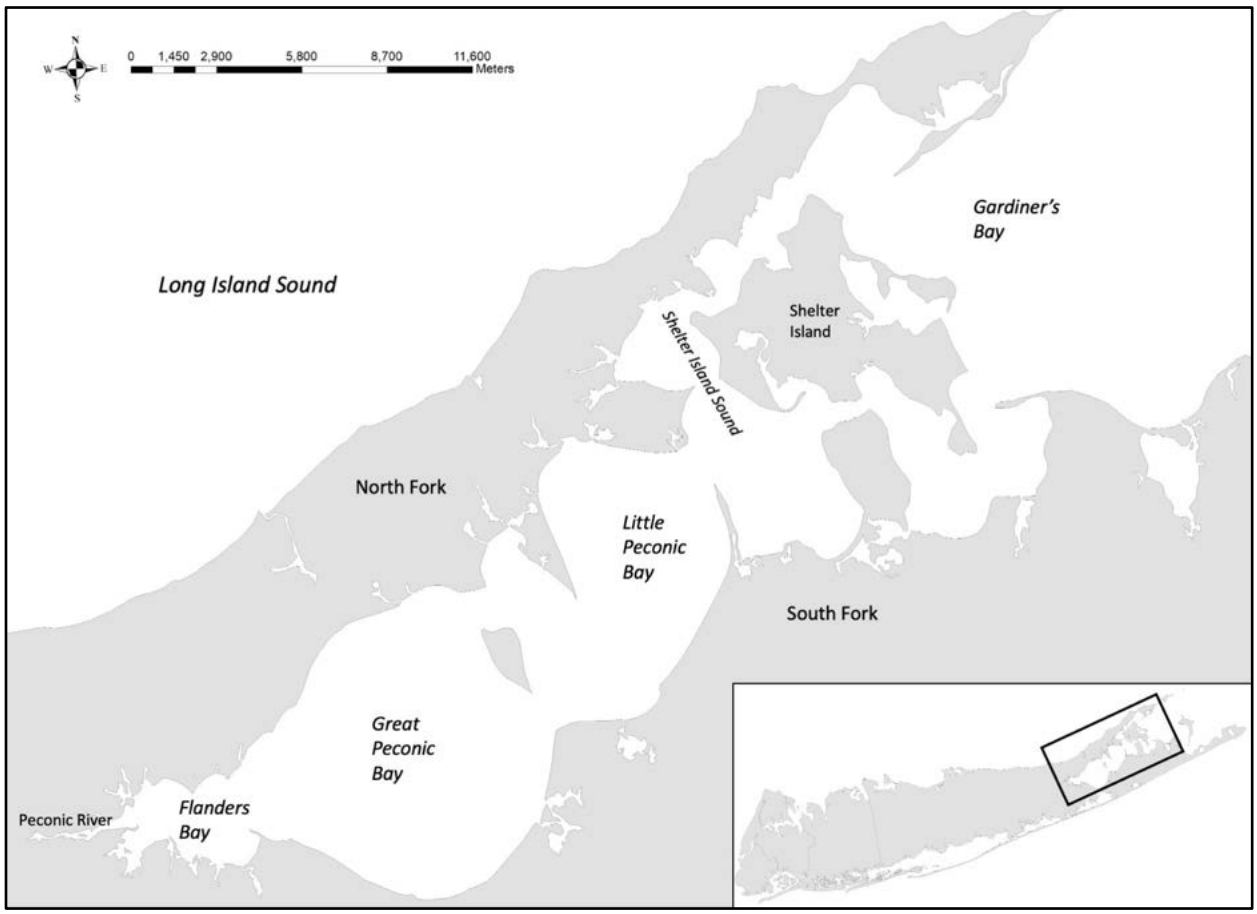

Figure 1: Peconic Bay, Long Island, NY.

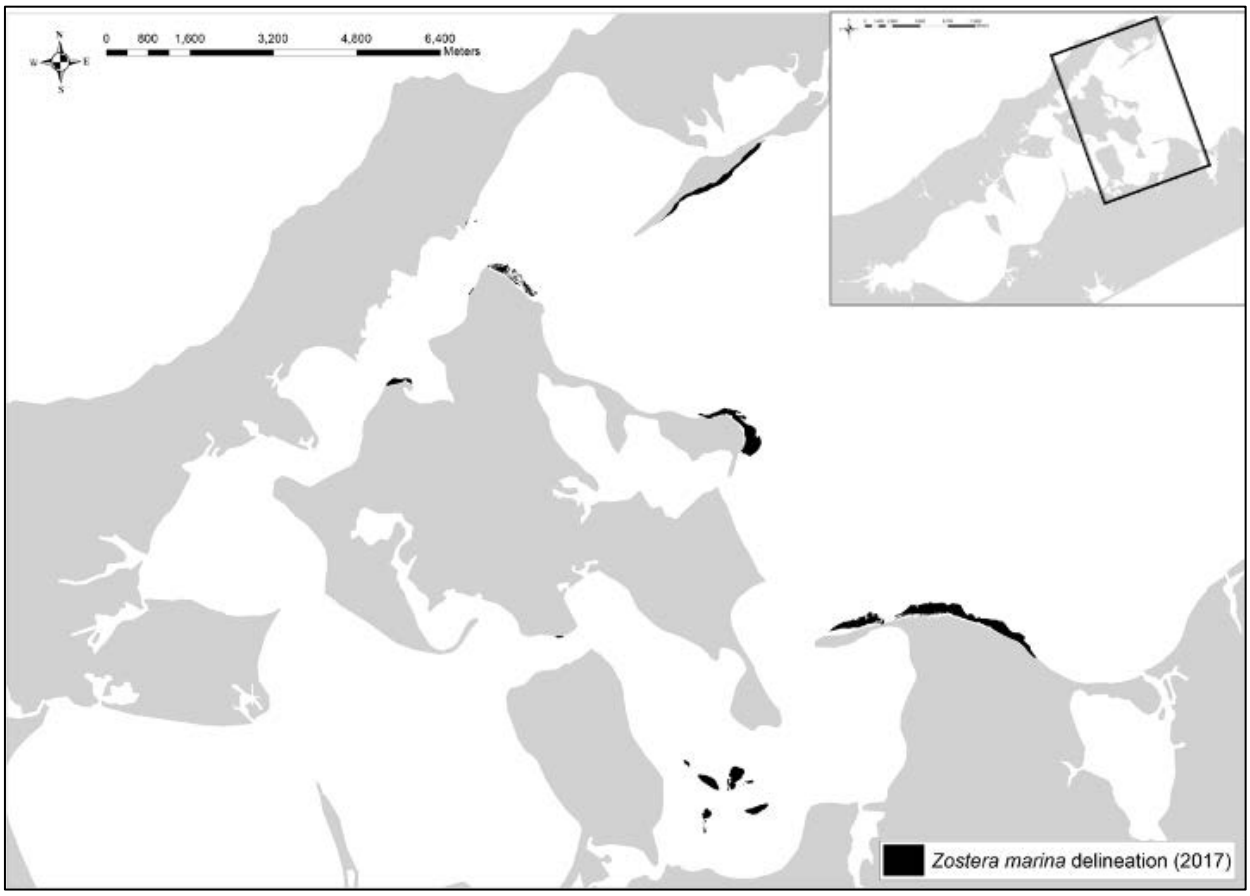

Figure 2: *Zostera marina* extent in Peconic Bay delineated from 2017 orthoimagery.

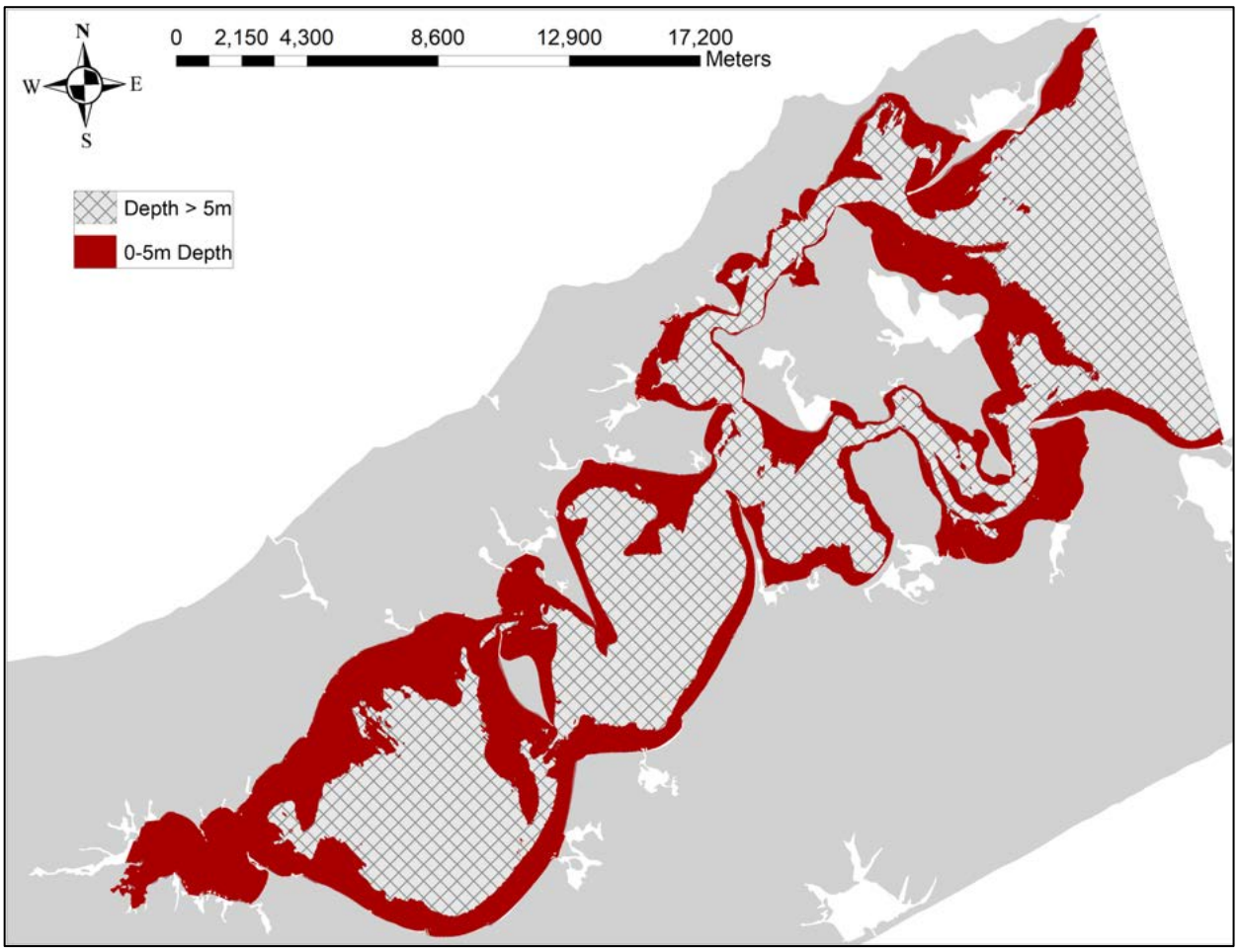

Figure 3: "Ideal" bathymetry mask used to create a random point sample file of 50,000.

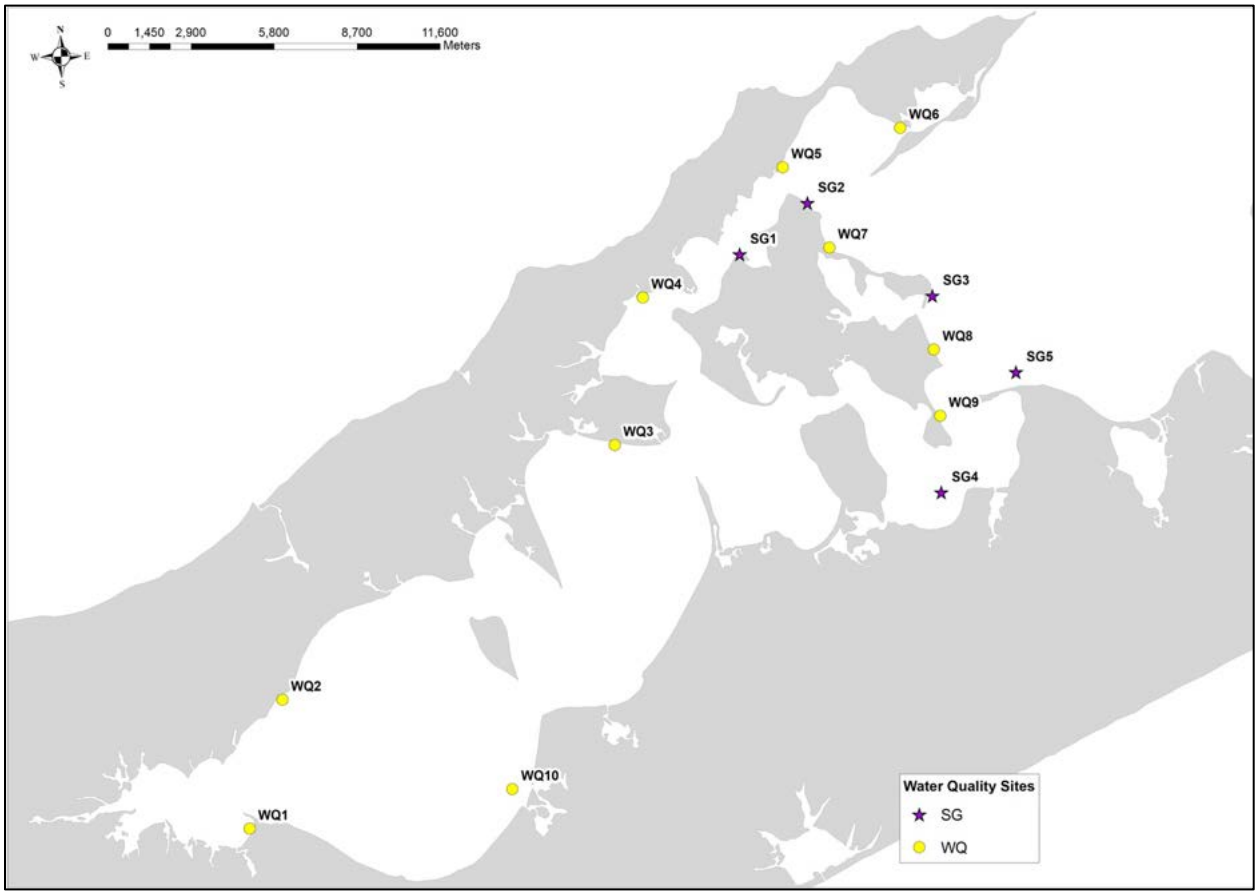

Figure 4: Water quality sampling locations in Peconic Bay for 2017 and 2018. Type indicates whether sampling occurred in seagrass (SG) or non-seagrass areas (WQ).

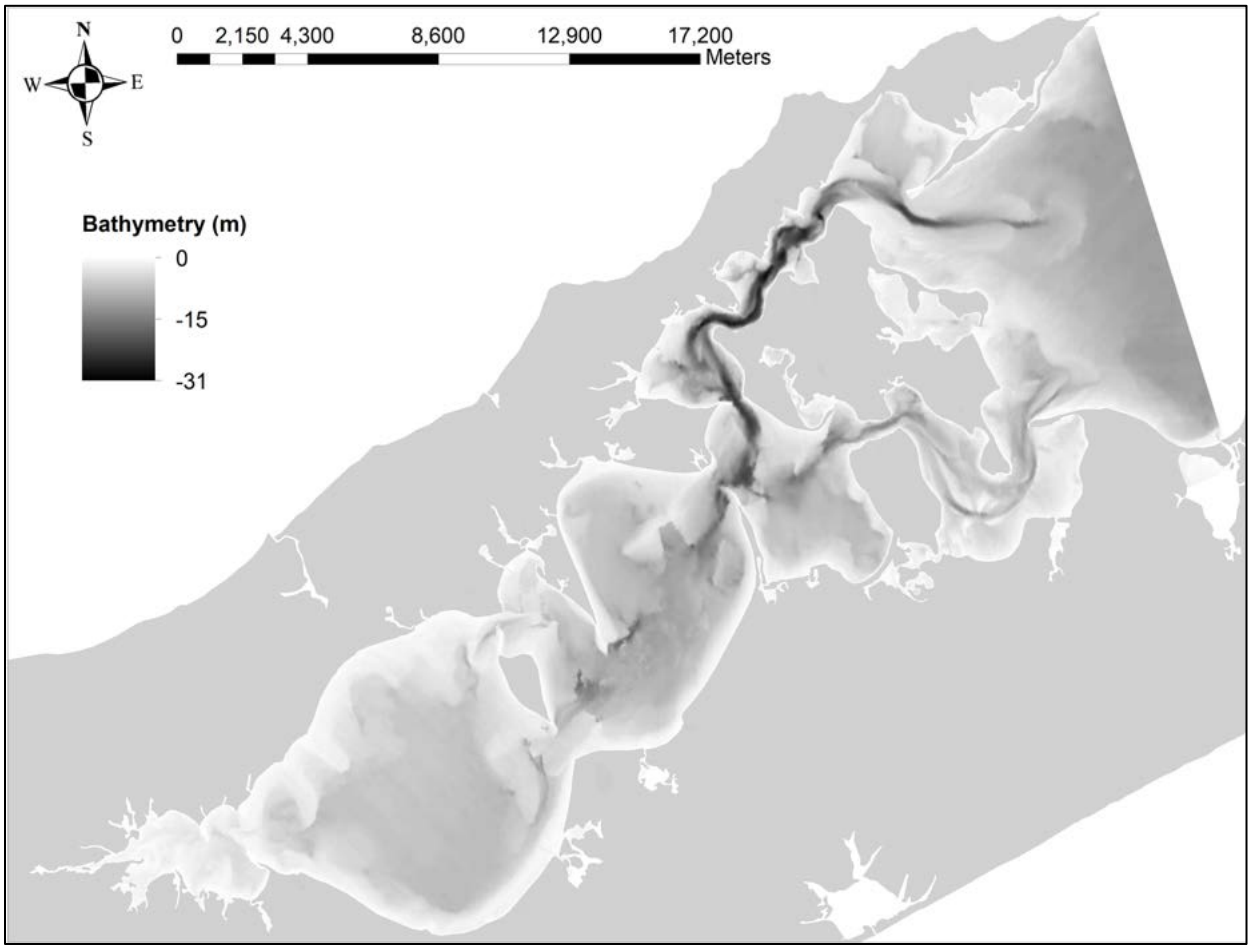

Figure 5: Water depth (m) at mean low water (MLW).

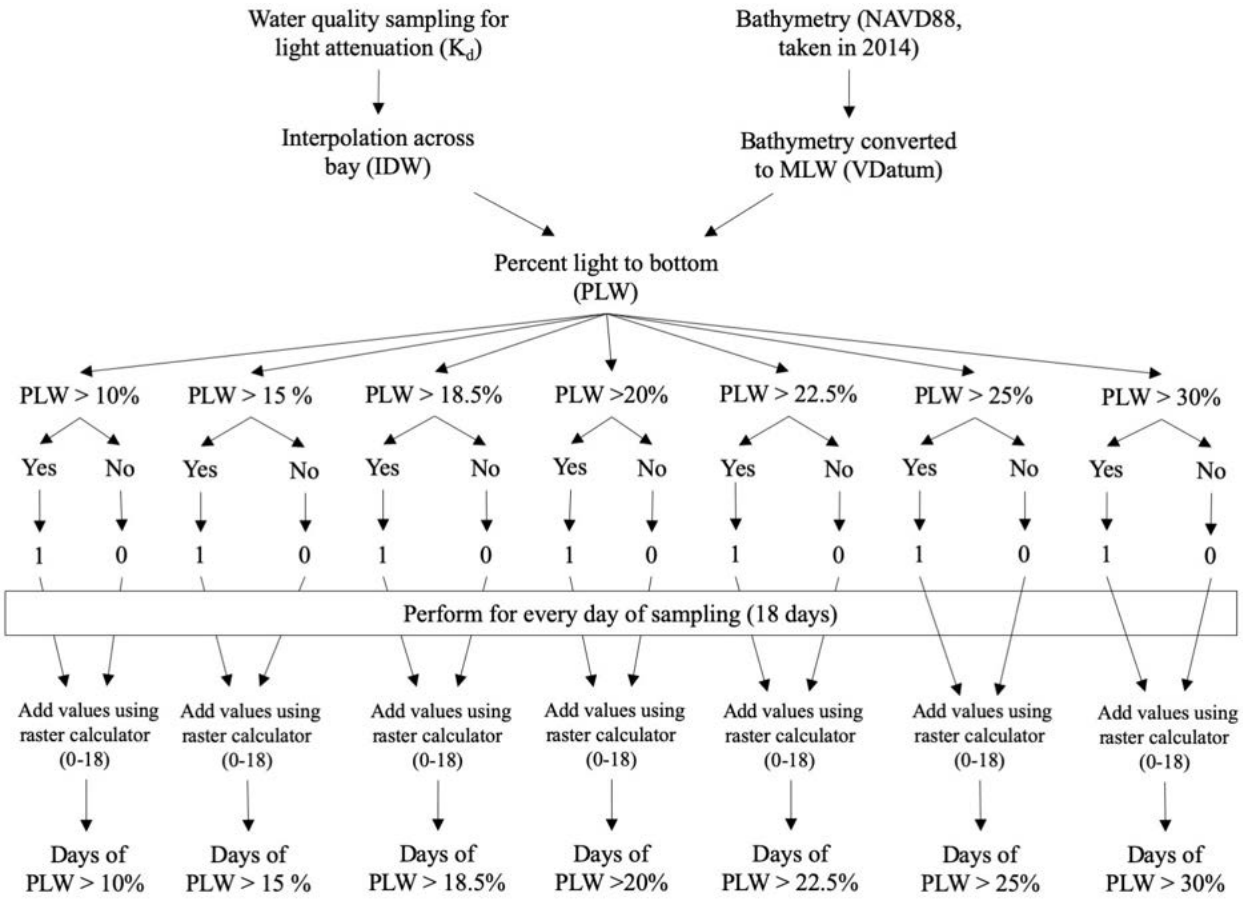

Figure 6: Percent light through water (PLW) schematic. Collected K_d (light attenuation) values are interpolated and used with bathymetry (m) to calculate percent light to bottom for every sampling day (18 days). The resulting raster layers were then classified into above (1) or below (0) 10, 15, 18.5, 20, 22.5, 25, and 30% thresholds to determine a single layer (0-18 values) of analysis for each light threshold incorporating all days.

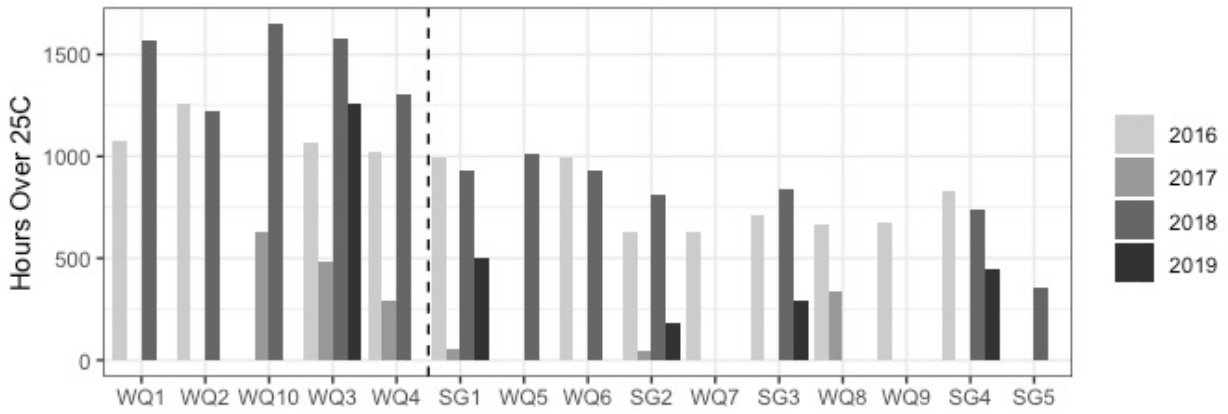

Figure 7: Cumulative hours of temperature over 25 ºC at each site determined from HOBO temperature loggers left out for the summers of 2016-2019.

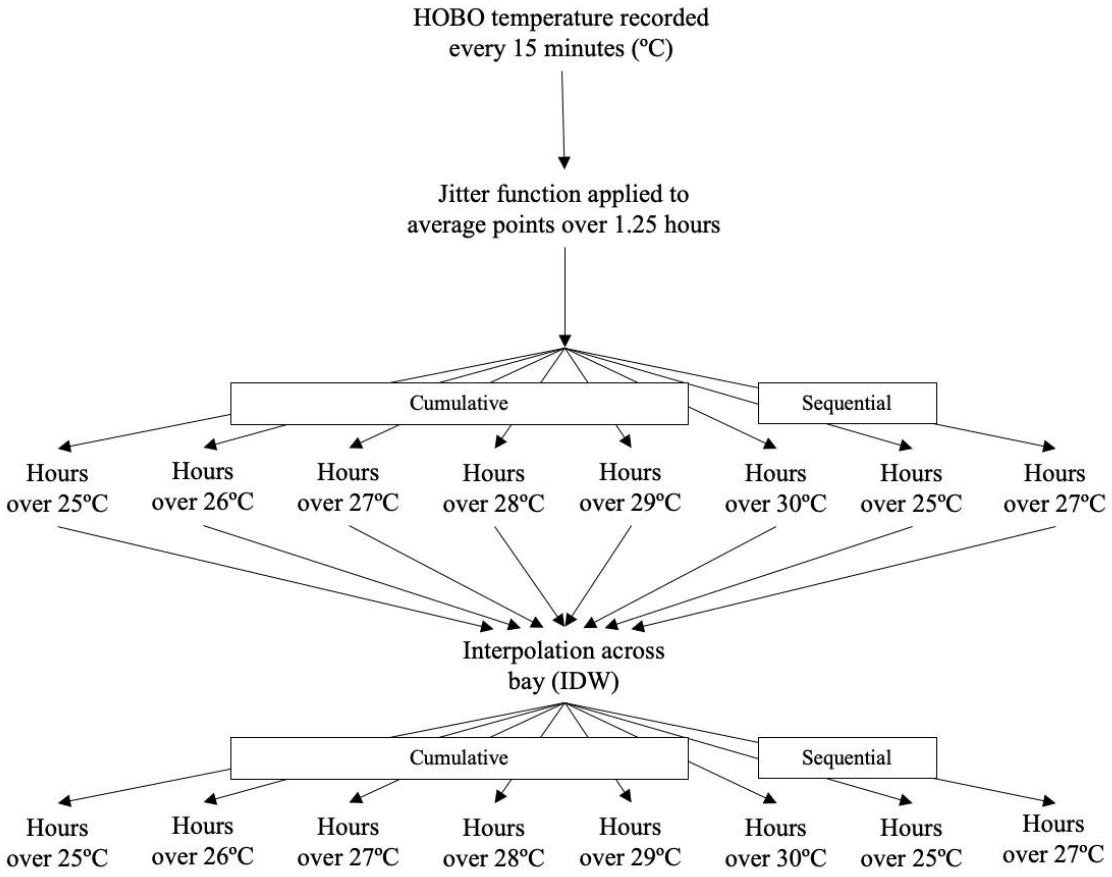

Figure 8: Schematic for creation of temperature layers. HOBO temperature from 2018 was used, this was the hottest year of data collection. Cumulative hours over temperatures of 25-30 ºC and sequential hours over 25 and 27 ºC were computed and interpolated across Peconic bay.

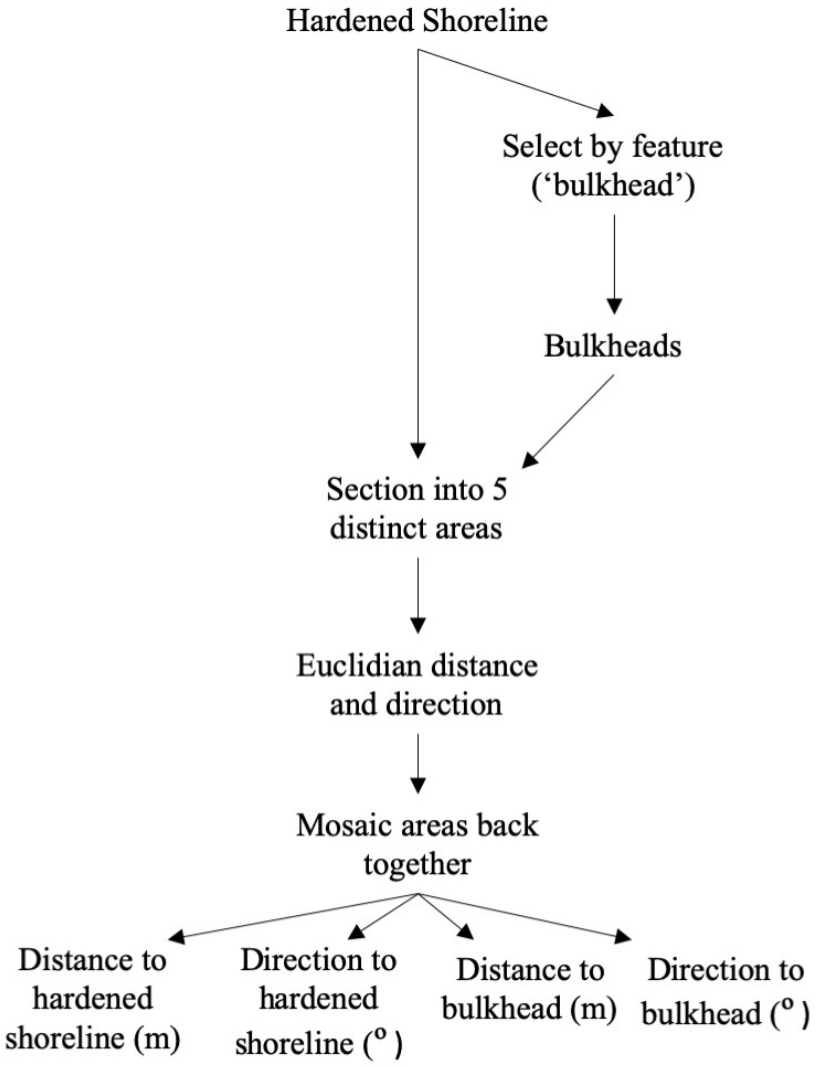

Figure 9: Schematic for creation of hardened shoreline and bulkhead raster layers for distance (m) and direction (°) by Euclidian distance and direction functions.

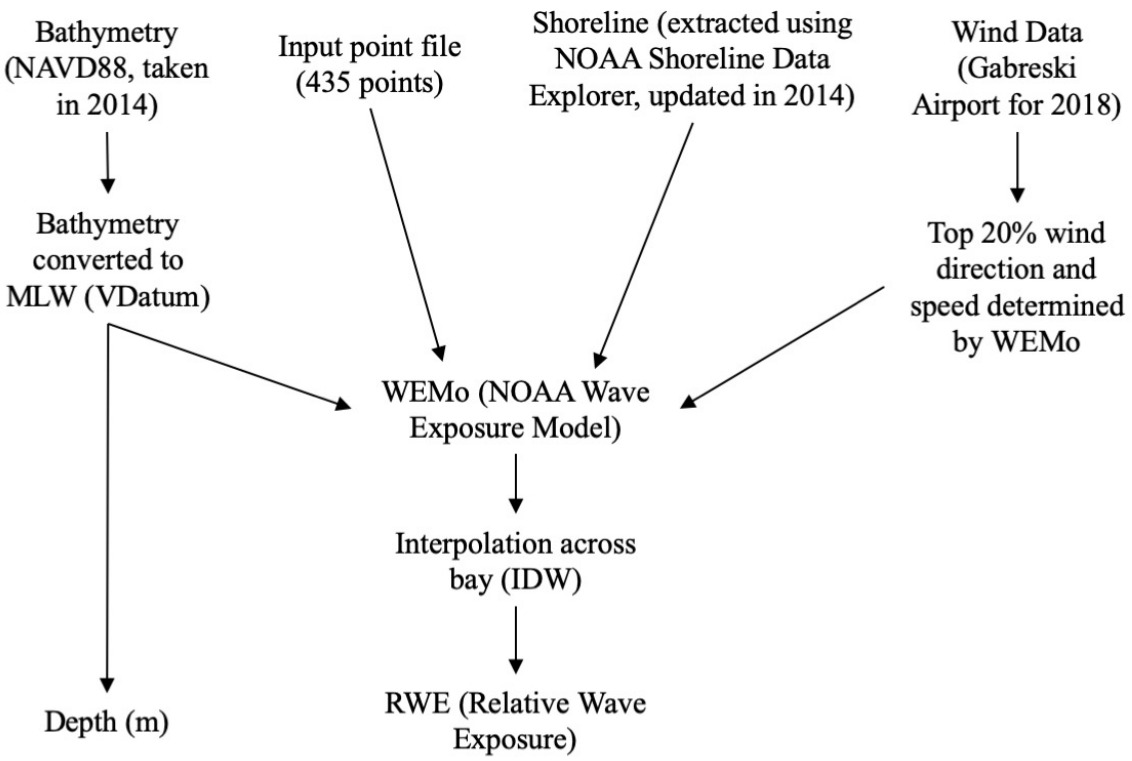

Figure 10: Wave exposure model schematic. Wind speed from Gabreski Airport in 2018, shoreline, and bathymetry at mean low water were used by the WEMo (Wave Exposure Model) to determine relative wave exposure at 435 points across Peconic Bay.

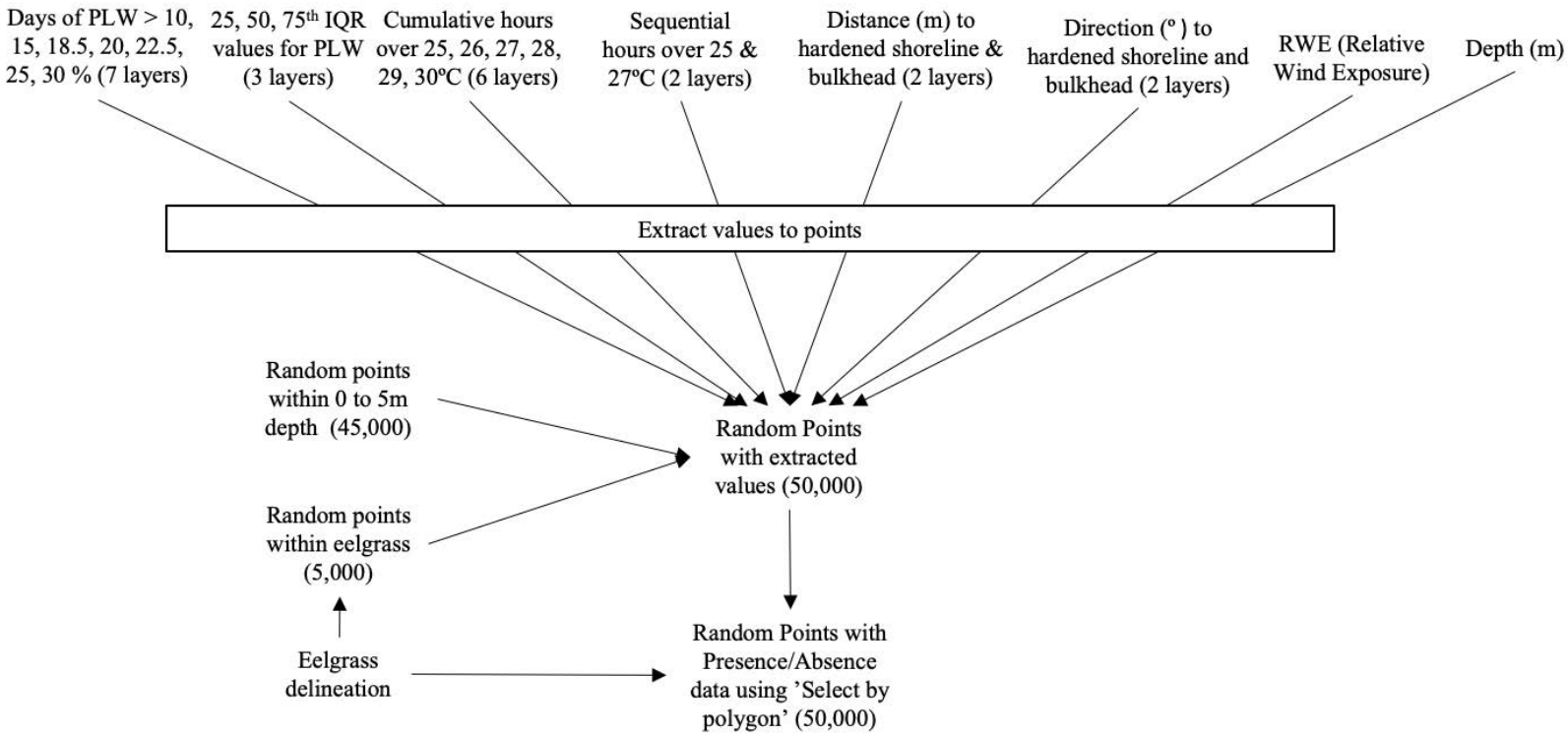

Figure 11: Schematic for creation of random points file to be used with the random forest modeling.

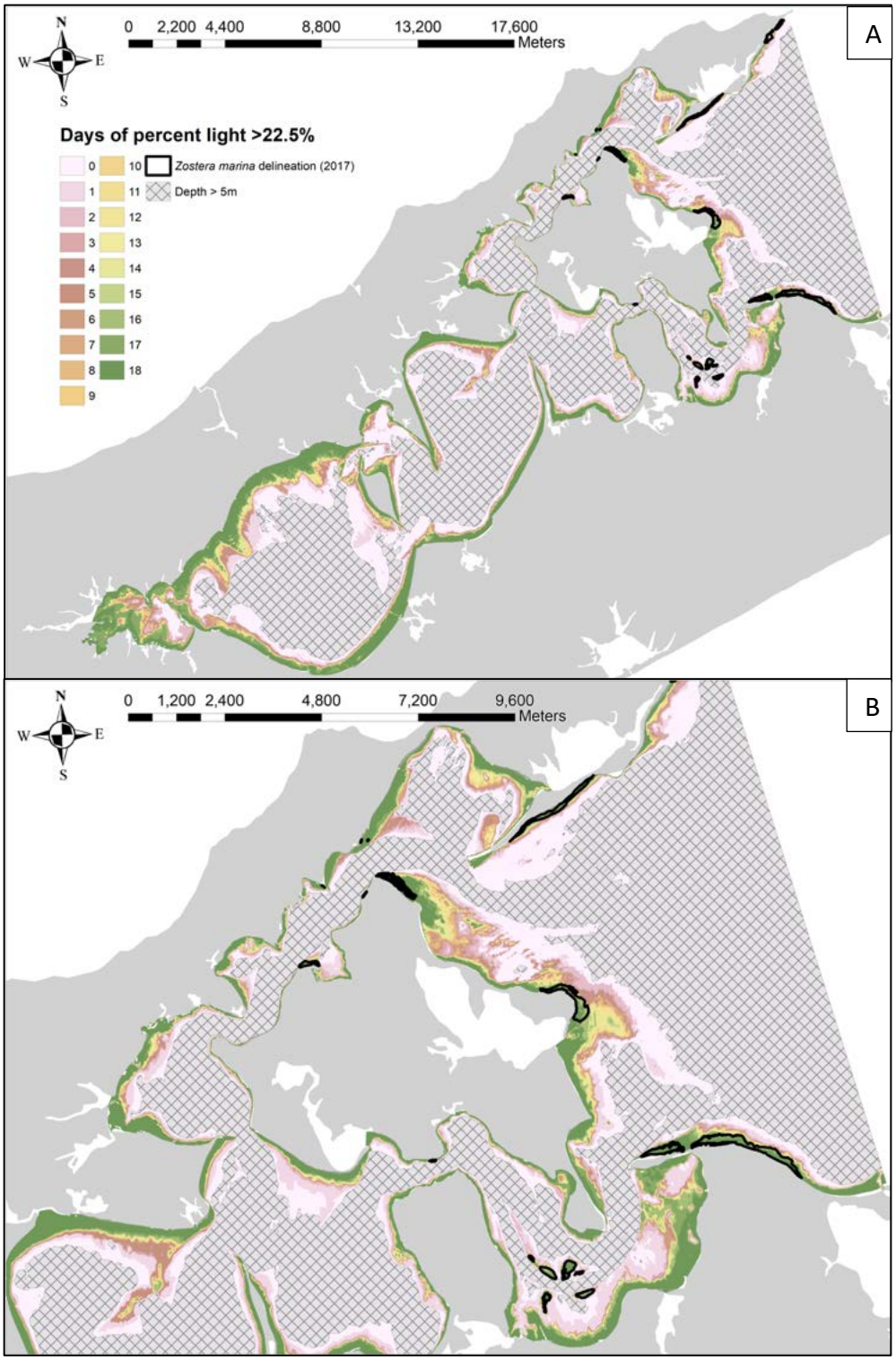

Figure 21: Days over PLW > 22.5% calculated from K_d and bathymetry. Depths > 5m were excluded (hash) due to low light levels and no *Z. marina* growing deeper than 4.5m at MLW. (A) All of Peconic Bay, (B) close-up.

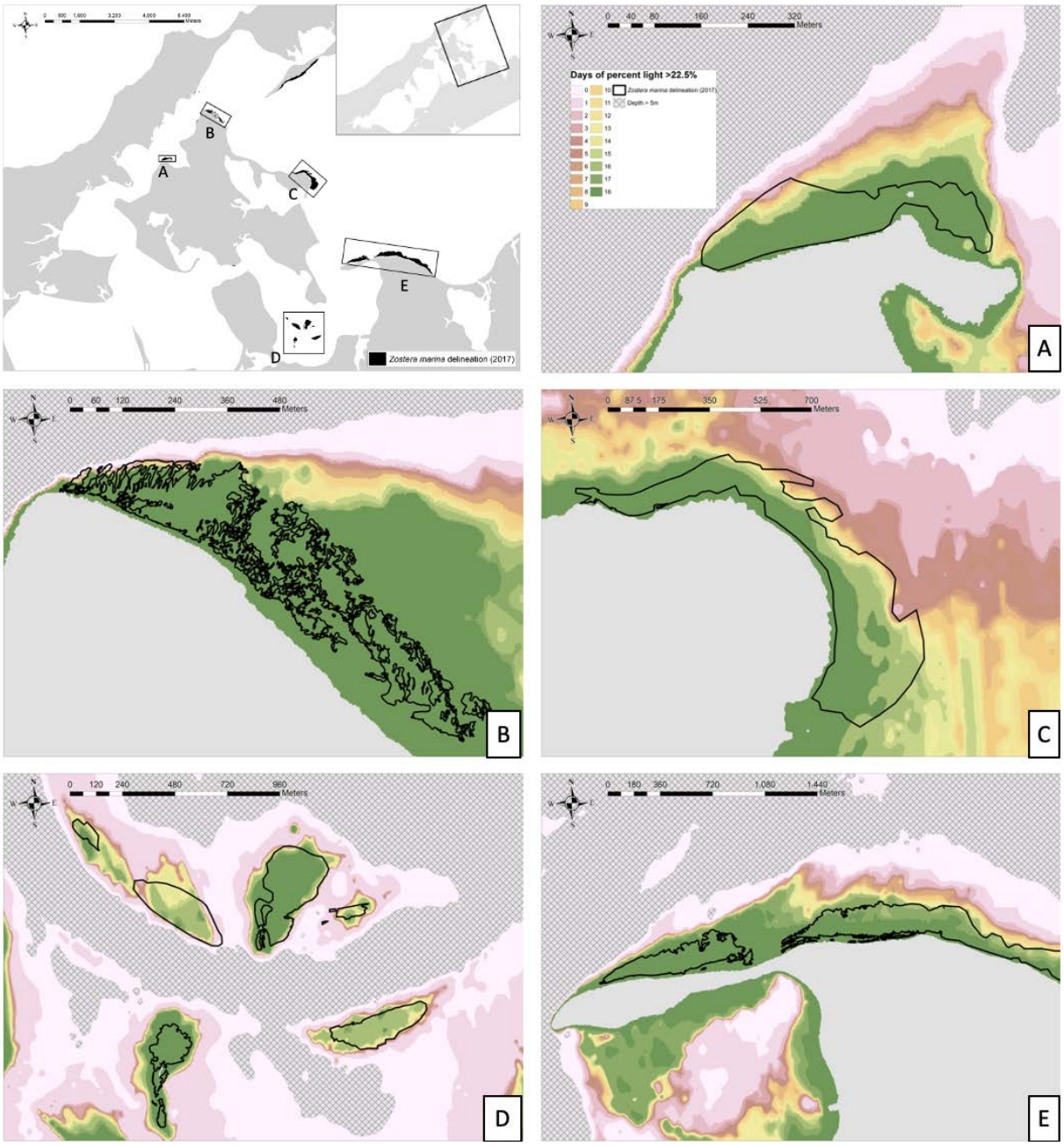

Figure 13: Days over PLW > 22.5% at *Z. marina* beds, (A) SG1, (B) SG2, (C) SG3, (D) SG4, (E) SG5, calculated from K_d and bathymetry. Depths > 5m were excluded (hash) due to low light levels and no *Z. marina* growing deeper than 4.5m at MLW.

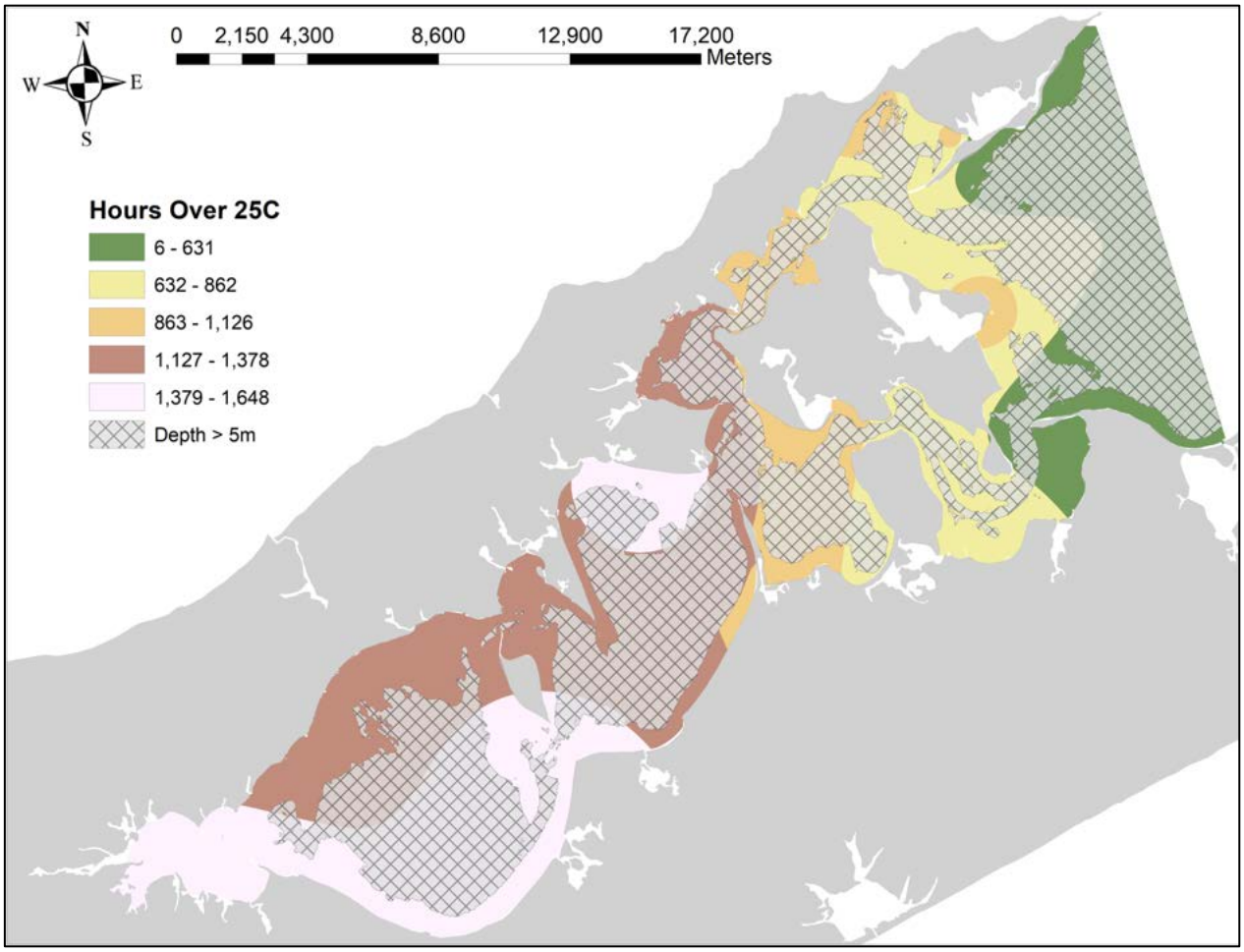

Figure 14: Cumulative hours over 25 ºC interpolated across Peconic Bay for 2018.

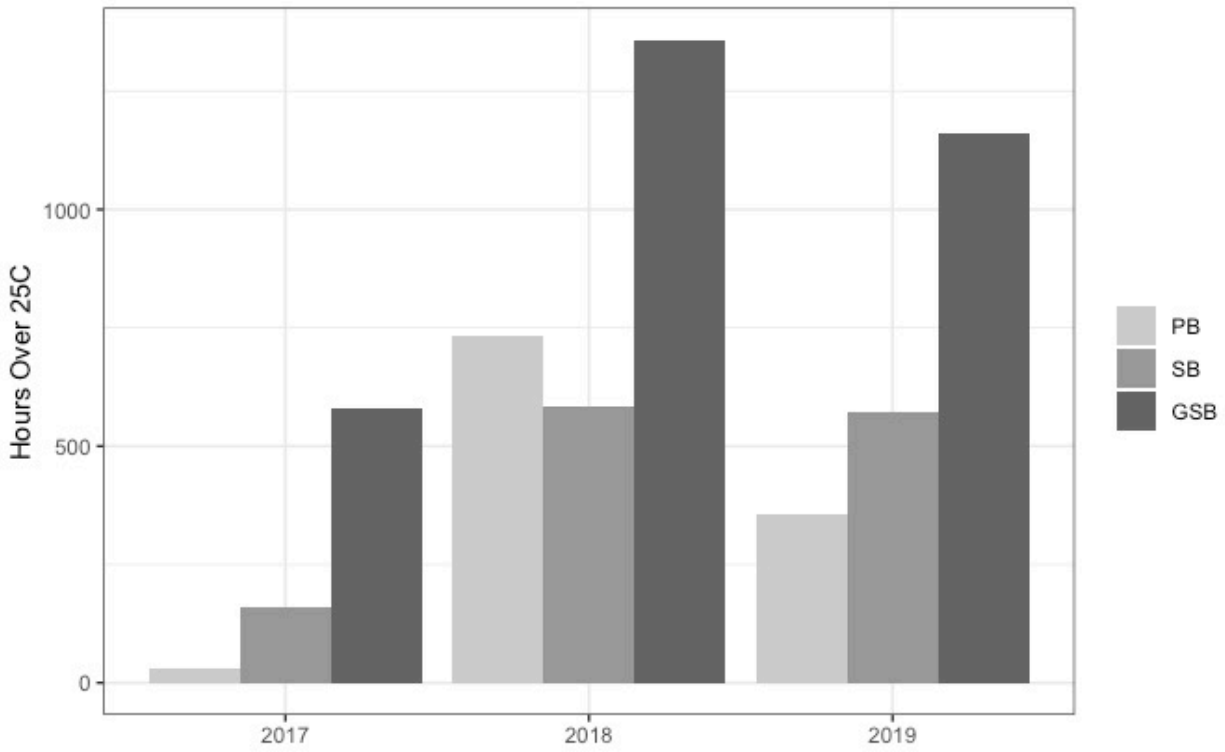

Figure 15: Cumulative hours over 25 ºC at locations with *Z. marina* between three bays (PB = Peconic Bay, SB = Shinnecock Bay, GSB = Great South Bay) on Long Island, NY for three years of sampling (2017-2019).

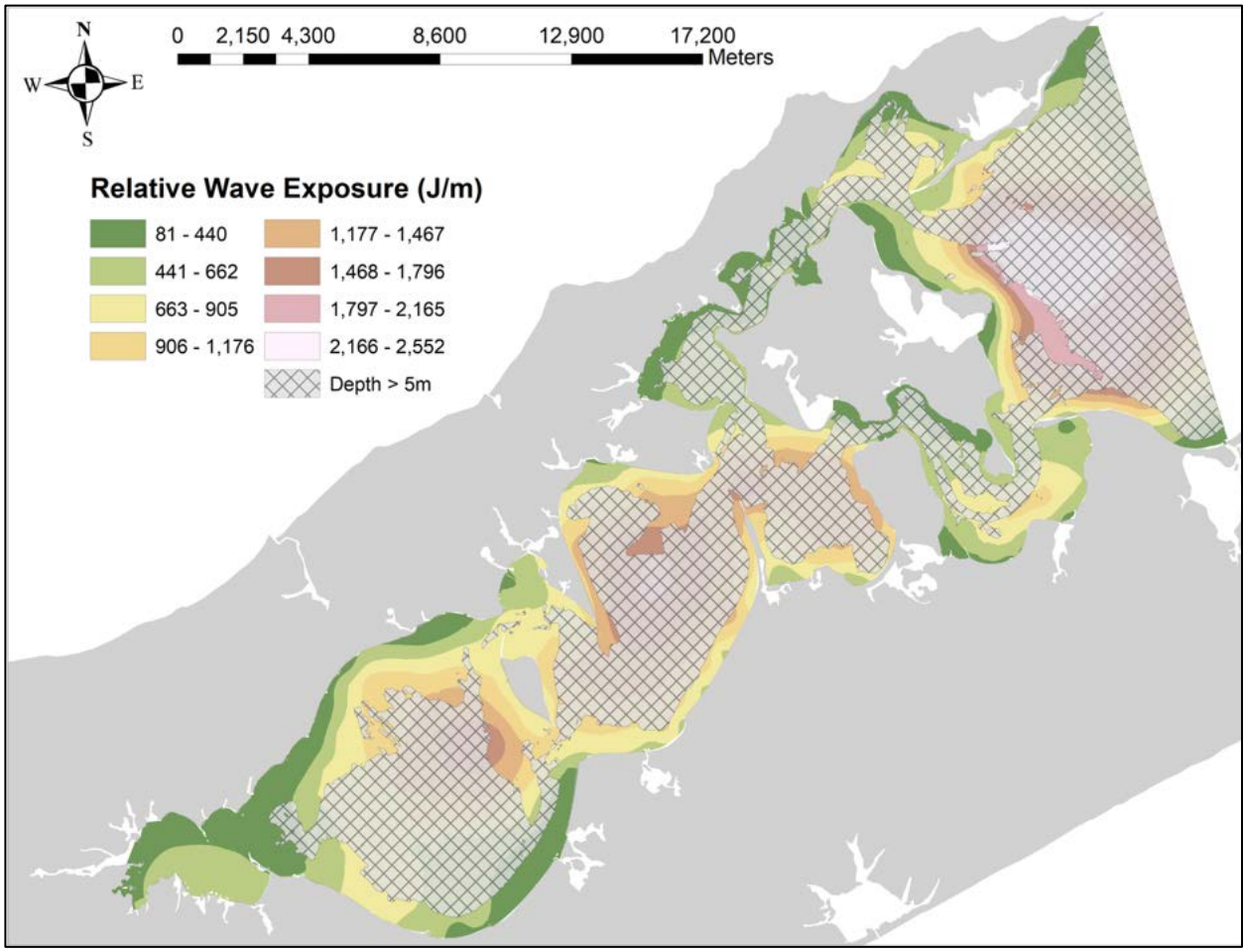

Figure 16: Wave exposure layer. Wind speed from Gabreski Airport in 2018, shoreline, and bathymetry at mean low water were used by the WEMo (Wave Exposure Model) to determine relative wave exposure at 435 points across Peconic Bay.

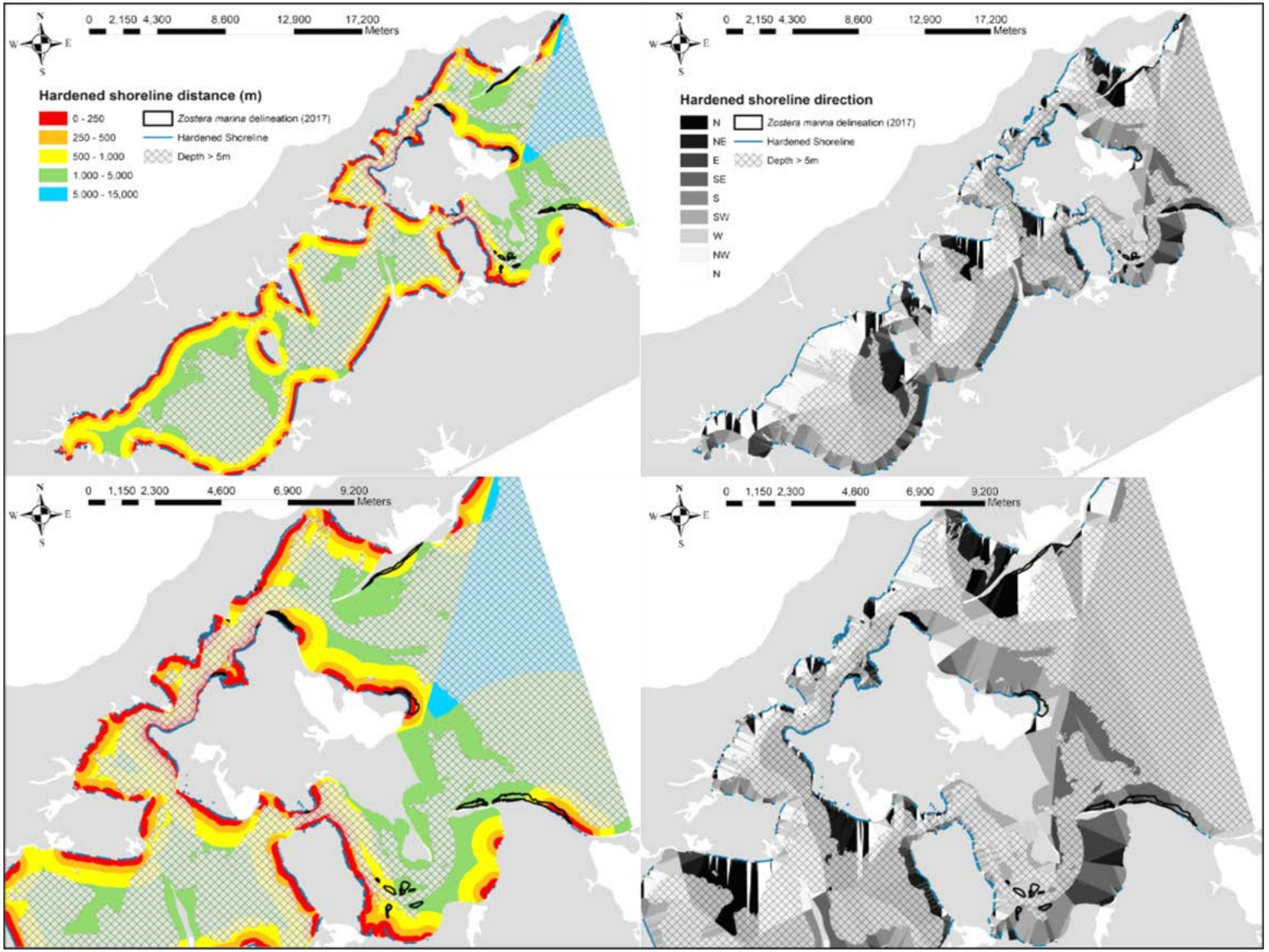

Figure 17: Distance (left) and direction (right) to hardened shorelines in Peconic Bay calculated through Euclidian distance.

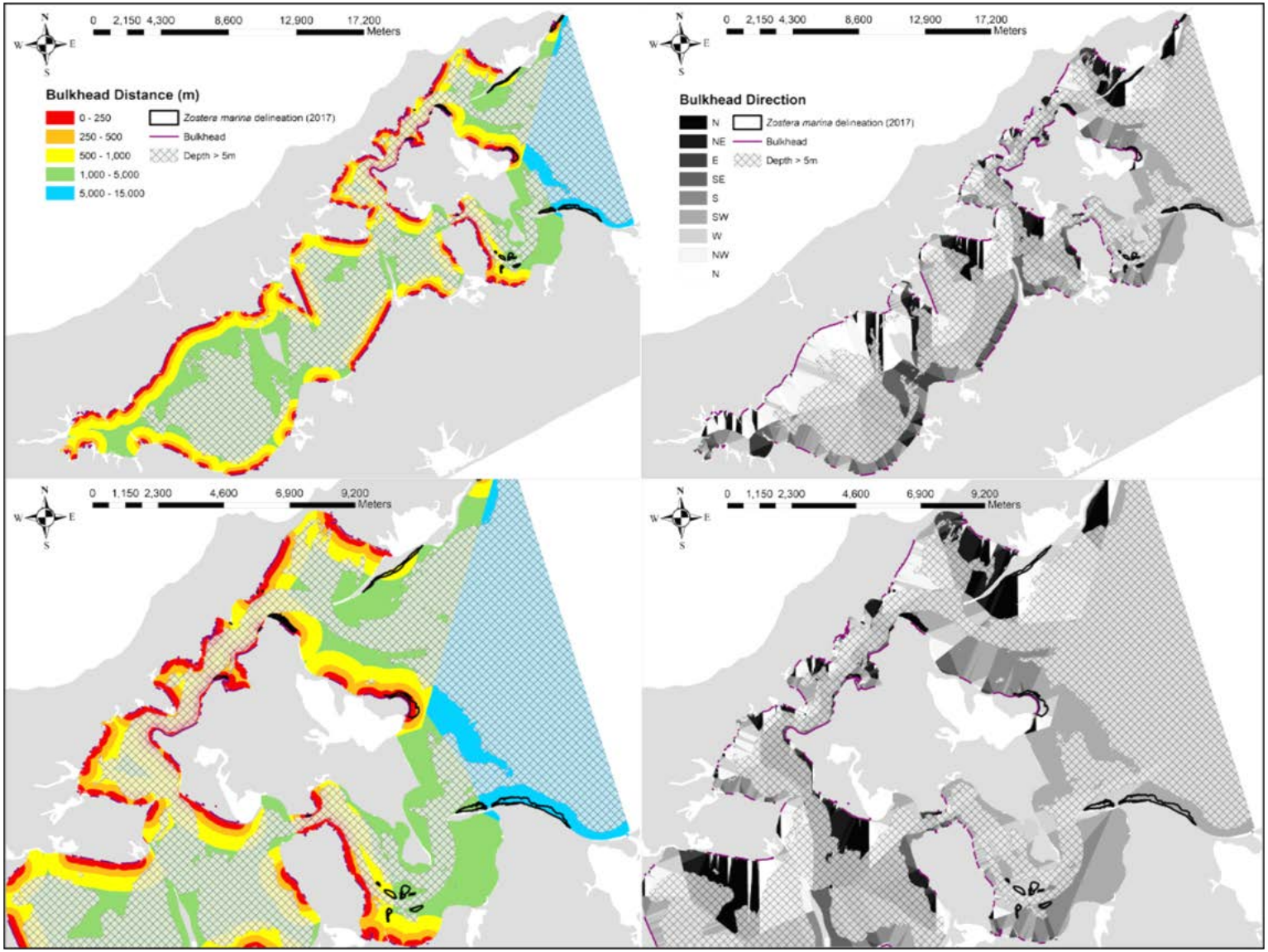

Figure 18: Distance (left) and direction (right) to bulkheads in Peconic Bay calculated through Euclidian distance.

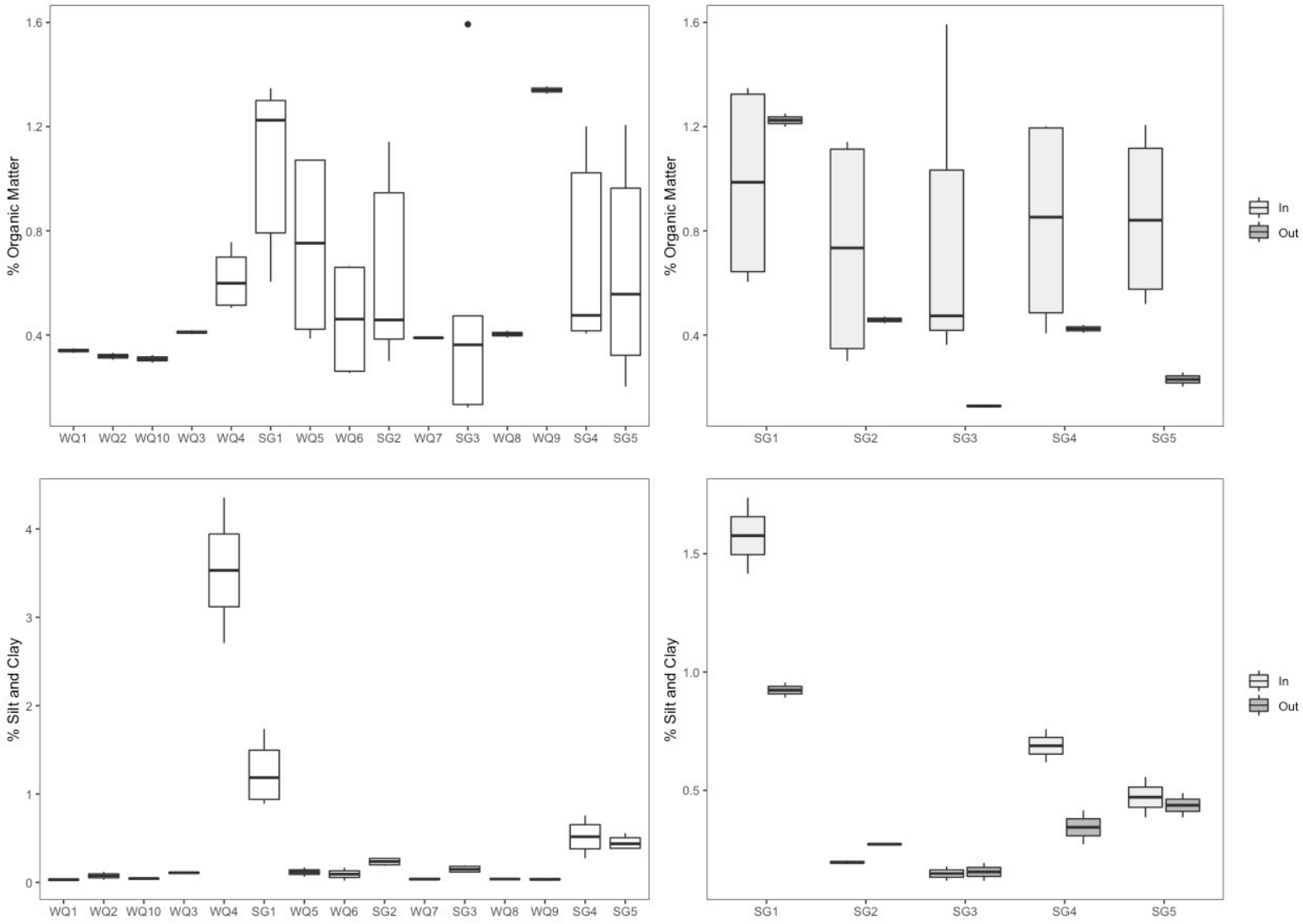

Figure 19: Boxplots of % organic matter and % silt and clay from sediment cores taken at all water quality sites in 2018 and 2019 (left). Boxplots displaying the difference in % organic matter and % silt and clay between *Z. marina* sites where samples were taken in and directly out of *Z. marina* (0.25m).

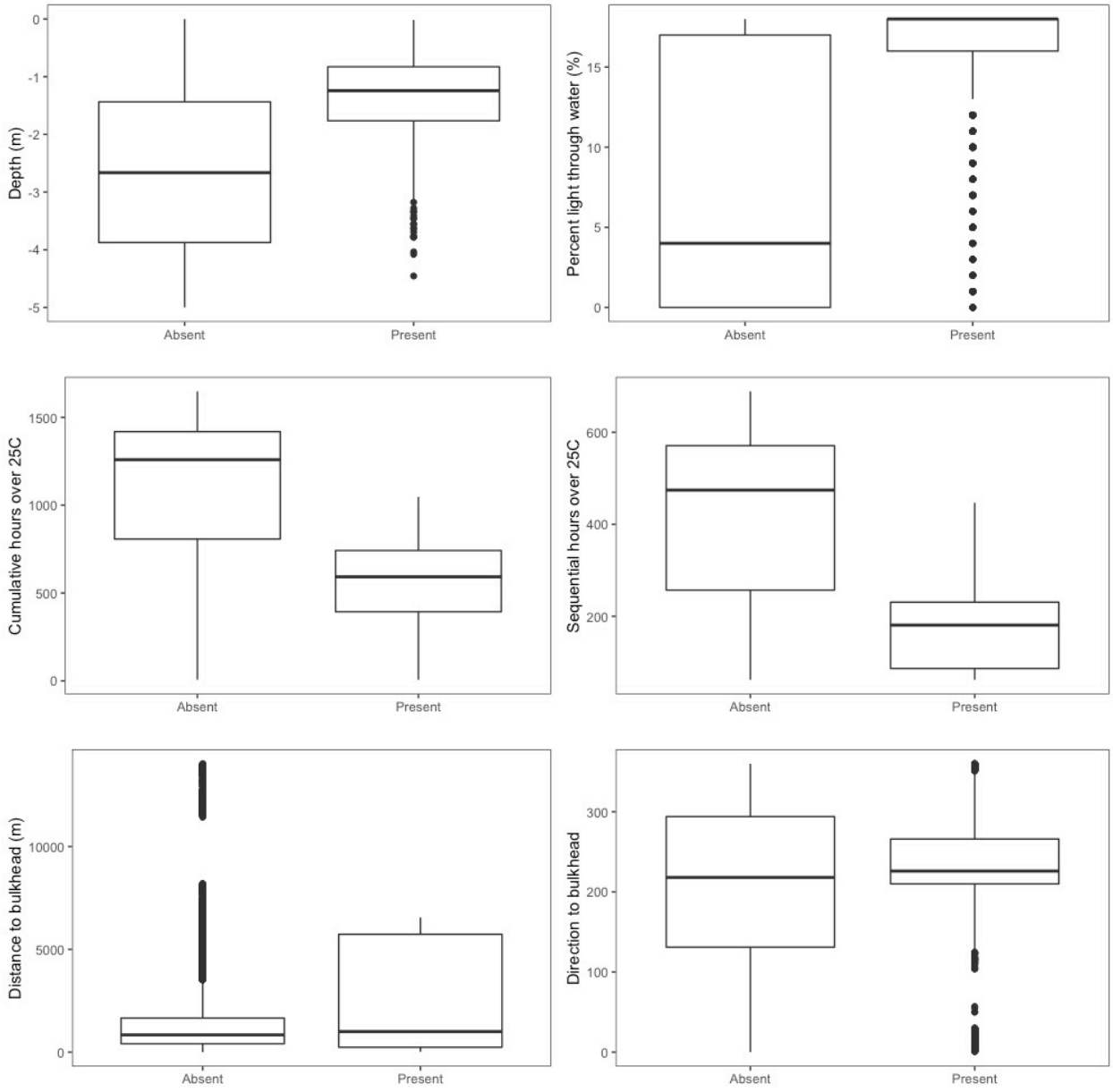

Figure 20: Boxplots between present and absent points of *Z. marina* for depth, percent light to bottom, cumulative and sequential hours over 25 ºC, and distance/direction to bulkhead.

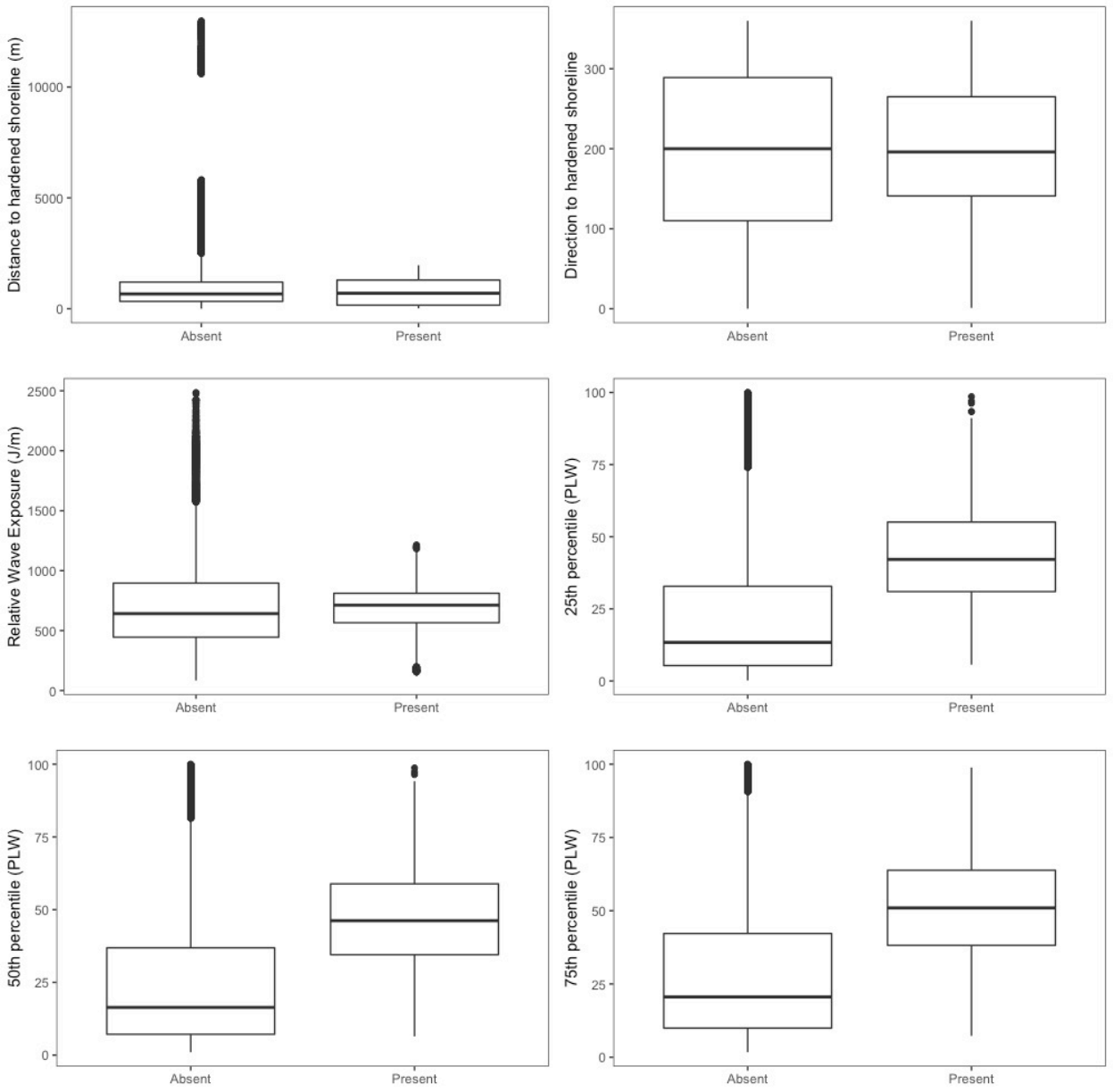

Figure 21: Boxplots between present and absent points of *Z. marina* for distance/direction to hardened shorelines, relative wave exposure, 25, 50, 75th IQR values for PLW.

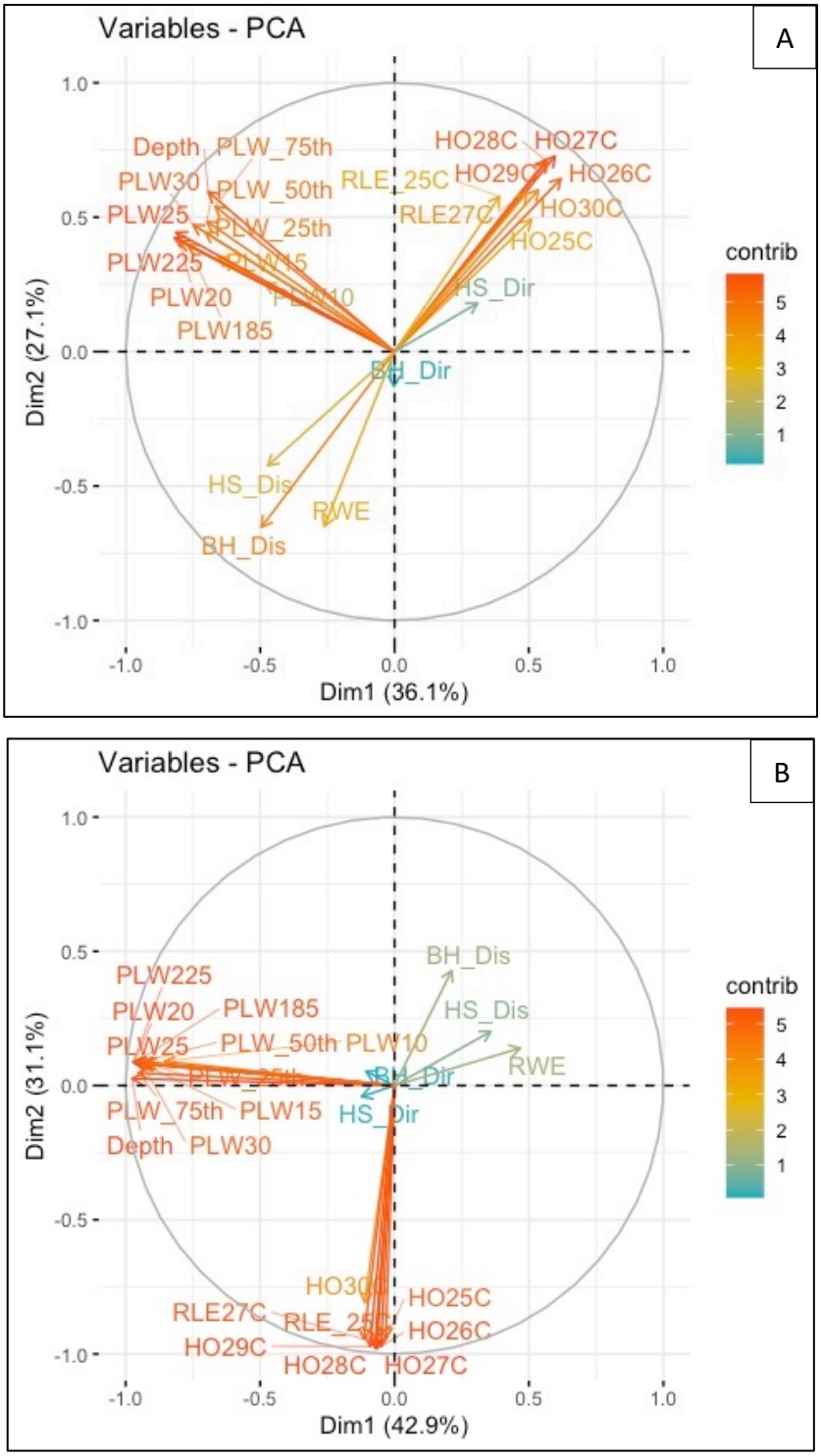

Figure 22: Principle component analysis of (A) variables with *Z. marina* and (B) variables with and without *Z. marina*. Variables were scaled and centered.

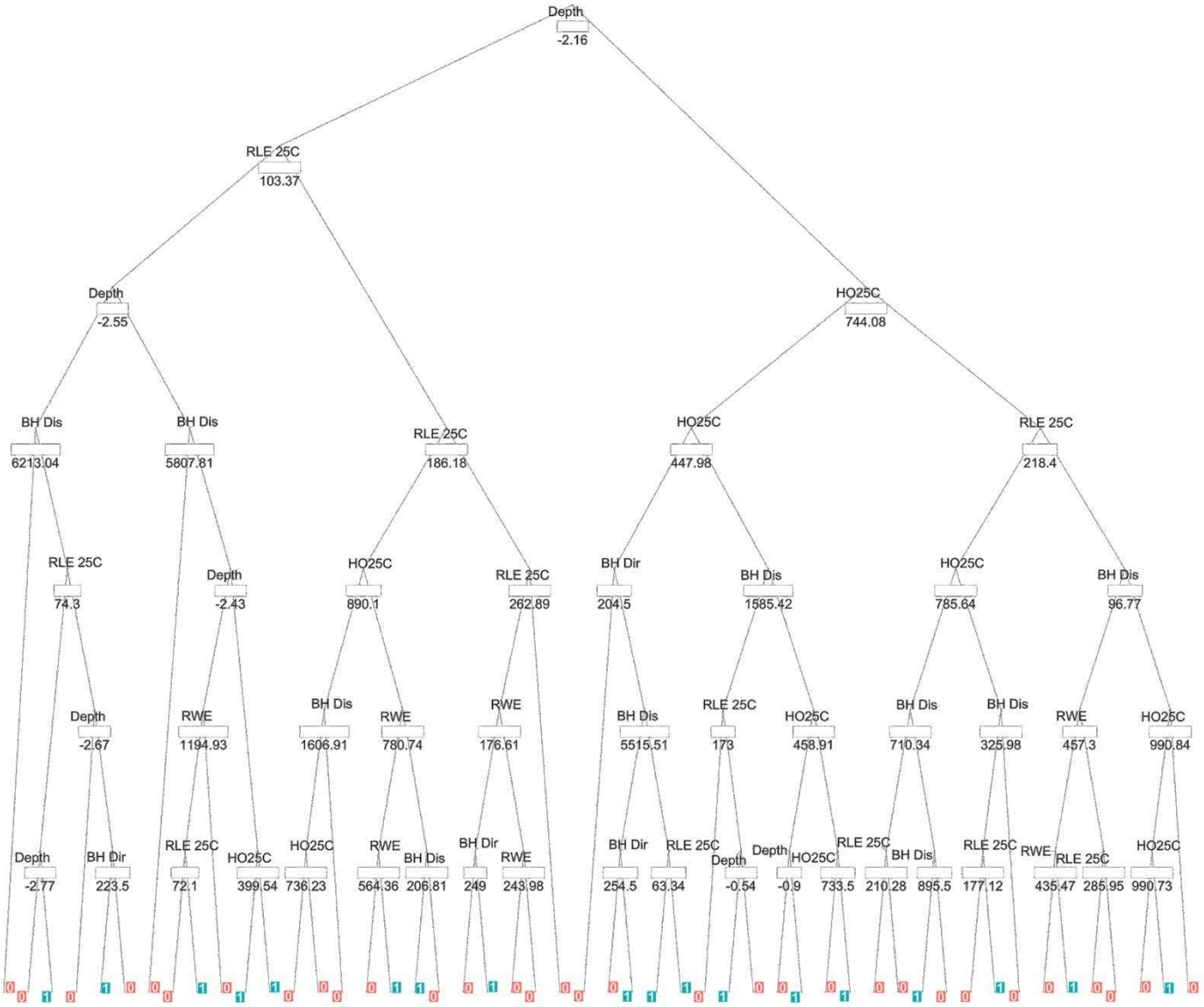

Figure 23: "Tree" of outcomes resulting from the Restoration Potential (RP) model, 1 = present *Z. marina*, 0 = absent.

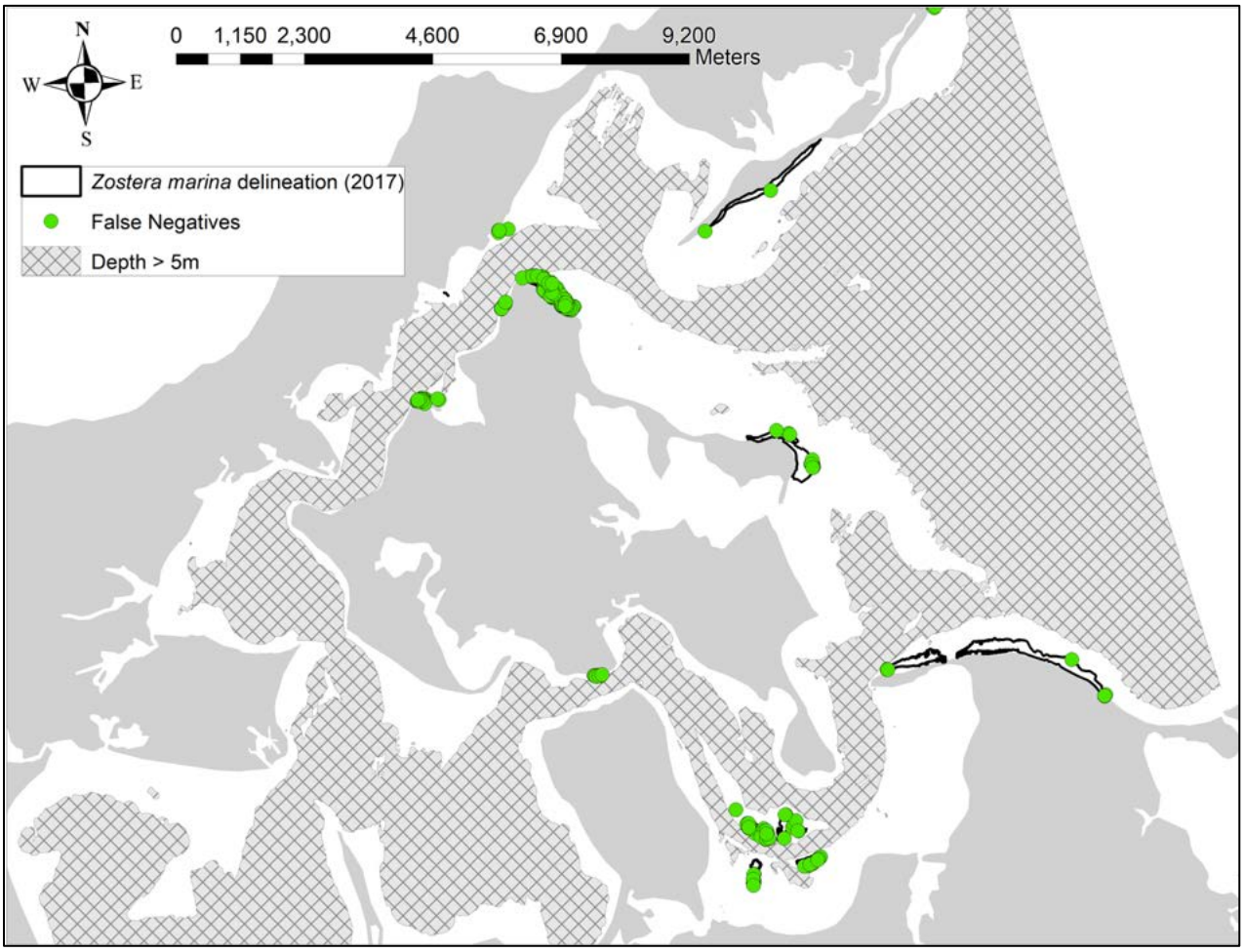

Figure 24: Locations of false negatives produced by the Restoration Potential (RP) model.

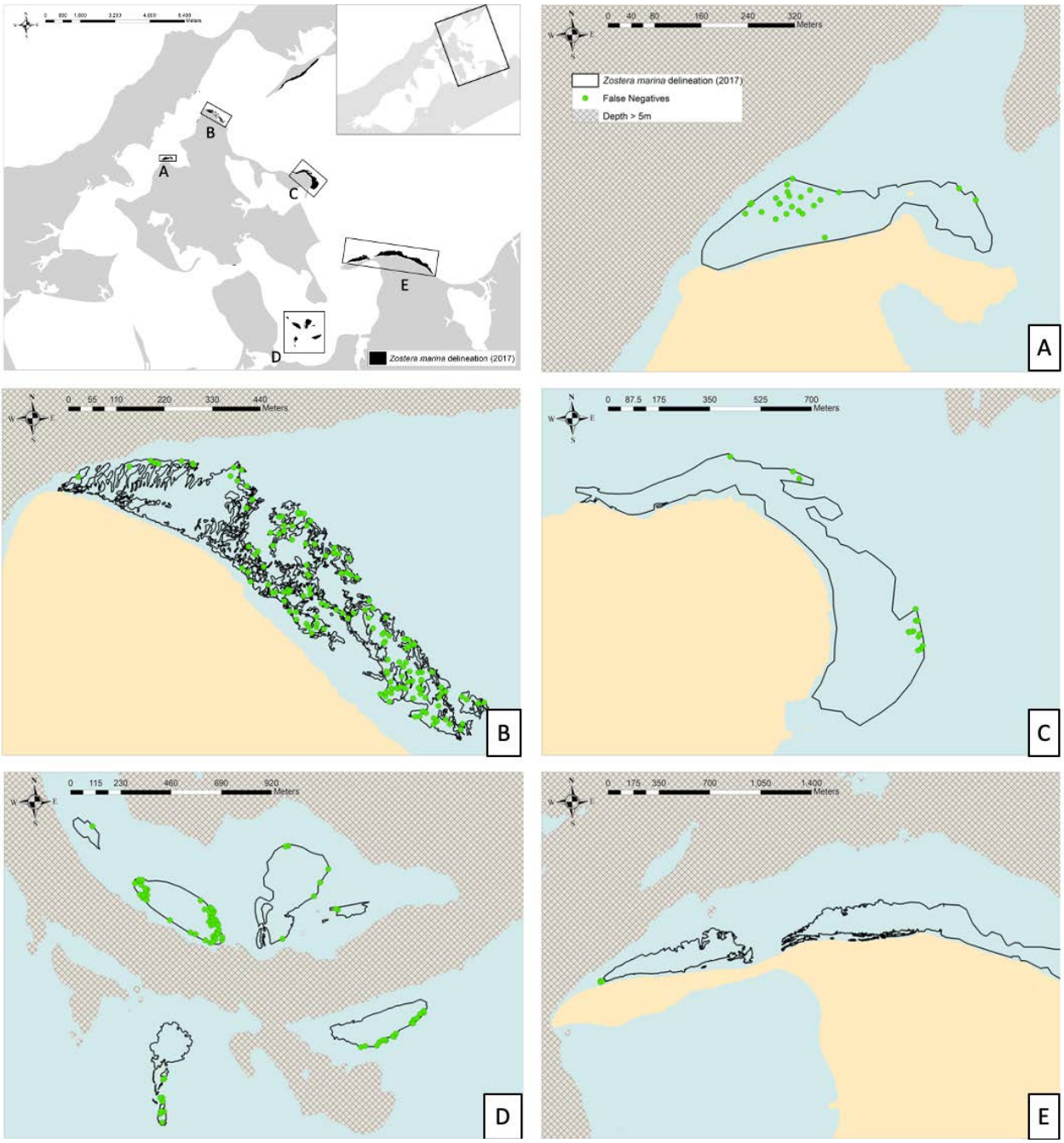

Figure 25: Locations of false negatives produced by the Restoration Potential (RP) model (close-up).

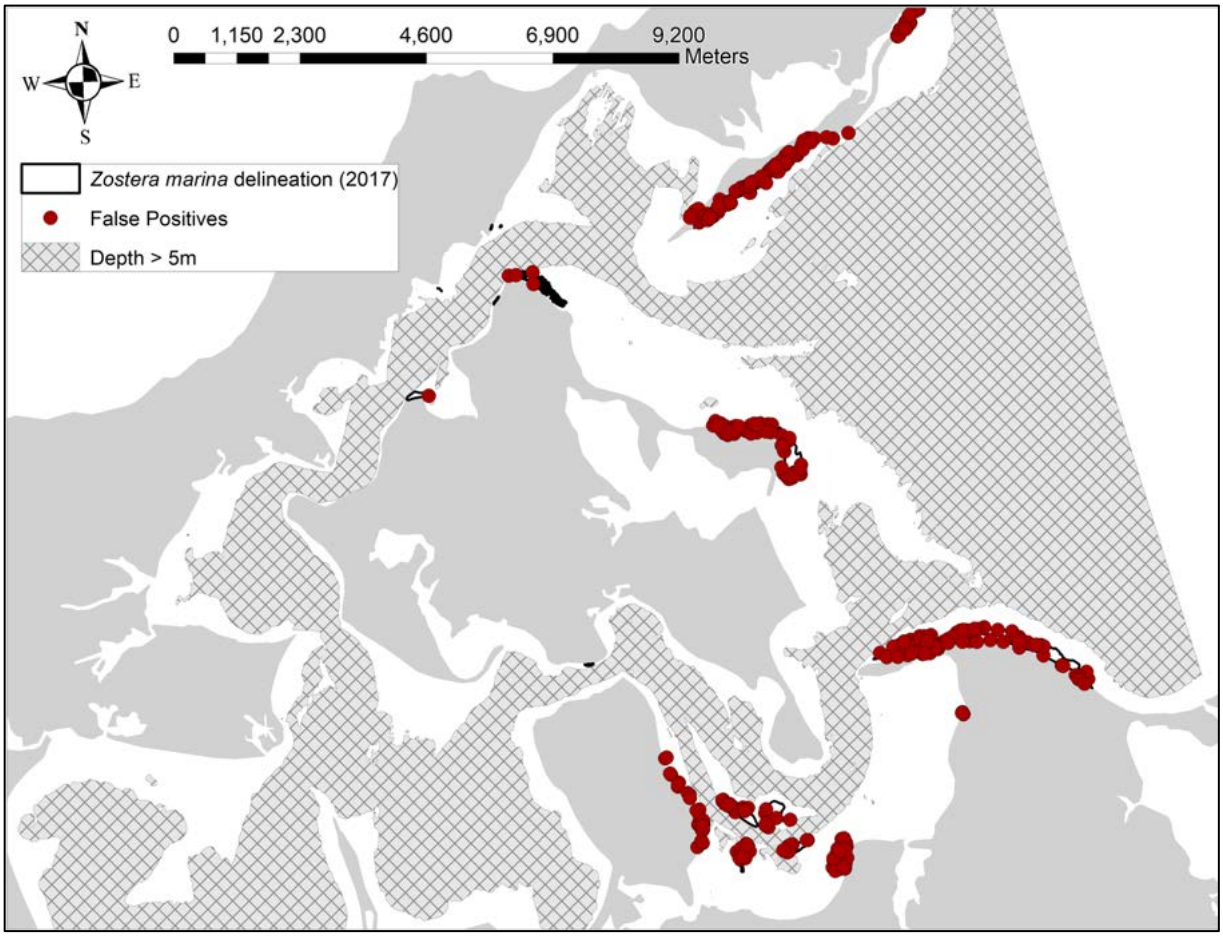

Figure 26: Locations of false positives produced by the Restoration Potential (RP) model.

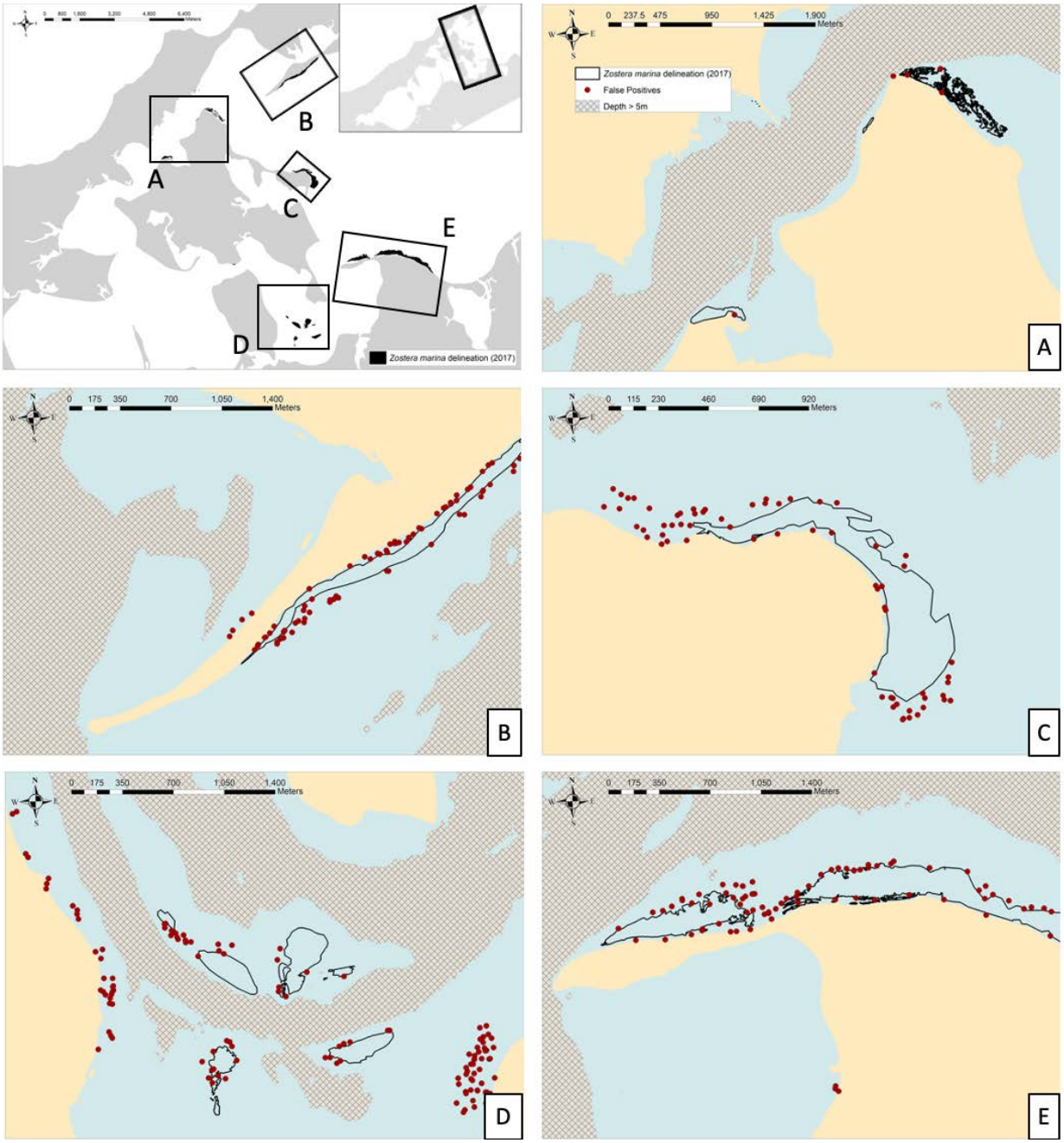

Figure 27: Locations of false positives produced by the Restoration Potential (RP) model (close-up).

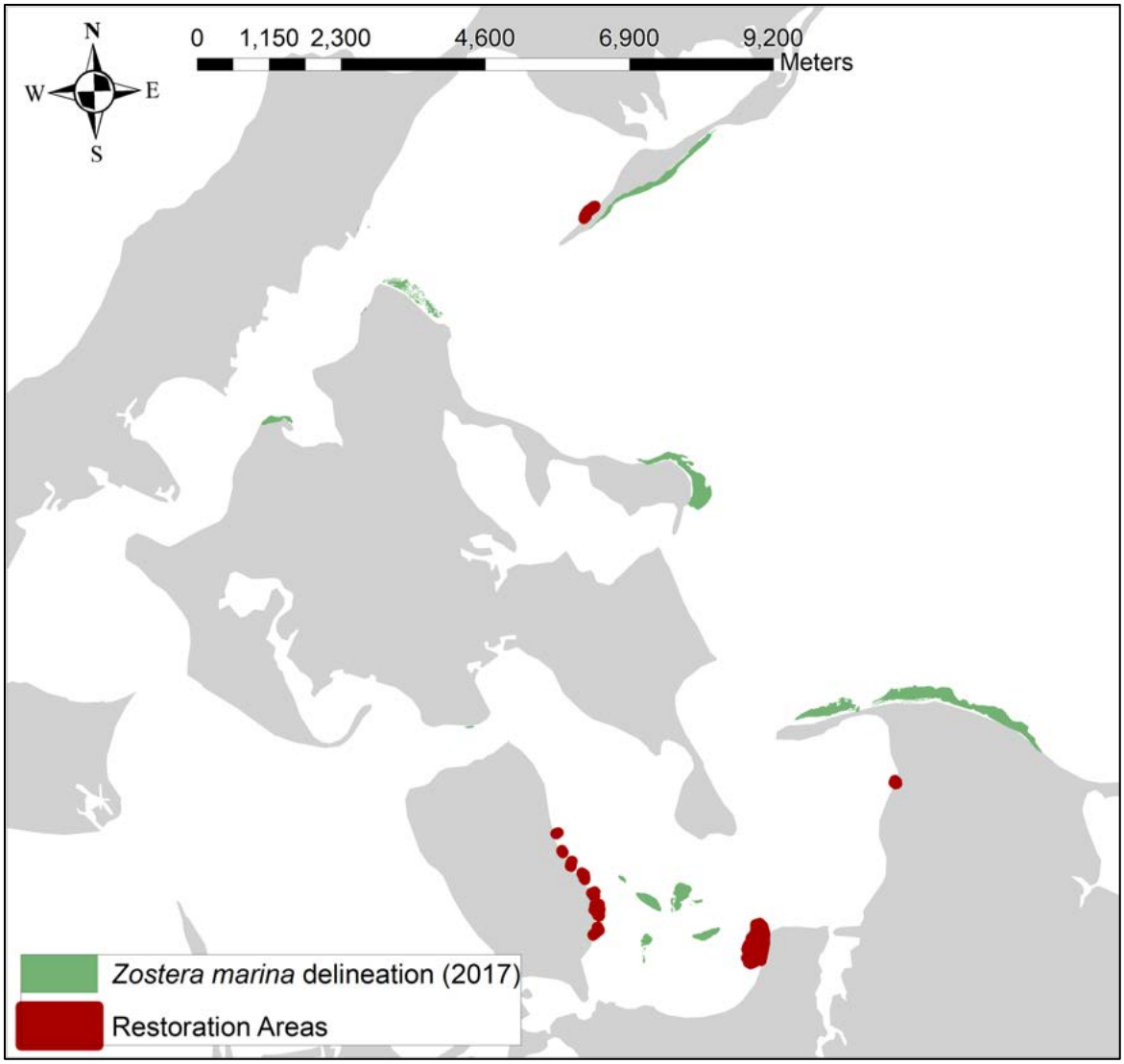

Figure 28: Locations of possible restoration areas for *Z. marina* produced by the Restoration Potential (RP) model (close-up).

TABLES

Table 1: Mean and SD (standard deviation) of variable values from present (with *Z. marina*) and absent (without *Z. marina*) points used for random forest modeling in the creation of the Habitat Suitability (HS) and Restoration Potential (RP) models.

		Present		Absent	
Variable	Metric	Mean	SD	Mean	SD
PLW 10%	Days	17.9	0.69	12	6.81
PLW 15%		17.7	1.27	9.8	7.66
PLW 18.5%		17.4	1.78	8.63	7.83
PLW 20%		17.2	2.08	8.18	7.84
PLW 22.5%		16.8	2.61	7.49	7.8
PLW 25%		16.2	3.30	6.87	7.73
PLW 30%		14.7	5.03	5.85	7.53
Q1	%	43.9	15.9	22.1	21.6
Q2		47.5	16.3	24.7	22.1
Q3		51.3	15.9	28.1	22.6
Depth	(m)	-1.31	0.60	-2.64	1.4
25	Cumulative hours	577	237	1124	344
26		202	113	672	336
27		43.2	41.7	319	214
28		11.1	13.8	119	87
29		2.25	2.84	25.6	19.8
30		0.33	0.51	2.84	3.41
25	Sequential hours	171	85.1	425	177
27		7.64	3.35	71.5	58.4
Hardened shoreline	Distance (m)	740	590	974	1211
Hardened shoreline	Direction ()	199	78	NA	NA
Bulkhead	Distance (m)	2514	2567	1374	1623
Bulkhead	Direction	226	70	NA	NA
RWE		681	243	714	374

Table 2: Random forest model results for all variables used, removed temperature layers, removed PLW layers, final model. Yellow indicates final model 1, green indicates final model 2. Accuracy, kappa, and AUROC were calculated with the 'rfUtilities' package. True positive rate (TPR), true negative rate (TNR), false positive rate (FPR), and false negative rate (FNR), were calculated from model predictions.

Model #	Total # of variables	# of nodes	# of variables at each split	OOB estimate of error rate	TPR	TNR	FPR	FNR	Accuracy	Cohen's Kappa	Area under the ROC	Variables used
1	24	309	4	0.57%	0.983	0.996	0.004	0.017	99.3%	0.961	0.971	All
2	24	50	4	1.94%	0.913	0.988	0.012	0.087	97.9%	0.886	0.933	All
3	7	339	2	0.58%	0.981	0.996	0.004	0.019	99.4%	0.966	0.979	RWE, bulkhead distance and direction, cumulative and sequential hours over 25°C, depth, and median PLW
4	7	50	2	1.87%	0.911	0.989	0.011	0.089	98.1%	0.897	0.948	RWE, bulkhead distance and direction, cumulative and sequential hours over 25°C, depth, and median PLW
5 (Habitat Suitability model or HS model)	6	340	2	0.54%	0.984	0.996	0.004	0.016	99.4%	0.966	0.979	RWE, bulkhead distance and direction, cumulative and sequential hours over 25°C, and depth
6 (Restoration Potential model or RP model)	6	50	2	1.54%	0.928	0.991	0.009	0.072	98.3%	0.906	0.949	RWE, bulkhead distance and direction, cumulative and sequential hours over 25°C, and depth

Table 3: Predicted area of ideal bathymetry (0-5m) when sea level rise scenarios (SLR) are added to present day bathymetry (2014).

Scenario	Depth change (m)	Year	Area (km^2)	% Change
Current	NA	2020	150	NA
Low	0.2	2050	149	**-0.7%**
Medium	0.4		145	**-3.3%**
High	0.8		137	**-8.7%**
Low	0.3	2080	147	**+2.0%**
Medium	0.7		139	**+7.3%**
High	1.5		132	**-12%**
Low	0.4	2100	145	**-3.3%**
Medium	0.9		136	**-9.3%**
High	1.8		129	**-14%**

Table 4: Predicted *Z. marina* presence/absence based on the HS (habitat suitability) model with temperature, sea level rise (SLR), and combinations of both.

Scenario	Present	Absent	% Change
Current (predicted)	5,495	44,505	NA
+0.25ºC	285	49,715	**-94.8%**
+0.5ºC	11	49,989	**-99.8%**
+0.75ºC	0	50,000	**-100%**
Low SLR (0.2m)	5,648	44,352	**+2.8%**
Medium SLR (0.4m)	5,626	44,374	**+2.4%**
High SLR (0.8m)	5,207	44,788	**-5.2%**
+0.25ºC & Low SLR	243	49,757	**-95.6%**
+0.25ºC & Medium SLR	140	49,860	**-97.5%**
+0.25ºC & High SLR	91	49,909	**-98.3%**
+0.5ºC & Low SLR	12	49,988	**-99.8%**
+0.5ºC & Medium SLR	11	49,989	**-99.8%**
+0.5ºC & High SLR	15	49,985	**-99.7%**